

2/83



77

BARD

FINAL REPORT

PROJECT NO. I-466-82

Crop Yield and Water Use Under Irrigation with Saline Water

H. Frenkel, A. Mantell

2

630.72
BAR/FRE
2nd copy

1988



000000083850

29333 0

Institute of Soils and Water,
ARO, The Volcani Center,
Bet Dagan, Israel.

Dept. Soil Science and Biomet.,
Utah State University,
Logan, Utah, U.S.A.

CROP YIELD AND WATER USE UNDER IRRIGATION
WITH SALINE WATER

Final Research Report
Submitted to

US-ISRAEL AGRICULTURAL AND DEVELOPMENT FUND

מכון וולקני לחקר הקרקע והמים
מחלקת המחקר והייעוץ
B.U.-RTI

July 1987

630.72 : 631.7 ; 631.52
BAR | FRE

2nd copy

Standard BARD Cover Page for Scientific Reports

Date: _____

BARD
P.O. Box 6
Bet Dagan, ISRAEL

BARD Project No. I-466-82

Title

CROP YIELD AND WATER USE UNDER IRRIGATION WITH SALINE WATER

Investigators' Names

(Principal listed first)

H. FRENKEL

A. MANTELL

R.J. HANKS, USA

Investigators' Institutions

AGRICULTURAL RESEARCH ORGANIZATION
BET DAGAN, ISRAEL.

AGRICULTURAL RESEARCH ORGANIZATION,
BET DAGAN, ISRAEL.

UTAH STATE UNIVERSITY,
DEPT. SOIL SCIENCE AND BIOMET

Project's starting date: 1983

Type of Report: 1st Annual _____ 2nd Annual _____ Final X

Signatures

Principal Investigator

Institution's Authorizing Official

Haim Frenkel

G. Gelse

State of Israel
Ministry of Agriculture
AGRICULTURAL RESEARCH ORGANIZATION
The Volcani Center Bet-Dagan

TABLE OF CONTENTS

	Page
Abstract	1
Introduction and Objectives	2
Physical and chemical properties of the soil studied	4
Soil hydraulic properties	12
Determination of the soil water retention curve in the laboratory	18
In-situ measurement of soil water retention curve	27
Soil hydraulic conductivity - laboratory and field measurements	34
Crop management during three years of experiments	40
Double line-source sprinkler system	47
Quantity and salinity of the irrigation water	51
Water and salt distribution in the soil	54
Field water balance and evapotranspiration	68
Effect of salinity and water application on yield	83
Literature cited	96
Appendix A:	
Basic program for calculating the soil water retention curve	99
Corn and wheat yields as a function of row number in the different treatments	103
Appendix B:	
Validation of a modified steady state model of crop response to saline water irrigation under transient conditions	119
Publications	

NOTE: This report includes only the Israeli contribution to the project.

CROP YIELD AND WATER USE UNDER IRRIGATION WITH SALINE WATER

ABSTRACT

The experiments in Israel were conducted in the southern Coastal Plain of the Negev. In order to determine the production function for the three crops studied - forage corn (Zea mays L., cv. Halameesh), sweet corn (Zea mays L., cv. Jubilee) and wheat (Triticum aestivum L., cv. H-945) - as affected by water and salinity, a modification of the line-source sprinkler system was developed. The double line-source system which we used consisted of two parallel lines, each supplying a uniform quantity of water of water but of different salinity (low salinity - 1.35 dS/m, and high salinity - 8.52 dS/m). This technique produces a wide range of water application amounts in combination with a large gradient in water salinity. Data on crop yield as a function of amount of irrigation, evapotranspiration, and salinity are presented.

In using semi-empirical simulation models for the prediction of crop response to irrigation with saline water the average irrigation water salinity must be corrected to account for rainfall or non-saline water given for crop establishment. Allowance must also be made for salts initially present in the soil profile. When local parameters are used, a steady-state model over-predicts yield losses when irrigation with saline water is under transient-state conditions. The latter situation is most common under semi-arid conditions where salinity is built up during the summer and partially leached by rainfall during the winter. Under these conditions when salinity changes with time and depth, the predicted yield under conditions of deficit irrigation is nearly independent of irrigation water salinity. The importance of the use of a transient-state modification will decline when irrigation continues over many seasons, especially if winter rainfall is low.

CROP YIELD AND WATER USE UNDER IRRIGATION WITH SALINE WATER

Introduction

Soil salinity is an important factor of the environment in which plants grow. In agriculture, soil salinity may become a problem because of accumulation of salts in the root zone to an extent that may cause crop yield reduction. The accumulation of soluble salts in the soil is the major problem in irrigated arid regions. Salts are concentrated in the soil as water is removed from the soil by evapotranspiration. Continual accumulation will occur unless excess irrigation is applied to leach the salts out of the root zone. With increased demands on our water supplies, water available for excess irrigation is becoming more limited. Moreover, the water leached out of irrigated lands is usually used as a source of irrigation water further downstream by other users. Thus, as our irrigation acreage increases, evapotranspiration also increases, which automatically causes more saline irrigation water and associated problems.

Thus, future irrigation practices will cause the irrigated soil to be affected by excess soluble salts and to be subjected to the deleterious effect of adsorbed sodium on the physical properties of the soil more than has been the situation in the past. Moreover, the continuing deterioration of the quality of both surface and ground water, coupled with the increased use of brackish, industrial and municipal waste water for irrigation underscores the need for sound irrigation management. Sound future irrigation management will require not only dependable information on water consumptive use and crop yield relations, but also the long-term consequences of

increasing salinity. Such information is scarce and difficult to obtain experimentally at a specific location. Previous information has been primarily derived from small "pot" type experiments where water of differing salinity characteristics has been used for irrigation in a near steady state mode. These methods have simulated past irrigation practices but do not give enough information on results to be expected from future, more closely managed, irrigation practices. A method which will permit estimation of crop yield based on known climatic, soil and crop parameters where salinity buildup is expected, is therefore highly desirable.

Objectives of the research

1. To study crop production functions under a wide range of water salinity and amounts.
2. To evaluate crop production under different water management practices and different root zone salinities.
3. To test (and possibly modify) semi-empirical simulation models for prediction of response functions of crops irrigated with saline water.

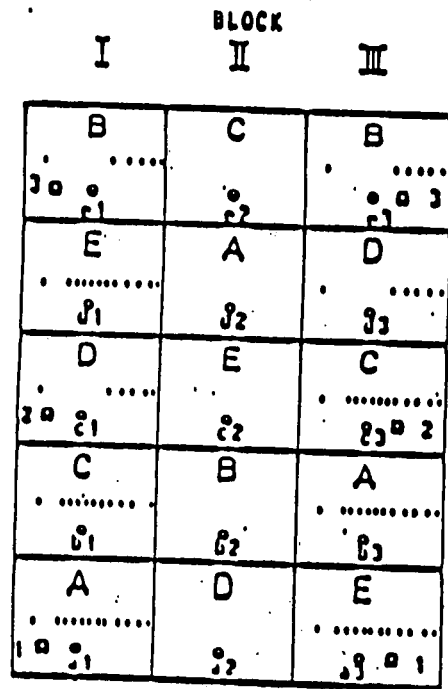
Physical and chemical properties of the soil studied

The experiment in Israel was conducted at Kibbutz Reim in the Southern Coastal Plain. The soil at the experimental field is a loess (Calcic mollic haploxeralf) of loamy texture.

The layout of the experimental plots is shown in Fig. 1. The field was 150 m long and 108 m wide, and divided into 3 blocks. Each block included 5 irrigation treatments, A-E. (A description of these treatments will be given later). Soil samples, marked $a_1 - e_3$, were taken in a grid, before sowing, in 30-cm increments to a depth of 210 cm. The samples were analyzed for chemical and physical properties as shown in Table 1. A detailed analysis of the uniformity of the field is given in Table 2 which shows the means, SD (standard deviation), and CV (coefficient of variation) of the clay, silt and sand contents for the various depths measured by the sedimentation method (Black, 1965).

From this data it can be seen that the coefficient of variation is relatively large for the clay and sand contents, whereas it is small for the silt content. When the mean values of clay, silt and sand contents, for all depths, are placed in the textural triangle (Fig. 2), we see that the soil texture according to the Soil Survey Staff (1975) is defined as a loam for all samples. Field soils display a variation in their properties. Depending on the property, these variations may be large or small.

According to Warrick and Nielsen (1980), it is possible to divide the soil properties according to their variability in a field into three groups as shown in Table 2.



- Soil water retention determinations
- Soil salinity measurements at the beginning and end of the experiment

Fig. 1: Plan of field

Table 1: Physical and chemical properties of REIM soil

Soil depth (cm)	Mechanical Composition*			CEC Cation exchange capacity meq/100gr	Surface area m ² /gr	CaCO ₃ (%)	O.N. Organic matter	Hygroscopic water content (%)
	Clay (%)	Silt (%)	Sand					
0 - 30	13.6	38.9	47.8	Mean 14.5 S.D. 1.03	119	Mean 10.14 S.D. 1.49	0.6	Mean 3.0 S.D. 0.21
30 - 60	15.4	40.1	44.5	14.2	116	12.65	0.8	3.35
60 - 90	16.4	45.0	39.9	14.0	114	14.74	0.3	3.57
90 -120	16.4	45.8	37.9	14.4	118	13.75	0.2	3.84
120 -150	17.2	40.7	42.5	13.8	113	11.47	0.2	3.77
150 -180	20.7	43.1	36.1	13.7	112	13.96	0.1	3.97
180 -210	21.2	42.6	36.1	14.1	115	14.5	0.1	4.1

Table 1a: Chemical Composition of saturated extrats REIM.

Soil depth (cm)	EC _e m ⁻¹ dS m ⁻¹		Na		Ca		Mg		Cl	
	Mean	S.D.	Mean	S.D.	Mean	S.D.	Mean	S.D.	Mean	S.D.
0 - 30	0.79	0.19	3.7	1.0	2.2	0.6	0.8	0.3	3.5	1.3
30 - 60	0.73	0.23	2.8	0.5	2.5	1.0	1.15	0.6	2.9	1.4
60 - 90	0.95	0.26	3.6	1.2	2.6	1.0	2.18	0.9	4.6	2.1
90 - 120	1.05	0.32	6.5	1.5	1.5	0.5	1.7	0.7	4.1	1.6
120 - 150	1.27	0.58	8.8	1.5	1.6	0.8	1.4	0.6	3.9	1.6
150 - 180	1.32	0.5	10.0	1.5	1.2	0.8	1.1	0.7	4.3	1.1
180 - 210	1.74	0.5	14.1	2.6	1.2	0.6	1.5	1.1	7.2	2.9

Table. 1b: Statistical analysis of the soil texture.

		Soil depth (cm)					
		0-30	30-60	60-90	90-120	120-150	150-180
Clay (%)	Mean	13,6	15,4	16,4	16,4	17,2	20,7
	Standard deviation	1,6	0,7	3,2	5,4	1,5	8,1
	Coefficient of variation	11,9	4,8	19,6	33,1	8,6	38,9
	Number of samples	7	8	8	8	6	7
Silt (%)	Mean	30,9	40,1	45,0	45,8	40,7	43,1
	Standard deviation	1,6	4,0	2,8	3,1	4,2	3,8
	Coefficient of variation	4,1	10,0	6,3	6,7	10,3	8,7
	Number of samples	7	8	8	8	6	7
Sand (%)	Mean	47,8	44,5	39,9	37,9	42,5	36,1
	Standard deviation	1,6	4,3	3,4	4,1	5,1	8,9
	Coefficient of variation	3,4	9,6	8,4	10,9	11,9	24,7
	Number of samples	7	8	8	8	6	7

Table 2: Classification of the variability of soil properties.

Variability	Soil Physical Parameter	Coefficient of Variation (%)
Small	Bulk density, Water content(%) at zero tension.	7-10
Medium	Sand, Silt, Clay (%), 0.1/15 Bar (% water content).	10-100
Large	Saturated hydraulic conductivity (HC), Unsaturated HC, 100-1000 Electrical conductivity for 1:1 and saturated extract.	

In the group of soil physical properties with low variability, we can find SP (amount of water in saturated paste). In the present experiment we took a large number of soil samples from Blocks I, II and III for salinity measurements.

The SP values were analyzed statistically and the distribution of SP values in the experimental field is shown in Fig. 3. No significant differences were found to a depth of 60 cm over the entire field, whereas significant differences were found between Blocks I and II, and Block III at the deeper depths. In Blocks I and II no horizontal differences were found, while in Block III SP values for the same depth increased from treatment E to B. In the vertical direction, the largest differences were found in Block III, where the SP values almost doubled from 0-30 cm to 180-210 cm.

It has been shown (Banin and Amiel, 1967) that for Israeli soils a high correlation exists between SP values and certain other physical properties, e.g. surface area, CEC, hygroscopic moisture, 1/3 atm moisture

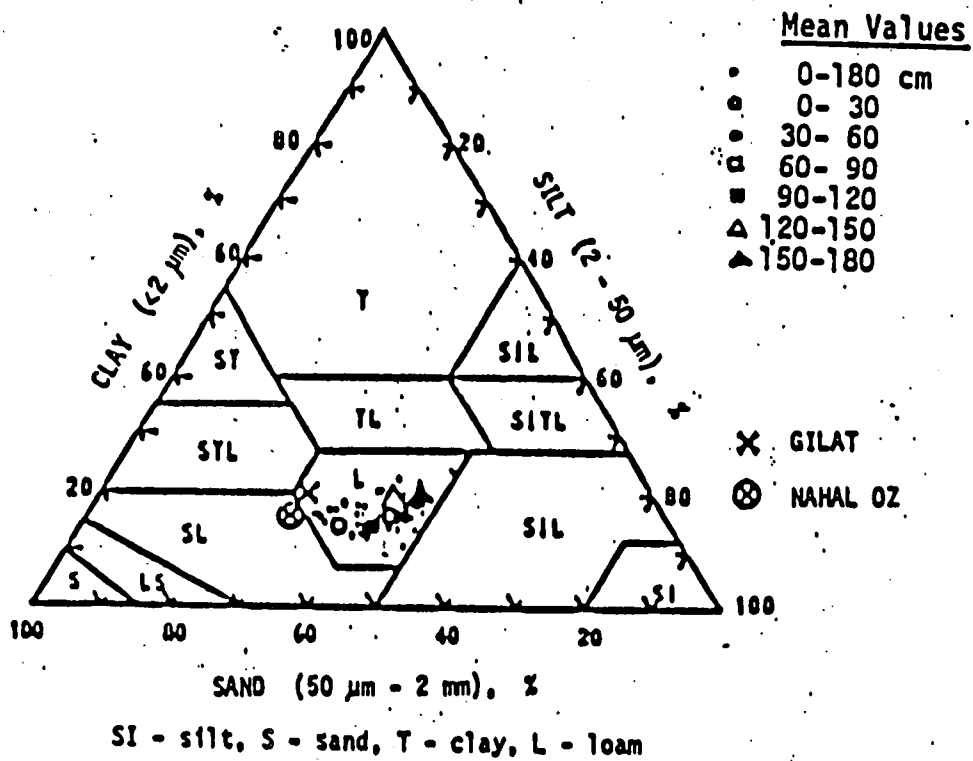


Fig. 2: Soil texture of REIM Soil for various depths.

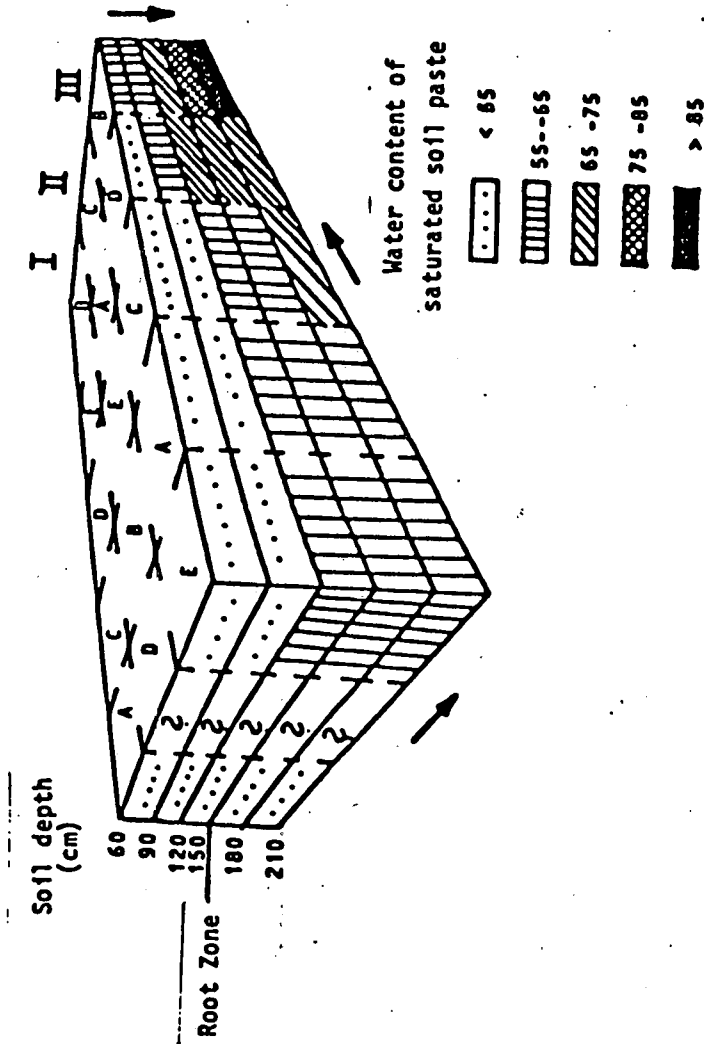


Fig. 3: Spatial distribution of saturation percentage (SP) of REIM Soil.

content, 15 atm moisture content, and clay content. The relationship between clay percentage, sand percentage and SP for the Reim field is shown in Figure 4 and Table 3. From the data in Table 3 it is evident that a strong linear correlation exists between SP and clay and sand percentages, and no correlation with silt. Using of the well-established relationship between SP, Field Capacity (FC), and Permanent Wilting Point (USSL,1954), SP:FC:PWP = 4:2:1, we found for the Reim soil that:

$$SP = 1.69 FC + 18.7 \quad r = 0.834$$

$$PWP = 0.58 FC - 20.6 \quad r = 0.951$$

Therefore Fig. 3, which describes the horizontal and vertical variability for SP, describes also the distribution of FC and PWP over the entire field. The same is true for the water characteristic curves (as will be discussed later).

Soil Hydraulic Properties

Salt transport is affected by a combination of several soil-water-plant factors. To estimate the magnitude of the hazard posed by salinity, it is important to understand and identify the processes involved in salt movement through the root zone. For one-dimensional vertical solution flow in the z direction, the condition for conservation of matter is

$$-\frac{\partial(\rho\theta)}{\partial t} = -\frac{\partial(\rho q)}{\partial z} \quad (1)$$

Table 3. Regression analysis between SP and clay, sand and silt contents.

1	2	3	4	5	6
Sand	-0.917	90.37	-0.7	4.45*	44
Silt	2.694	-101.62	0.159	1.04	44
Clay	0.601	-15.53	0.797	8.54*	44

1 - Soil fraction

2 - Linear regression coefficient

3 - Intercept

4 - Correlation coefficient

5 -
$$t = r \frac{n - 2}{1 - r^2}^{\frac{1}{2}}$$

6 - Number of samples

* - Significant at 0.1% level.

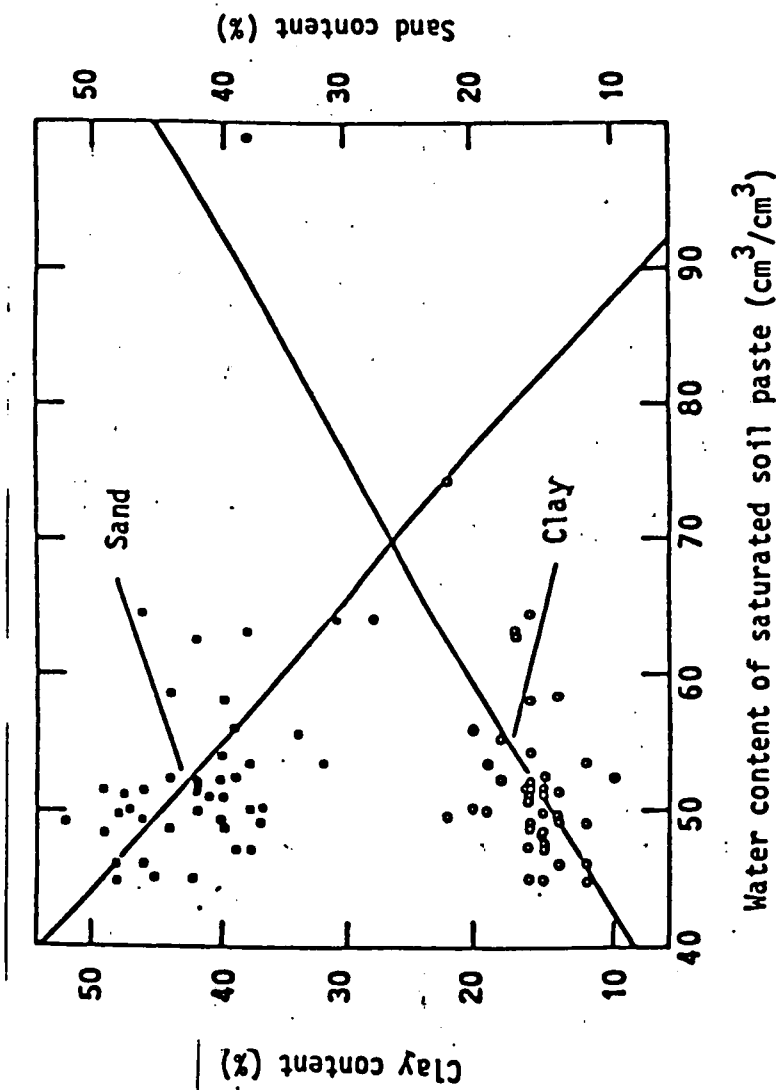


Fig. 4: Linear regression lines between SP and Clay, Sand contents.

where ρ is the density of the solution (generally assumed constant). Elimination of q by substituting the Darcy equation $q = V\theta = -K(\theta) dh/dz$ into the conservation equation (1) gives the general non-steady one-dimensional (vertical) water flow equation:

$$\frac{\partial \theta}{\partial t} = \frac{\partial}{\partial z} \left[K(\theta) \frac{\partial h}{\partial z} + K(\theta) \right] \quad (2)$$

where $K(\theta)$ is the unsaturated hydraulic conductivity function; $h = h(\theta)$ is the soil water pressure head function; and H is the hydraulic head (sum of pressure head and gravitation head, z). Since h and θ are interrelated by the soil water retentivity function, $h(\theta)$, Eq. (2) can be written in terms of either h or θ .

Reliable estimates of the unsaturated hydraulic conductivity are especially difficult to obtain, partly because of its extensive variability in the field, and partially because measuring this parameter is time-consuming. For these reasons, several investigators have used models for calculating the unsaturated hydraulic conductivity from the more easily measured soil-water retention curve.

Brooks and Corey (1964) used the Burdine theory (1953) to predict the relative hydraulic conductivity and the soil water diffusivity. They derived the following expressions:

$$\theta = (h/h_p)^{-\lambda} \quad (\theta \leq 1) \quad (3)$$

$$K_r(\theta) = \theta^{3+2/\lambda} \quad (4)$$

$$K_r(h) = (\alpha h)^{-2-3\lambda} \quad (5)$$

$$D(\theta) = \frac{K_s}{\alpha \lambda (\theta_s - \theta_r)} \theta^{2+1/\lambda} \quad (6)$$

The dimensionless water content is given by Eq (7)

$$\theta = \frac{\theta - \theta_r}{\theta_s - \theta_r} \quad (7)$$

where s and r indicate saturated and residual values of the soil water content (θ), respectively, K_r is the relative hydraulic conductivity, h is the pressure head and h_p is the bubbling pressure, λ is a characteristic soil parameter, and K_s is the saturated hydraulic conductivity

Brooks and Corey (1964, 1966) obtained fairly accurate predictions with their equations, even though a discontinuity was present in the slope of both the soil water retention curve and the unsaturated hydraulic

conductivity curve at some negative values of pressure head. Such a discontinuity occasionally prevents a rapid convergence in numerical saturated - unsaturated flow problems.

Another relatively simple equation for the soil water content pressure head curve $h(\theta)$ was suggested recently by van Genuchten (1980). This simple equation form enables one to derive a closed-form analytical expression for the relative hydraulic conductivity K_r when substituted into the predictive conductivity models of Burdine (1953) or Mualem (1976a).

The soil-water content as a function of the pressure head is given by Eq. (8) and (9)

$$\theta = \left[\frac{1}{1+(ah)^n} \right]^m \quad (8)$$

$$\text{or } \theta = \theta_r + \frac{(\theta_s - \theta_r)}{[1+(ah)^n]^m} \quad (9)$$

where h is positive and $m = 1-1/n$

This equation contains four independent parameters θ_r , θ_s , α and n , which have to be estimated from the observed soil water retention data.

In this study, we used both the methods described above. A schematic presentation of the water retention curve by both methods is given in Fig. 5.

The parameters h_b , α and m were determined by using the following equations:

$$\log \theta = (\log h_b - \log h) \quad (10)$$

$$\log (\theta^{-1} + 1) = m(\log \alpha + \log h) \quad (11)$$

A computer program (in BASIC) for making all of these calculations is given in Appendix 1.

Determination of the soil water retention curve in the laboratory

The soil water retention curve was obtained with the procedure suggested by Richards (1965). The pressures used were 0.33, 0.66, 1, 3, 10 and 15 Bars. Soil samples (10-20 g each) from depths of 0-30, 30-60, 60-90, 90-120 and 120-150 cm from Plots AI, DI, BI, BIII, CIII, and EIII (see Fig. 1) were run in three replicates.

The data are shown in Table 4, and the statistical analysis of the data is shown in Table 5.

The soil water retention curve was also determined by packing the soil in pressure cells which allowed θ -metric potential measurements to be made in the range of 0-0.5 bar. An acrylic cylinder was fitted into pressure cell (see Fig. 6). The soils were first saturated with NaCl-CaCl₂

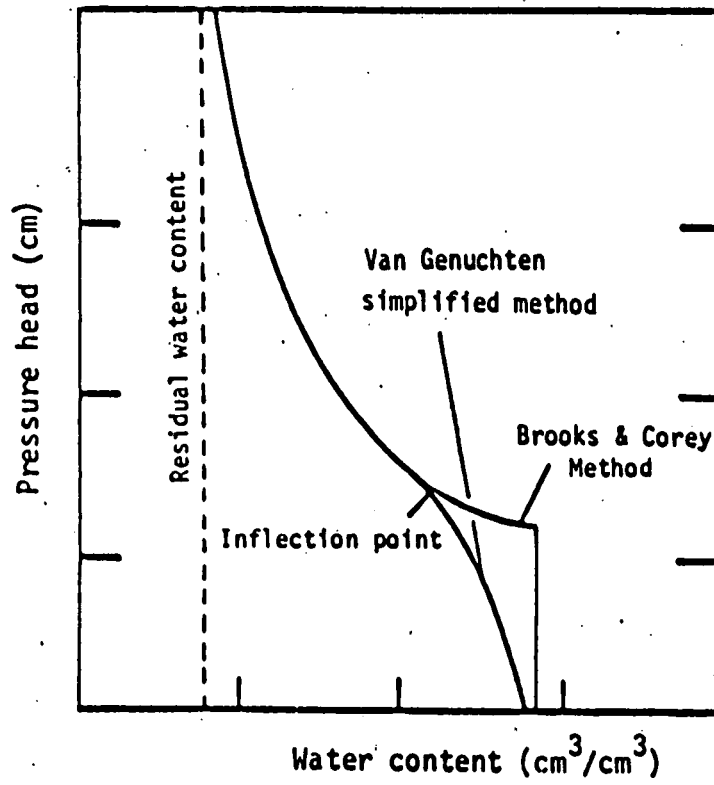


Fig. 5: Schematic presentation of soil water pressure head (h) as a function of water content (θ)

Table 4. Soil water content as a function of pressure applied to soil samples from various depths (Richards, 1965)

Soil depth (cm)	Treatment	Pressure head (cm H ₂ O)					
		330	660	1000	3000	10000	15000
0 - 30	1III	25,55	18,27	15,55	11,71	10,14	9,28
	1III	26,57		15,04		9,39	8,70
	2I	27,46		15,73		10,03	9,65
	2III	25,68	17,86	13,99	11,43	8,93	8,37
	3I	23,23	17,46	15,04	11,18	9,77	8,56
	3III	26,75	19,05	10,08	11,98	9,84	9,33
30 - 60	1I	25,14	18,68	16,06	12,07	10,82	10,11
	1III	27,84		16,52		10,17	9,20
	2I	28,72		16,80		10,71	10,43
	2III	27,10	19,51	15,36	12,01	9,41	8,53
	3I	25,08	18,58	15,99	11,89	10,44	9,04
	3III	26,25	19,59	17,92	13,19	10,83	9,90
60 - 90	1I	27,45	22,07	19,49	13,96	12,61	11,28
	1III	28,57		17,68		12,31	10,30
	2I	28,23		18,22		11,73	11,70
	2III	27,85	21,77	17,64	14,31	11,35	10,66
	3I	27,55	21,40	18,35	14,25	12,06	10,75
	3III	33,26*	27,90	26,96*	20,14	15,86	14,26
90 - 120	1I	27,55	13,21	19,43	15,05	13,14	12,20
	1III	28,57		17,82		11,64	10,70
	2I	30,65		19,93		12,49	11,74
	2III	29,63	25,22	21,01	18,55	14,07	13,61
	3I	28,63	23,10	19,62	15,83	13,59	11,29
	3III	38,44	32,47	31,00	25,23	20,90	19,71
120 - 150	1I	27,54	22,55	19,63	14,75	13,08	12,24
	1III	28,13		20,49		14,21	12,50
	2I	31,19		20,90		13,80	13,02
	2III	31,08	27,55	24,22	20,06	17,32	16,08
	3I	29,59	24,45	20,65	16,61	14,90	12,72
	3III	42,19	35,46	33,57	27,32	23,02	21,07

Table 5. Statistical analysis of data shown in Table 4.

Suction tension (bars)	Statistical parameters	Soil depth (cm)				
		0 - 30	30 - 60	60 - 90	90 - 120	120 - 150
0,33	\bar{x}	25,87	26,69	27,93	29,01	29,51
	S	1,48	1,47	0,47	1,18	1,66
	CV	5,71	5,51	1,68	4,06	5,64
	N	6	6	5	5	5
0,66	\bar{x}	18,16	19,09	20,99	23,84	24,85
	S	0,68	0,53	1,32	1,19	2,52
	CV	3,74	2,80	6,32	5,01	10,16
	N	4	4	3	3	3
1	\bar{x}	15,34	16,44	18,28	19,56	21,18
	S	0,74	0,88	0,75	1,15	1,77
	CV	4,83	5,33	4,10	5,88	8,34
	N	6	6	5	5	5
3	\bar{x}	11,43	12,29	14,17	16,48	17,14
	S	0,22	0,60	0,19	1,84	2,69
	CV	1,90	4,92	1,32	11,15	15,72
	N	4	4	3	3	3
10	\bar{x}	9,68	10,40	12,01	12,99	14,00
	S	0,45	0,55	0,49	0,95	0,76
	CV	4,65	5,25	4,09	7,33	5,44
	N	6	6	5	5	4
15	\bar{x}	8,98	9,54	10,94	11,91	12,63
	S	0,51	0,73	0,55	1,10	0,35
	CV	5,65	7,61	5,04	9,25	2,78
	N	6	6	5	5	4

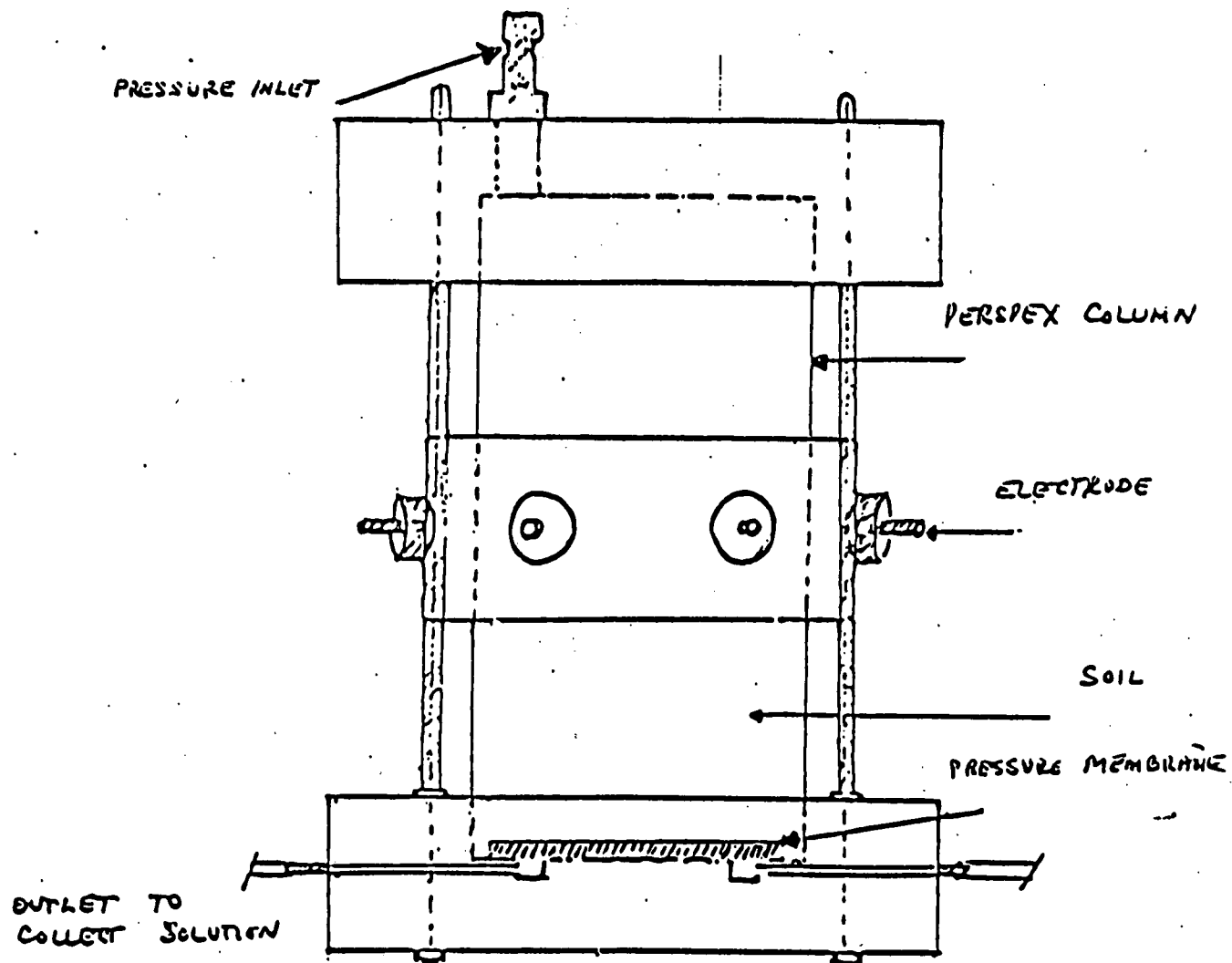


Fig. 6. Pressure cell for measuring the effect of moisture on electrical conductivity of soil.

of various concentrations having an SAR = 5. After the soils were saturated, cell weight (to compute water content) was determined. Then a constant pressure was applied for 72 hr. The amount of water released was calculated from i) the change in the weight of the soil column, and ii) the amount of water released (collected in bottles).

Statistical analysis of the data is given in Table 6. For predicting the $h(\theta)$ function, the saturation water content is needed. However, θ_s of the disturbed samples was not determined, so we assumed $\theta_s = 50\%$. In the Brooke and Corey method this value is only of a limited importance. However, it has a significant effect on the bubbling pressure (h_b) which tends to decrease as θ_s increases. In contrast, the θ_s value has a significant effect on the soil water retention curve shape calculated by the simplified van Genuchten method, especially in the range of high water contents.

Table 4 presents the data obtained with the different soil samples and Table 5 gives the statistical analysis of the data. It is evident that samples from plots 3III and 2III differ significantly from the rest of the samples. This is in agreement with the SP data shown in Fig. 3. The coefficient of determination (r^2) (Table 7) for the regression with the Brooks and Corey method shows good correlation between the measured values and the exponential function $r^2 = 0.9917-0.9951$. With the Van Genuchten method $r^2 = 0.9873-0.9922$.

Figures 7 and 7a give the soil water retention curves for all soil depths as calculated by the two methods (A = Brooks and Corey, and B = van Genuchten). For the same pressure head there is a shift in the curves to a

Table 6. Statistical analysis of water content as a function of pressure applied (in pressure cells).

h						Statistical parameters
0,05	0,10	0,15	0,20	0,30	0,50	
44,60	42,71	38,11	29,00	22,64	18,67	\bar{x}
2,51	2,34	2,48	2,39	1,67	1,77	s
5,61	5,47	6,51	8,25	7,37	9,50	cv
8	8	8	8	8	8	N

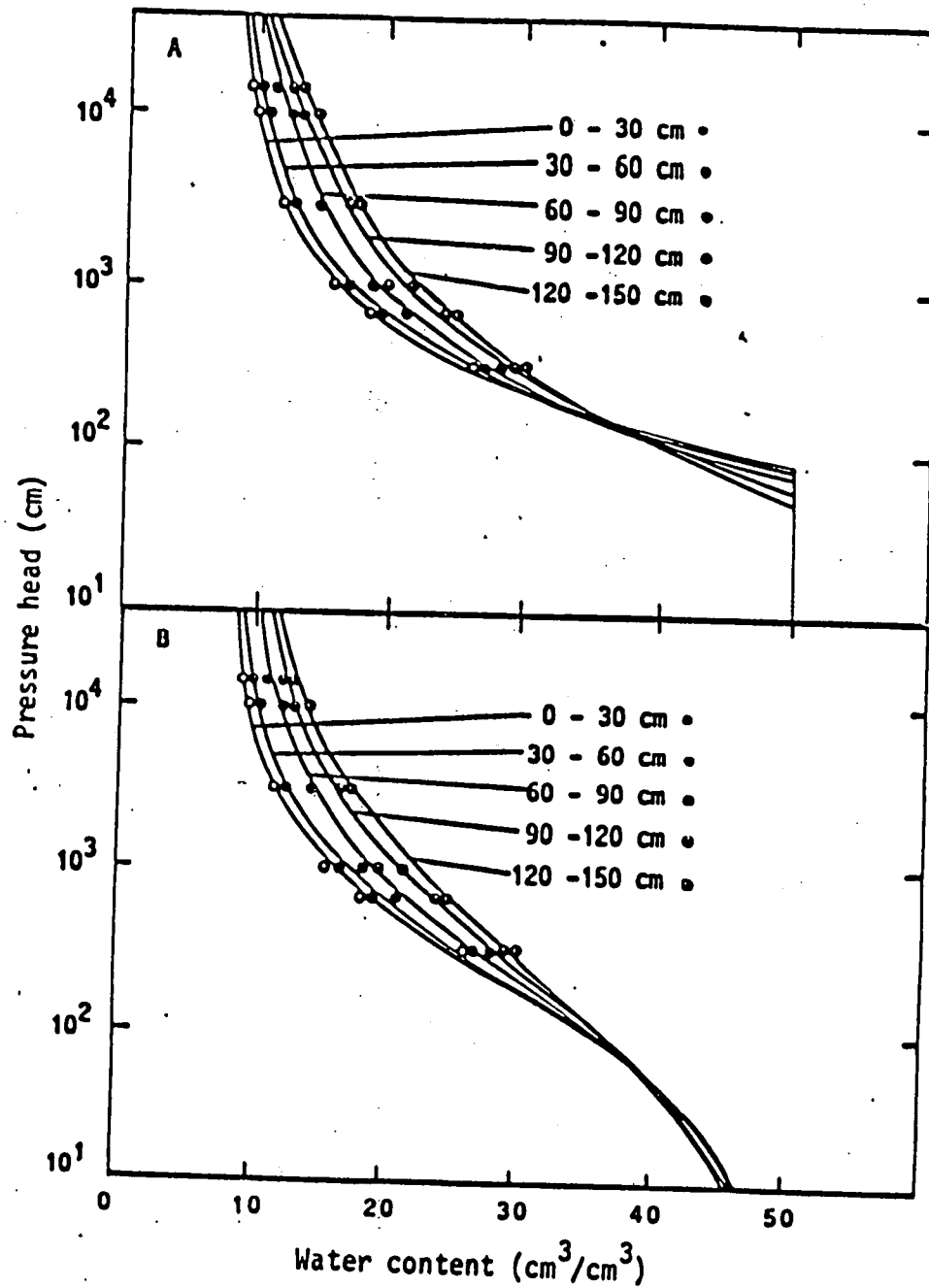


Fig. 7: Soil water pressure head (h) as a function of water content (θ) for REIM soil calculated by:
 A - Brooks and Core method
 B - Van Genuchten Method

מכון המחקר
 לתכנון ולקונסטרוקציה
 ב"ח-11

Table 7. Estimated parameters for soil water retention curve from disturbed soil samples.

Soil depth (cm)	θ_s	$h(\theta)$ - Function Brooks & Corey Method					$h(\theta)$ - Function Van Genuchten simplified method						
		θ_r	λ	h_b	r^2	s_a	N	θ_r	m	α	r^2	s_a	N
30	50	7.8	0.6813	86.8	0.9948	3.68	6	8.2	0.8905	0.0051	0.9896	6.78	6
60	50	8.0	0.6200	80.9	0.9937	3.68	6	8.6	0.8505	0.0049	0.9881	6.90	6
90	50	8.7	0.5320	70.7	0.9930	3.32	6	9.6	0.7705	0.0046	0.9873	6.5	6
120	50	8.0	0.4253	61.6	0.9917	2.90	6	9.8	0.6955	0.0038	0.9883	5.6	6
150	50	7.4	0.3659	53.3	0.9951	1.91	6	9.9	0.6407	0.0035	0.9922	4.23	6
0-30 Pressure cell	46.13	11.5	0.9107	98.7	0.9986	4.47	5	15.6	2.385	0.005	0.9120	1.1599	6

θ_s = Saturation water content

r^2 = Coefficient of determination

S = Standard error

N = Number of samples

higher water content as soil depth increases. Again, these data are in complete agreement with the data presented in Fig. 3. Therefore, we can conclude that the spatial distribution of SP in the field describes also the spatial distribution of the soil water retention curve. This is also in agreement with Warick and Nielsen (1980), who showed that the soil water retention curve is in the soil properties class of medium variability (see Table 2).

In-situ measurement of soil water retention curve

These measurements were made in the field in treatments CI and DI with the use of tensiometers and a neutron probe, during the first year experiment before irrigation. (The soil before irrigation was relatively dry). However, in order to obtain a reliable estimate of drainage, the part of the soil water retention curve at high water content is needed. Therefore, we used the parameters h_b , θ_r and θ_s of Russo and Bresler (1980) for Gilat soil which is very similar in texture to Reim soil. Table 7 gives the linear regression of the parameters λ , h_b , m and α by the Brooks and Corey and simplified van Genuchten methods.

Saturated water content was calculated from $\theta_s = [1 - (p_b/2.65)]/b$ (McBride and Mackintosh, 1984). θ_s values calculated by this method are similar to those found in the laboratory experiments [measurements of saturated hydraulic conductivity (Table 9) and infiltration Table (10)]. Residual water content, θ_r was estimated by extrapolating available soil water retention data with the highest regression coefficient. We also used θ_r from Russo and Bresler (1980) for Gilat soil. The parameters (λ , h_b , m , α) estimated from the in situ measurements are given in Table 8.

The coefficient of determination of these parameters was in the range $r^2=0.78-0.83$. The differences between the water retention curves estimated with the value of θ_r calculated by the best fit and those calculated using θ_r of Gilat soil was less than 1.5%.

θ_r of Gilat soil which is significantly smaller than the one found for Reim soil, (Table 7) had a large effect on λ , α and m and therefore on the curvature of the water retention curves (Table 8 and Fig. 8). The small effect that θ_r has on the coefficient of determination and its relatively large effect on the curvature of the curves indicates that there is a large variability of the measurements and also that the range of water content in the field when the tensiometers reading were taken was too small. Considering these two facts, it is clear that the this range of water content was not enough to predict the water retention curve for the full range of water content (from $\theta_r - \theta_s$). Furthermore, θ_r must be a parameter which adjusts to the function and is not a measured one (see also Van Genuchten, 1980). Russo and Bresler (1980a) determined experimentally the parameters θ_s , θ_r , λ and h_b by the Brooks and Corey method and then described the $h(\theta)$ function for Gilat soil. θ_r for the Gilat soil was 3% (cm^3/cm^3). Therefore, we chose to use the Russo and Bresler value for θ_r rather than the one we obtained by the best estimate procedure.

In order to evaluate the variability of the "predicted" portion of the soil-water retention curve, the 95% confidence intervals were calculated for the effective saturation data (Figure 8) and superimposed on the semi-logarithmic plot of $h-\theta$ for the tensiometer readings from all depths.

The soil water retention curves were calculated by the Brooks and Corey

Table 8. Estimated parameter for soil water retention curves using various θ_r values (of Gilat soil).

Soil depth (cm)	θ_s	h (θ)- Function Brooks & Corey Method					h (θ)- Function Van Genuchten simplified method						
		θ_r	λ	h_b	r^2	s_a	N^*	θ_r	m	α	r^2	s_u	N
30	34	5,1	0,4176	-23,1	0,7846	4,33	40	8,4	0,8783	0,0111	0,7839	9,08	40
60	34	5,9	0,3285	-12,25	0,8013	3,30	42	9,7	0,7291	0,0153	0,7982	7,41	42
90	36	9,7	0,3471	-6,7	0,8252	3,09	43	12,0	0,6504	0,0292	0,8252	5,79	43
30	34	2,2	0,3284	-19,02	0,7841	3,41	40	2,2	0,5913	0,0063	0,7779	6,25	40
60	34	2,2	0,2450	-9,25	0,8010	2,47	42	2,2	0,4647	0,0063	0,7901	4,84	42
90	36	2,5	0,1841	-2,87	0,8228	1,65	43	2,5	0,3452	0,0080	0,8169	3,16	43
0 - 90	34	2,2	0,2616	-11,28	0,7567	2,96	125	2,2	0,49038	0,0006	0,7643	5,04	125

θ_s = Saturation water content

r^2 = Coefficient of determination

S_u = Standard error

N = Number of samples

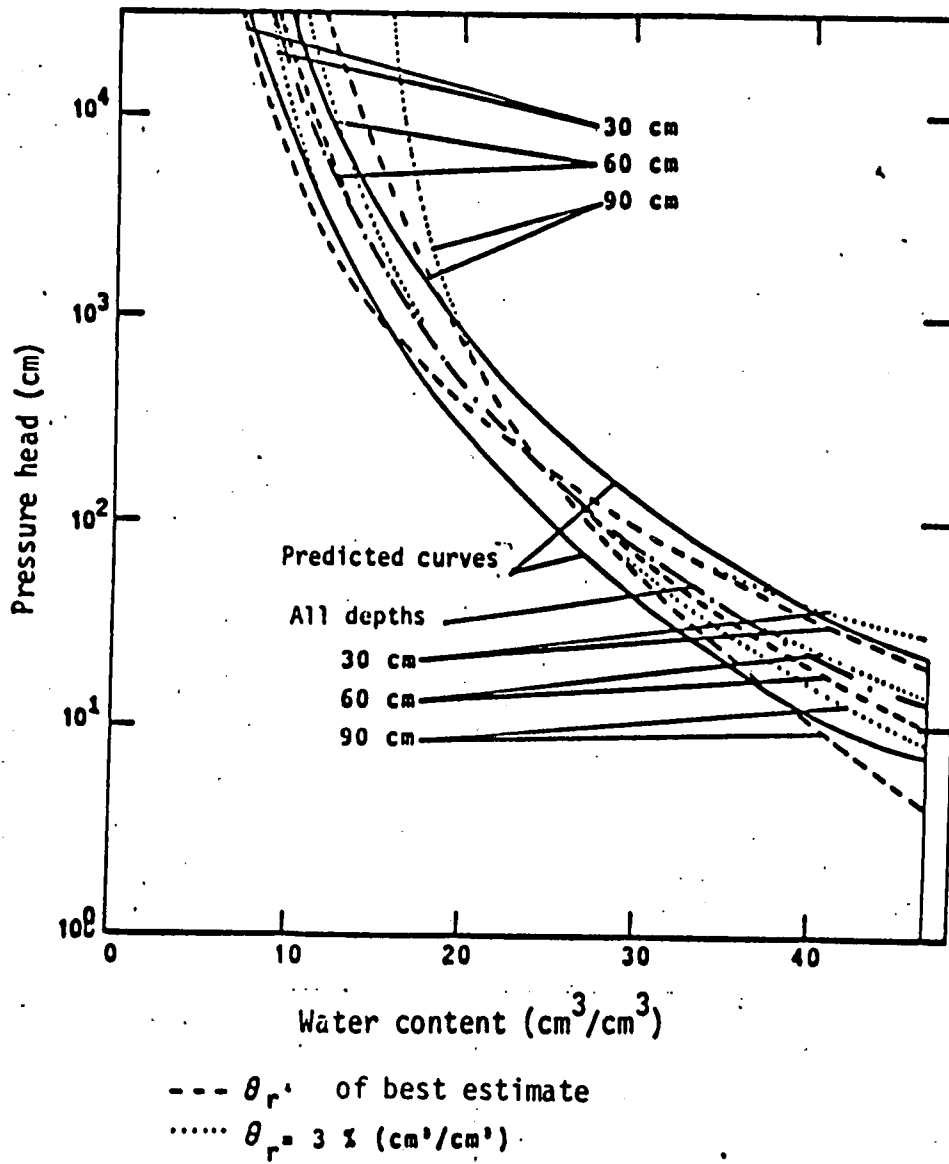


Fig. 8: Soil water pressure head (h) as a function of water content (θ) using various θ_r

method for the soil depths of 30, 60 and 90 cm and for the 0-90-cm layer (Table 8). Large deviations from the 95% confidence intervals were in the range of high and low water content. However, the major part of the water retention curve with the various θ_r is in the 95% confidence interval.

A comparison between the soil water retention curve determined in the laboratory with those measured in the field shows large deviations especially in the range of low pressure head. However, there is good agreement at high pressure head (Fig. 9). The deviations of those curves is a result of several factors: 1) In the laboratory measurements we destroy and rearrange the macro- and medium-size pores. Therefore, the largest deviation occurs at low pressure head. 2) The differences between drying and wetting (hysteresis). 3) All parameters which were measured in the laboratory such as weight and pressure head, were measured with high accuracy (e.g. weight ± 0.01 gr, whereas in the field the neutron probe measurement is $\pm 0.1\%$; tensiometer 0.05 bars, and the soil volume which the tensiometer measures is much smaller than that measured with the neutron probe. This explains also the scattering of the data.

The same results were obtained in other investigations. For example, Shaykewich (1970) found large differences in water content at 1/3 and 15 bars, between disturbed and undisturbed soil samples. Hanks and Ashcroft (1980) showed that water content at 1/3 bar in the laboratory is equivalent to 1/10 bar in the field. In Fig. 10 field capacity as measured in the laboratory is equivalent to 0.1 bar measured in the field. Moreover, all the values measured in the laboratory for all soil samples and depths fall within the confidence interval predicted from in situ measurements. When

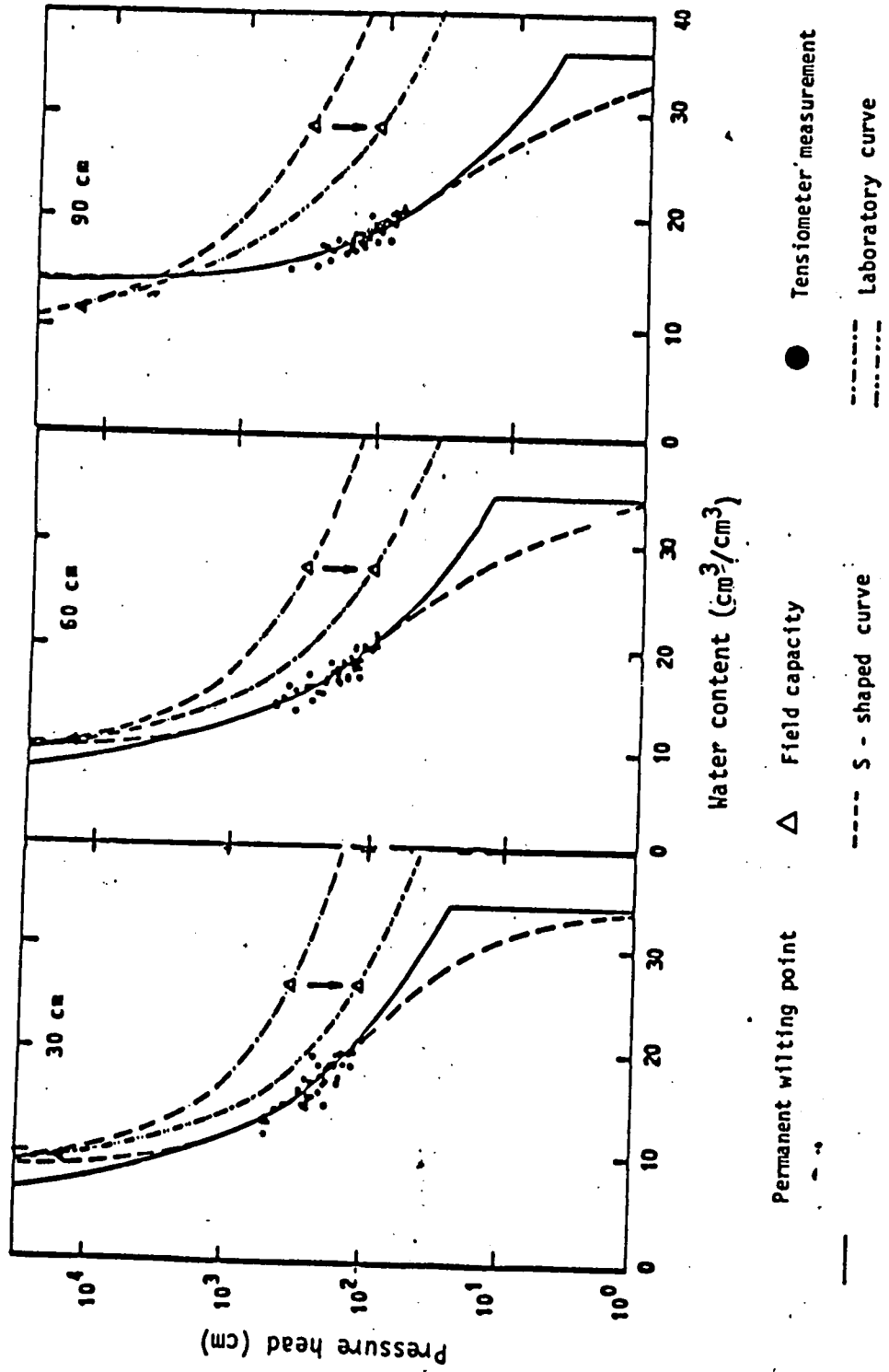


Fig. 9: Comparison of REIM soil water retention curves determined in the laboratory and in the field.

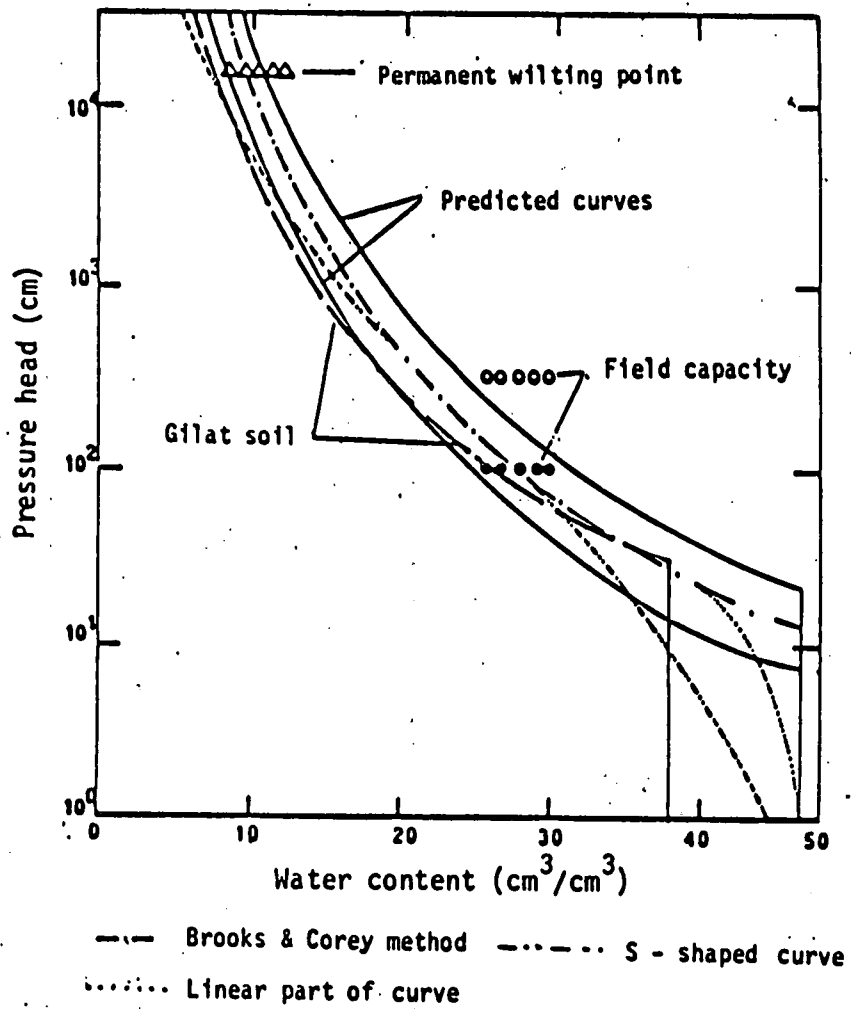


Fig. 10: Comparison of REIM soil water retention curve calculated by various methods.

we used the mean value of θ_r from Gilat soil for the 0-90-cm depth the soil water retention curve was in close agreement with the laboratory curve. In Fig. 10 we also present the water retention curve as calculated after McBride and MacKintosh (1984), which assumes a linear relationship between preessure head and water concent (from the inflection point to saturation). If we assume that h at saturation equals 1 cm H₂O, then for $\theta > 40\%$ (cm³/cm³).

$$-h = +2.938\theta - 141.197 \quad (12)$$

Soil hydraulic conductivity - laboratory and field measurements

Soils were packed by the Yaron et al. (1966) method to a bulk density of 1.39 g/cm³, into soil columns 10 cm long and 5 cm in diameter. The soils were first flushed with CO₂ (Frenkel, et al., 1983) for 45 minutes, and the column was then saturated from the bottom with 0.01 M NaCl-CaCl₂

solution having SAR = 5. After saturation, the soil was leached with the same solution from the top under a constant head. Leachate volumes were collected and saturated hydraulic conductivity was calculated. Saturated hydraulic conductivity was measured on soil samples from different depths in field plots lIII, 3III and 2I. Statistical analysis of the saturated hydraulic conductivity of soil samples and saturation water content is given in Tables 9 and 10.

It is important to note the large coefficient of variation of 45.2% for the 0-30-cm layer and 53.8% for 0-150 cm (combined soil samples).

Table 9. Saturated hydraulic conductivity as measured in the pressure cells.

	K_s		θ_s [cm ³ /cm ³]	K_s		θ_s % [cm ³ /cm ³]
	cm/h	m/s		cm/h	m/s	
Mean	0,49	$1,36 \cdot 10^{-6}$	50,3	0,39	$1,08 \cdot 10^{-6}$	44,8
Standard deviation	0,26	$7,33 \cdot 10^{-7}$	2,47	0,18	$4,9 \cdot 10^{-7}$	2,9
Coefficient of variation	53,8 %		4,9 %	45,2 %		6,5 %
Number of samples	13			14		
Sampling depth	0 - 150 cm			0 - 30 cm		

Table 10. Hydraulic conductivity values for different soil depths as measured by the Young (1964) method.

	K		θ_s
	cm/h	m/s	% [cm^3/cm^3]
Mean	0,152	$4,22 \cdot 10^{-7}$	30,52
Standard deviation	0,005	$1,28 \cdot 10^{-8}$	0,87
Coefficient of variation	3,1 %		2,85 %
Number of samples	4		
Sampling depth	0 - 30 cm		
Mean	0,131	$4,19 \cdot 10^{-7}$	30,98
Standard deviation	0,014	$3,89 \cdot 10^{-8}$	0,94
Coefficient of variation	9,0 %		3,02 %
Number of samples	5		
Sampling depth	30 - 60 cm		
Mean	0,166	$4,61 \cdot 10^{-7}$	34,83
Standard deviation	0,002	$5,8 \cdot 10^{-8}$	1,94
Coefficient of variation	1,25 %		5,57 %
Number of samples	3		
Sampling depth	60 - 90 cm		
Mean	0,154	$4,28 \cdot 10^{-7}$	33,76
Standard deviation	0,014	$3,89 \cdot 10^{-8}$	1,20
Coefficient of variation	9,08 %		3,56 %
Number of samples	4		
Sampling depth	90 - 120 cm		
Mean	0,165	$4,58 \cdot 10^{-7}$	36,19
Standard deviation	0,0042	$1,17 \cdot 10^{-8}$	1,18
Coefficient of variation	2,57 %		3,26 %
Number of samples	2		
Sampling depth	120 - 150 cm		

The unsaturated hydraulic conductivity was measured in the laboratory by the Young (1964) method. The total amount of water infiltrated into a vertical soil column can be described by eq. (13).

$$Q = \int_0^t [K \left(\frac{dp}{dz} + 1 \right)] dt \quad (13)$$

where K = the unsaturated hydraulic conductivity; p = matric potential; z = depth and t = time. Under a long time of infiltration $dp/dz = 0$, then

$$Q = A + Kt \quad (14)$$

where A is the integration constant.

The hydraulic conductivity could be determined from the graphical relationship between Q/t against $1/t$, where K is the intercept on the Q/t axis. The water content which relates to this value may be determined from the slope of the line described in eq. (15).

$$Q = a - bz \quad (15)$$

where Q = volume of water, b = slope, a = intercept and z = depth.

We used the Young (1964) method with a slight modification. A peristaltic pump with a constant flux was used to supply the water and we measured the advance of the water front every 30 and 60 min for a period of 16 hr. Because of the use of a constant flux, K is predetermined. Therefore, graphical presentation of Q/t against $1/t$ will give a straight

line with zero slope. In order to measure K we needed to have soil water content as a function of time. By assuming that water content during infiltration is equally distributed in the wetted soil volume, and by measuring the volume of water infiltrated, time, depth of wetting, diameter of the column and soil bulk density it is possible to calculate water content by using eq. (16).

$$Q = V/t.A.b. + \theta_i \quad (16)$$

where b is the slope of the line obtained from eq. (17).

$$Z = bt + a \quad (17)$$

where Z = depth of wetting front, t = time and a = intercept (on the Z axis).

Soil samples from different depths from plots 1I, 1III, 2I, 3I and 3III were measured by this method. The results are given in Table 1a and Fig. 11.

In another method we used 2m x 2m plots. These were flooded and covered by plastic sheets to prevent evaporation. In the center of each plot we installed two access tubes (for neutron probe measurements) and tensiometers at 15-cm intervals to a depth of 120 cm. We measured water content and matric potential for the different soil depths and time. Hydraulic conductivity was calculated according to Hillel (1980a) (data are given in Fig. 11).

We also used the procedures suggested by Brooks and Corey and Van Genuchten to calculate the $K(\theta)$ function from the soil water retention curves (Fig. 11). This procedure was carried out for soil samples from

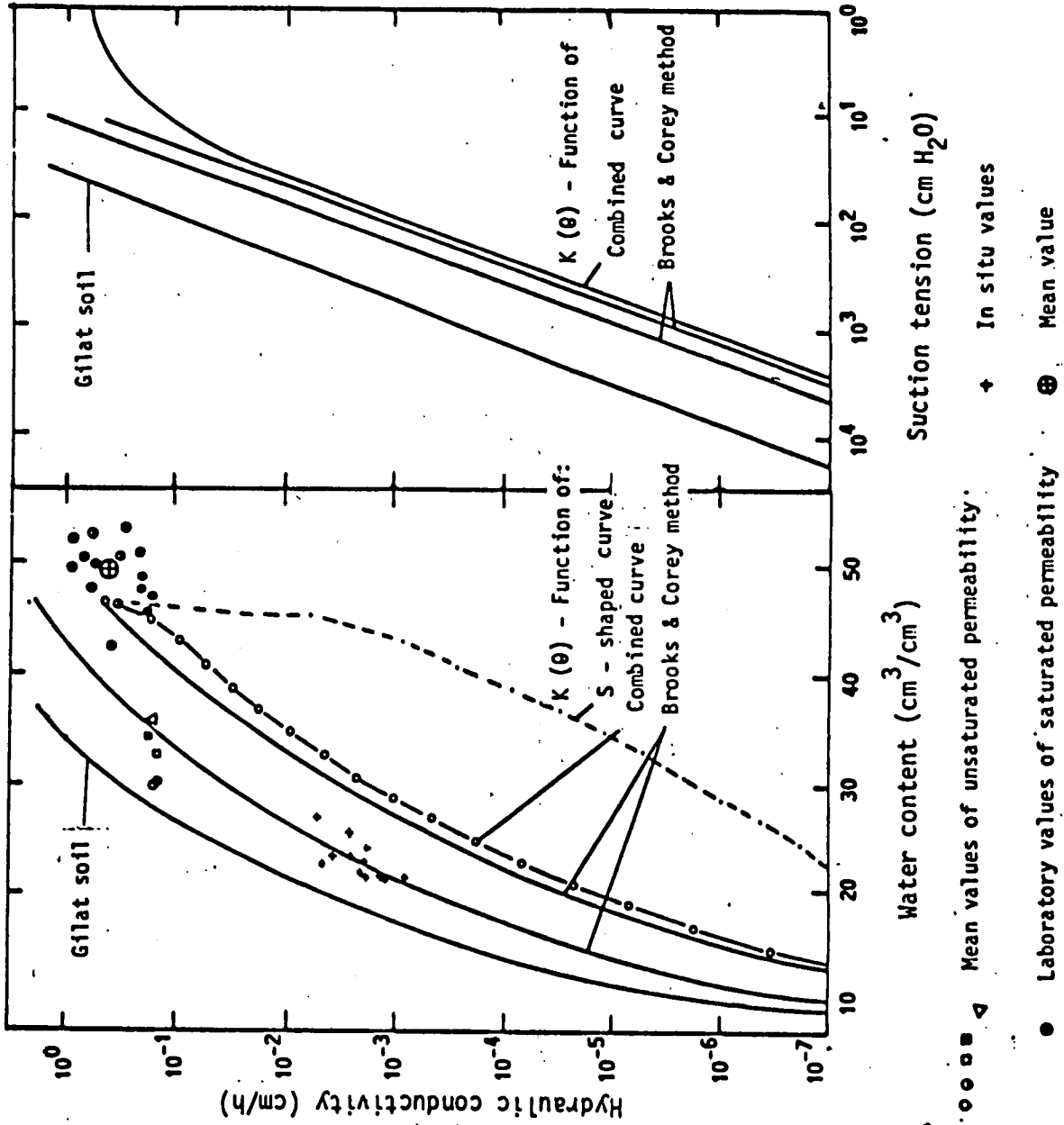


Fig. 11: Hydraulic conductivity as a function of soil water content (θ) and pressure head (h).

depths of 30, 60 and 90 cm (Fig. 12). Because of the large variability in K_s we used

$K_{rel} = K/K_s$ relative hydraulic conductivity

$S = \theta/\theta_s$ relative water content

In all cases, K values calculated by the van Genuchten method gave lower values compared with those calculated by Brooks and Corey method. Van Genuchten (1980) found also the same kind of deviations in his analytical procedure. This means that calculating the $K(\theta)$ function by the Brooks and Corey method over-predicts K, and the van Genuchten method under-predicts the K values. In Fig. 10 soil hydraulic conductivity as a function of water content was calculated by various methods (sec 1) using data collected from disturbed soil samples in the laboratory and in situ measurements in the field. For comparison we also presented the data for Gilat soils. From all the physical properties measured on Reim soil in the laboratory and in the field it seems that most of the properties described very well the soil parameter, especially in Block I. For a better evaluation of soil hydraulic conductivities more measurements are needed. In the water balance calculation the variability in K must be taken into account.

Crop management during the three years of experiments

first year:

Forage corn (*Zea mays* L., c. "Halameesh") was sown on 28th June 1984, in rows 1 m apart at a spacing of 5-7 plants/m on a furrowed surface. The field was uniformly fertilized before sowing with 250 kg N/ha as urea and 50 kg P/ha as superphosphate. During the irrigations on 12th July, 2nd

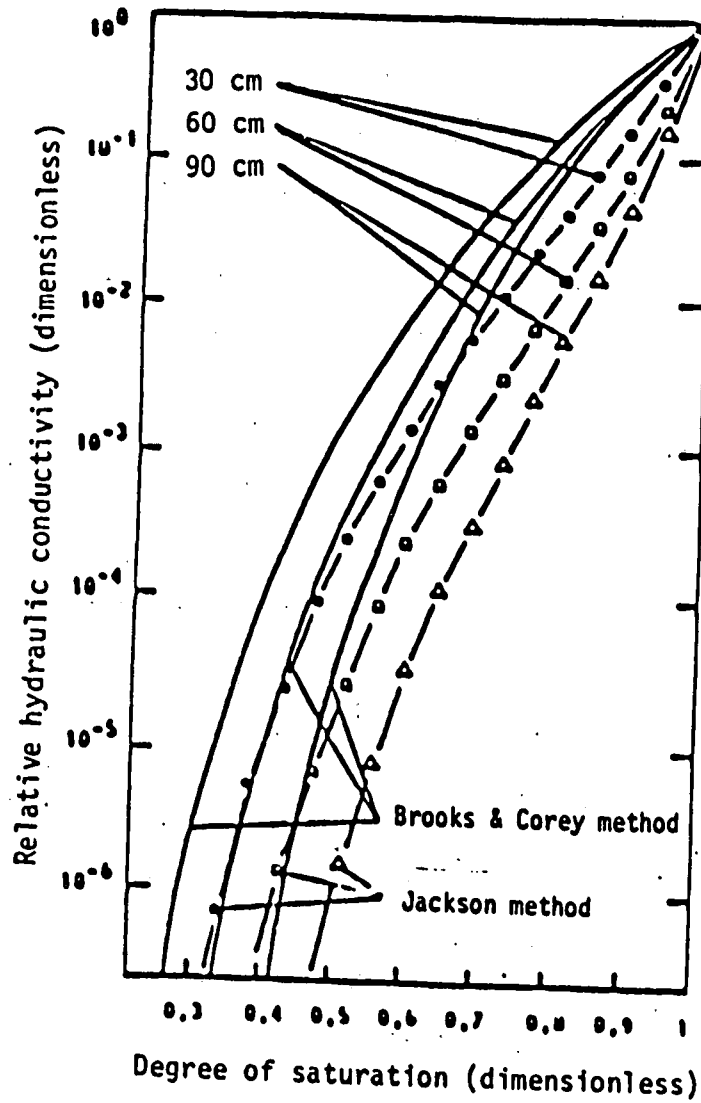


Fig. 12: Relative hydraulic conductivity as a function of the degree of saturation for 30, 60 and 90 cm depth.

Table 11. Details of instrumentation

Instrument	Treatment	Replicates	Inter-row numbers	Depth (if applicable)
Collection cans	A, B, C, D, E	I and III	1, 3, 5, 7, 9, 11, 13, -23 25, 27, 29, 31, 33, 35.	-
Neutron access tubes	C	I and III	As collection cans	0 - 1.50 m
Salinity sensors	A, C, E	I and III	13, 16, 19, 23	0 - 1.50 m
		I	14, 18, 22	0.30m, 0.60 m 0.90 m
Suction cups	A, C, E	I	-----	As sensors -----
Tensiometers	A, B, C, D	I	-----	As sensors -----
4-probe	A, C, E	I	-----	As sensors -----

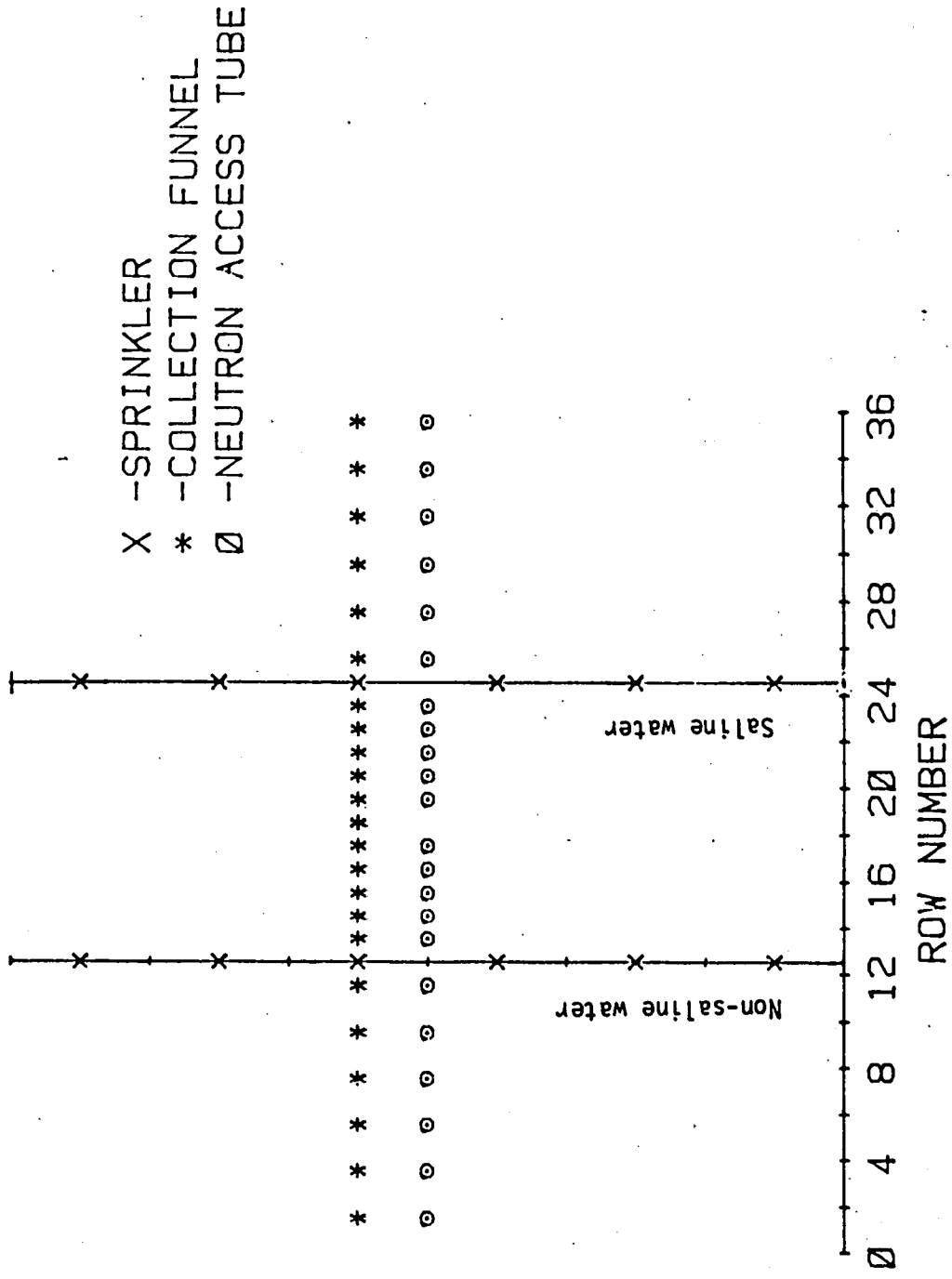


Fig. 14. Layout of instrumentation in a representative plot

August, and 9-12 August, 147 kg N/ha was applied with the irrigation water.

Instrumentation

The field was instrumented to follow water and salt movement in the soil as a function of time. Table 11 summarizes the locations of these instruments and fig.14 shows their relative positions in a representative plot. The neutron probe and four-electrode probe were calibrated using field and laboratory data, and the salinity sensor readings were based on the calibration supplied by the manufacturer. Measurements were made regularly once a week before (neutron probe, tensiometers) or after (salinity sensor, 4-probe, suction cups) irrigation. Soil was sampled in a grid before sowing, five samples being taken in a transect through each replicate. Intermediate soil sampling was done in treatments A, C and E, blocks I and III. Samples were taken after rows 14, 16, 20, 22 and 24 of all three treatments, and after rows 3, 6, 9, 27, 30 and 33 of treatment C. After harvest, samples were taken in row 6 (A - E), rows 12, 14, 16, 18, 20, 22 (A, C and E), and rows 24, 27, 30, 33 and 36 (A, C, E) of blocks I and III. Initial and final samples were taken to a depth of 210 cm.

Plant measurements

Plant height was measured weekly, based on the tip of the youngest emerging leaf before tasseling, and on the tip of the tassel after tasseling. Leaf water potential was measured diurnally from 12 - 3/9 using a pressure chamber. Dry matter production was determined periodically by harvesting a single plant every two weeks in rows 3, 6, 9, 13, 16, 20, 24, 27, 30, 33 and 36 of all treatments and blocks. The final harvest was based on 2-m long sections in all the rows of each plot. Ears (both primary and

secondary) and stover were weight separately. Samples for dry matter and ion concentration (Na and Cl in leaf and stem) were taken in all rows of all plots.

Second year

Sweet corn (zea mays L., cv. Jubilee) was sown on july, 1985, in rows 1 m apart at spacing of 5-7 plants/m on a furrowed surface. the rows were located in exactly the same position as in 1984. The field was uniformly fertilized before sowing with 250 kg N/ha as urea and 50 kg P/ha as superphosphate. During the irrigations on 12, 18 and 25 August and 2 September 108 kg N/ha was applied with the irrigation water.

The lay out of the double line - source system, plant measurments and soil sampling were the same as in the year befor (same treatments in the same locatins).

Third year

After the corn harvest (October, 1985) the field was fertilized with 100 kg N/ha and 800 kg superphosphate/ha, and disced to prepare the seed bed. Wheat (cv H - 945) was sown on wide beds 1.97-m wide beds on November 1985, at a rate of 140 kg/ha using a commercial planter with 15 cm between rows. After sowing, a uniform sprinkling irrigation of 30 mm was given for gemination, using reservior water. Full emergence was recorded on November 24th. After this date, irrigation was applied with the double line -source system, repeating again the same treatments and locations as before. Water distribution was measured in the same way (see next section). Rain gauges were placed in several locations in the field. Rain was also measured with the collecting funnels. Soil water measurments were made

during the season with a neutron probe. Access tubes were inserted on the same locatin and depths as in the years befor.

On 21st December, 1985 plants were removed from 75 - cm sections of each row ,in five treatments of blocks I and III to determine dry matter production. On 21st may 1986, plant were removed from 75 - cm sections of each row, in the middle of each bed, in every treatment and in all three blocks. Plant hieght, dry matter, number of ears, ear weight, number of grains per ear, single ear weight, were determined for all the samples.

The plots ($\approx 20 \text{ m}^2$) were harvested on 3rd june by combine to obtain the grain yield per unit area.

A double line-source sprinkler system for determining the separate and interactive effects of water and salinity on crop growth

The line-source sprinkler technique (Hanks et al., 1976) has gained wide acceptance as a most useful tool in irrigation studies. It provides a water application pattern which is uniform along the length of the plot and continuously, but uniformly variable across the plot. A number of variations have been suggested (Lauer, 1983; Stark, et al., 1982) which make it possible to superimpose different variables (e.g. fertilizer application, leaching) on the water application treatments. In order to determine the yield function for a given crop and the crop's response to water and salinity using the line-source method, a fairly large experimental field is required. Also, there are considerable technical difficulties involved in preparing water of various salinity levels and supplying it to the different sprinkler lines.

To overcome these problems, we used a modification of the line-source sprinkler system, employing two parallel lines - each supplying a uniform amount of water but of different salinity level. The technique produces a wide range of water application amounts in combination with a large gradient in water salinity. It enables one to determine the separate effect of both factors as well as their interaction, while at the same time permitting use of an experimental field of reasonable size. This paragraph describes the design of the double line-source sprinkler system and presents results obtained with its use in these studies.

The layout of the double line-source system is shown in Figure 13. Two irrigation lines were placed 12 m apart in each of 3 replicates. Low-salinity water from a local reservoir (1.35 dS/m) was supplied to one line and high-salinity water from a local well (8.52 dS/m) was supplied to the other. The chemical composition of the irrigation water is presented in Table 12. Consequently, a gradient of water salinity was produced between the two lines, but the quantity applied in this area was uniform. On one side of each line were 12 plant rows which received water in decreasing quantity but of uniform quality, as in the conventional line-source arrangement (Hanks et al., 1976). Along each line, impact-type sprinklers (Na'an 323/91) were spaced at 6-m intervals. These were mounted on 2-m risers with pressure regulators assuring a uniform operating pressure of 200 kPa and a 24-m diameter of coverage. Sprinkler with different nozzle diameters (3.2, 3.5, 4.0, 4.5, and 4.8 mm) were placed in groups of five along each pair of lines to give five different water application rates. Between the two lines these rates were nominally 7.3, 9.7, 11.3, 15.0 and 16.9 mm/hour. The plots receiving these different application rates were designated A, B, C, D, and E, respectively. Plot size was 30 m x 36 m, with 36 rows per plot numbered from 1 to 36, beginning 12 m from the low-salinity line. Surface runoff between plots was prevented by preparing mini-basins 1 m apart along each furrow.

Two uniform irrigations were given for germination (total 40 mm), after which the double line-source was installed (about 15 days after sowing). A serious problem that may result from sprinkler application of saline water to salt-sensitive plants is leaf burn (Maas, 1985). The

FIELD DESIGN OF THE DOUBLE LINE-SOURCE SYSTEM

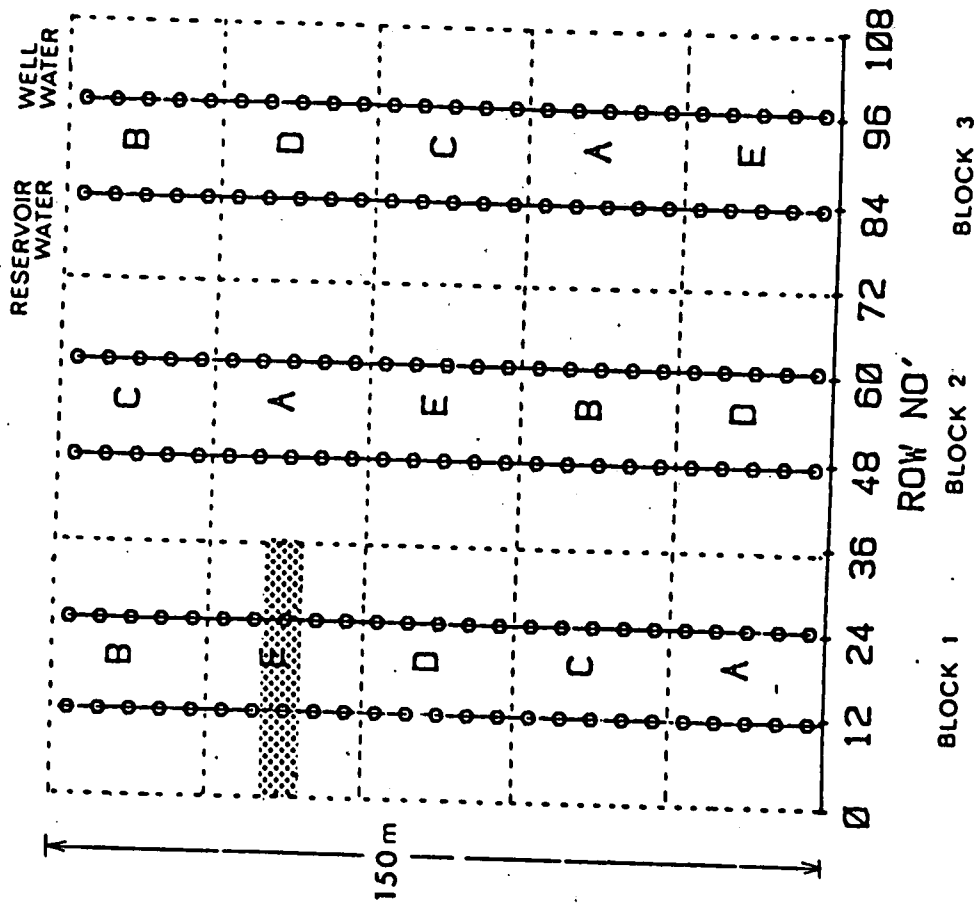


FIG. 13 Diagram of the irrigation system, showing the location of the sprinkler laterals. The broken lines indicate plot borders, and the letters designate rates of water application (see text for explanation). The various water, soil, and plant measurements in each plot were carried out within the shaded area.

Table 12. Composition of water from A) Well B) Reservoir at Kibbutz Reim

Water	pH	EC	Na	me/l		
				Ca + Mg	Cl	SO ₄ + HCO ₃
A. WELL	7.5	8.52	55.0	23.3	58.2	20.1
B. RESERVOIR	7.7	1.35	3.9	6.7	6.8	3.8

damage becomes more severe with increasing salinity level of the water. The irrigations were carried out at night, when wind speed did not exceed 2 m/sec, to guarantee uniform water distribution and to reduce direct evaporation of saline water from the leaves which could cause burning. As a further precaution, reservoir water was injected into the high-salinity sprinkler lines for a 10-min period at the conclusion of each irrigation.

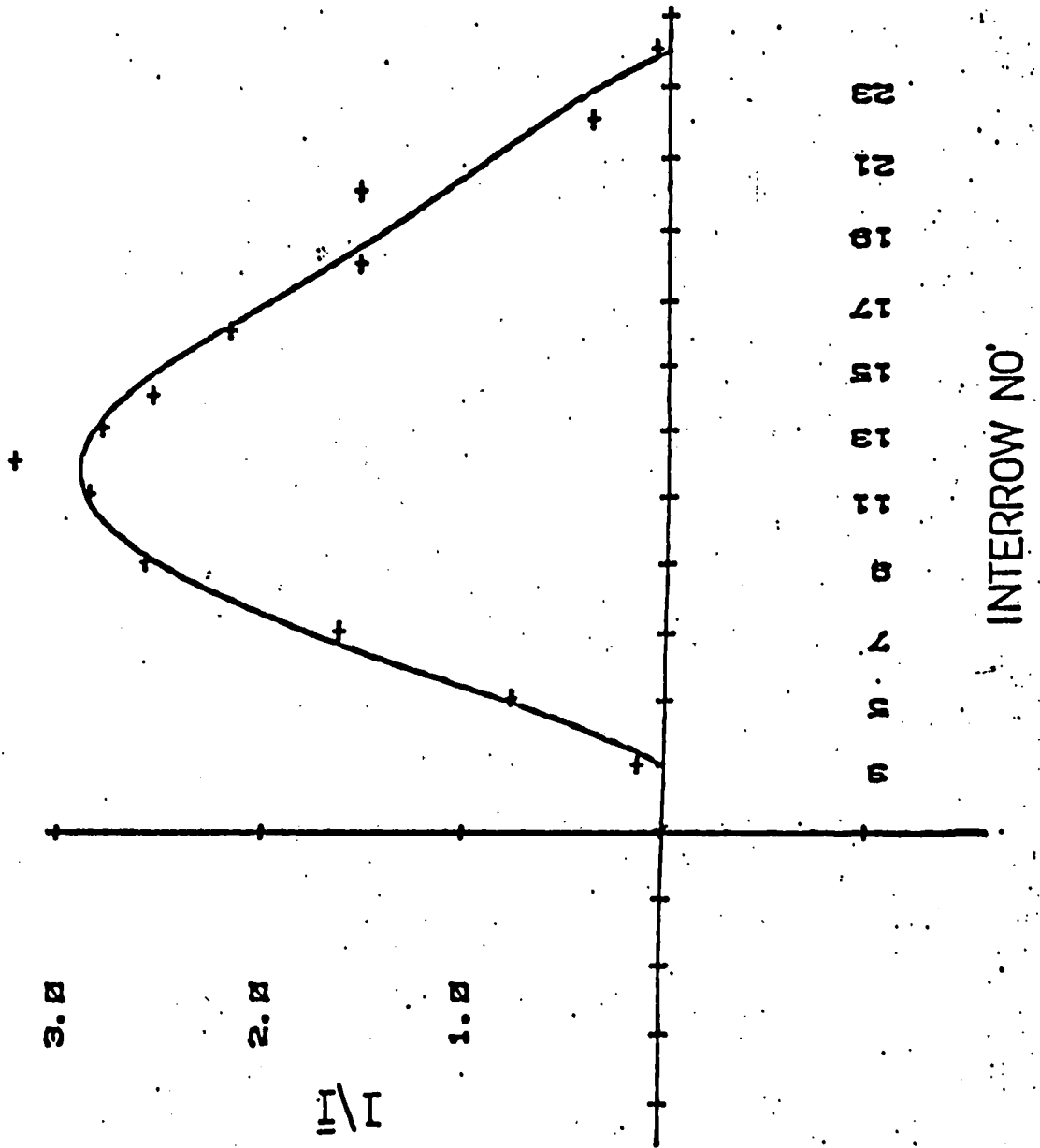
The quantity and quality of the applied water was measured during the growing season by catching the irrigation water in 10-cm diameter plastic funnels mounted on stakes and connected by tubing to collection bottles. The funnels were located at 1-m intervals in rows perpendicular to the sprinkler lines, in the center of all the plots. After each irrigation the water volumes were measured and samples taken to the laboratory for quality analysis. At the head of each sprinkler line was a water meter to measure the total quantity applied of each water type.

Soil water content was measured weekly (before irrigation) with a neutron meter, to a depth of 180 cm in three treatments - A, C, and D - in three blocks and at 2-m intervals from the sprinkler line.

Quantity and salinity of water

Fig. 15 shows the normalized water distribution as a function of distance from the sprinkler line, where I = water quantity (in mm) at each measuring point and I = average water quantity (in mm) applied to the entire experimental plot. There is a linear decrease in water application with distance from the water source. The ratio I/I , for every treatment in relation to the sprinkler type, as measured and as calculated from the

Fig. 15. Water distribution of the double line-source system expressed as the ratio between the water quantity measured at each location (I) and the average quantity of water applied to the entire plot (\bar{I}).



INTERROW NO.

Table 13. Relative irrigation water amount for each sprinkler type.

Sprinkler type	I/\bar{I}	I/\bar{I} Expected*
A	0,59	0,61
B	0,86	0,81
C	0,91	0,94
D	1,17	1,25
E	1,47	1,40

* From manufacturer's specifications

Distance from sprinkler line (m)	I/\bar{I} (24 m)	Standard deviation
1	2,37	0,41
2	2,11	0,30
3	1,82	0,20
4	1,57	0,22
5	1,29	0,23
6	1,07	0,16
7	0,77	0,19
8	0,55	0,14
9	0,34	0,16
10	0,19	0,14
11	0,11	0,09
12	0,03	-

manufacturer's specifications, is given in Table 13. There is very good agreement between the measured and calculated values. The agreement is also expressed in the quality of the water collected between the two overlapping sprinkler lines. Fig. 16 describes the relation between calculated and measured electrical conductivity of the water obtained between the two lines. A similar relation is shown in Fig. 16b for chloride concentration in the water. In both cases the correlation between calculated and measured values was quite high, with only a slight deviation from a slope of 1, indicating optimal mixing of the two water types. The slope deviation is attributed primarily to the effect of wind. The water distribution as a function of distance is described separately in Fig. 11 for each of the two lines (well and reservoir). Due to wind, no reservoir water reached row 2 and no well water was caught in row 1. As a result, the dilution ratio was not uniform over the entire distance between the two lines, and this was responsible for the above-mentioned deviation. The distribution of E_c and SAR in the double line source irrigation system is shown in Fig. 18, and the total amount irrigated along one season is given in Fig. 19.

The pattern of water and salt distribution between the lines was expressed also in the soil. For example, Fig. 20 shows the soil water distribution measured with a neutron probe at 2-m intervals in a direction perpendicular to the sprinkler line. The non-uniform water application accordingly produced a lack of uniformity in soil water content, and this condition continued throughout the growing season. The effect of sprinkler type on soil water content between rows 6-7 at different depths is shown in

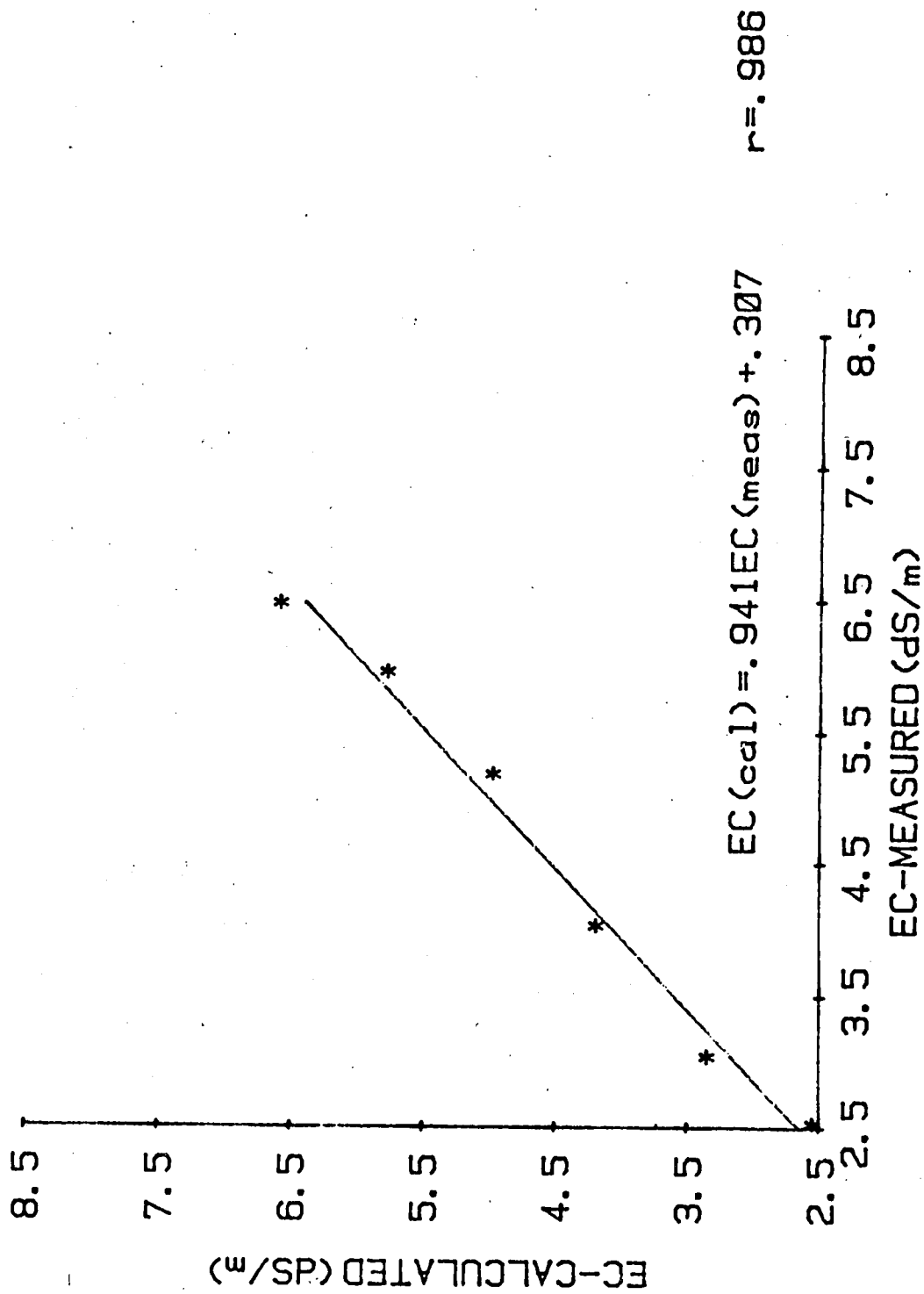


Fig. 16. Relationship between EC_{cal} and EC_{meas} . Means of treatments A,B,C,D, and E. Corn, Reim, 25.8.85.

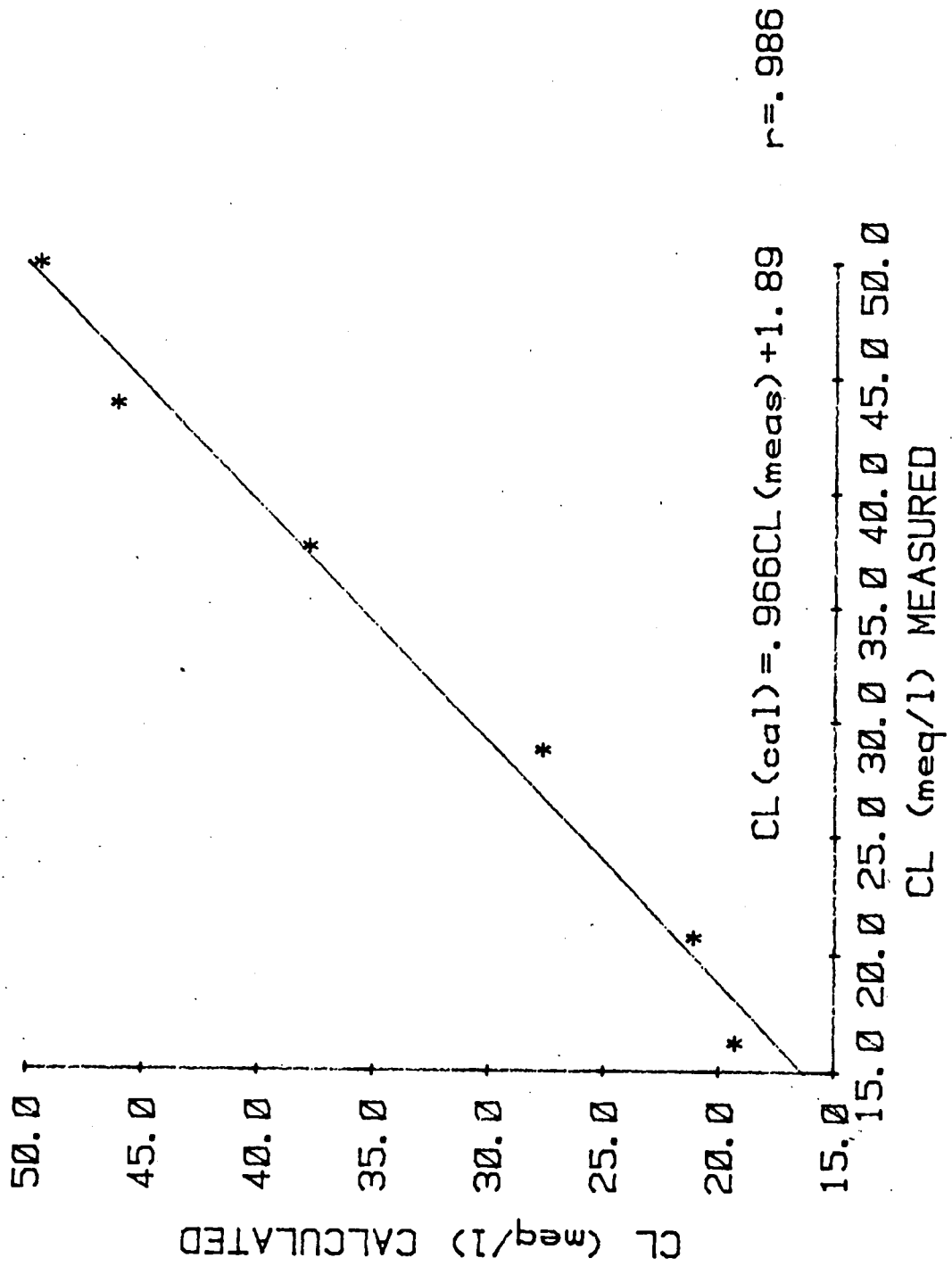


Fig. 16a. Relationship between Cl_{cal} and Cl_{meas} . Means of treatments A,B,C,D, and E. Corn, Reim, 25.8.85.

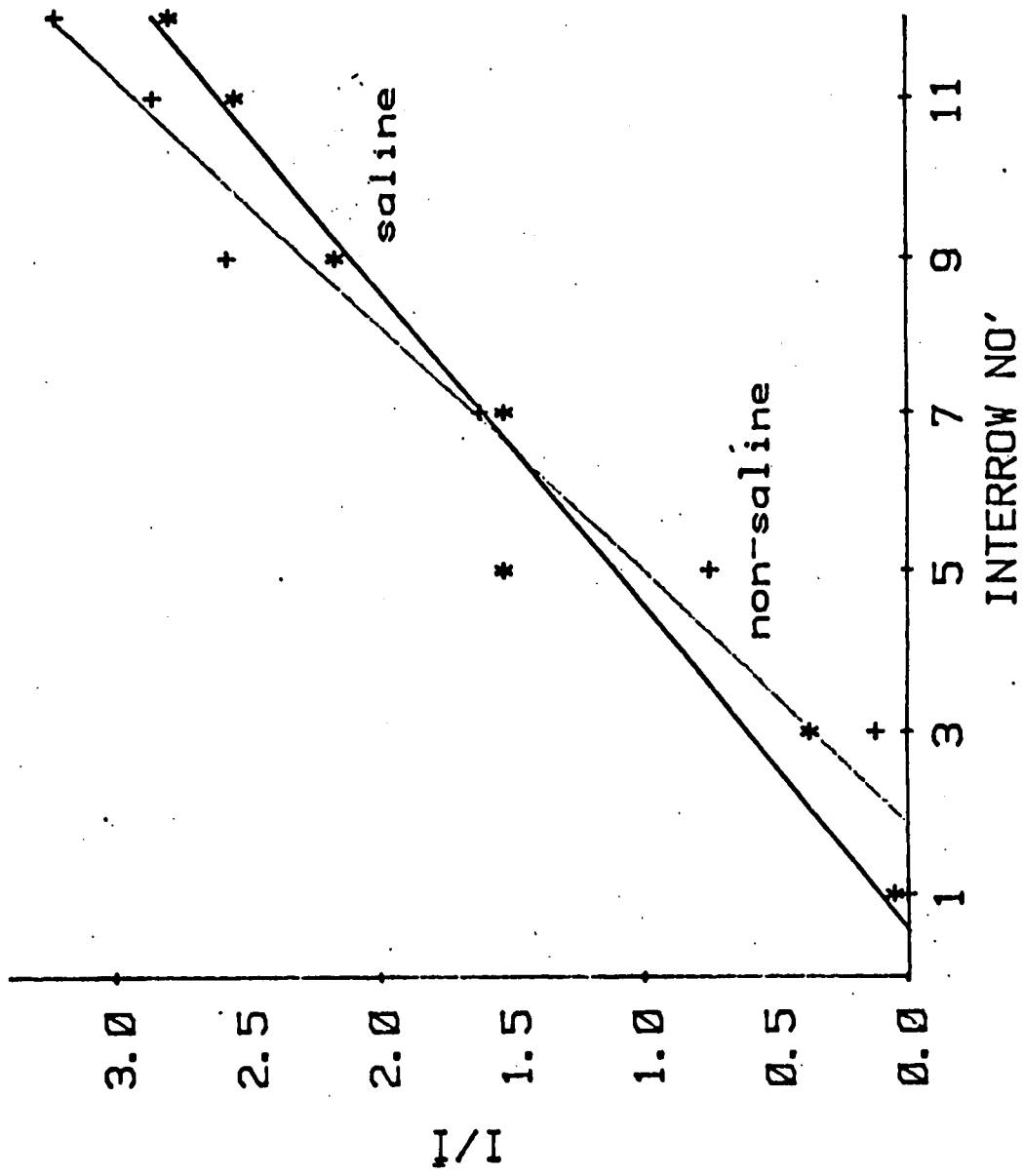


Fig. 17. Relative water distribution as a function of distance from the sprinkler line, for the two types of irrigation water.

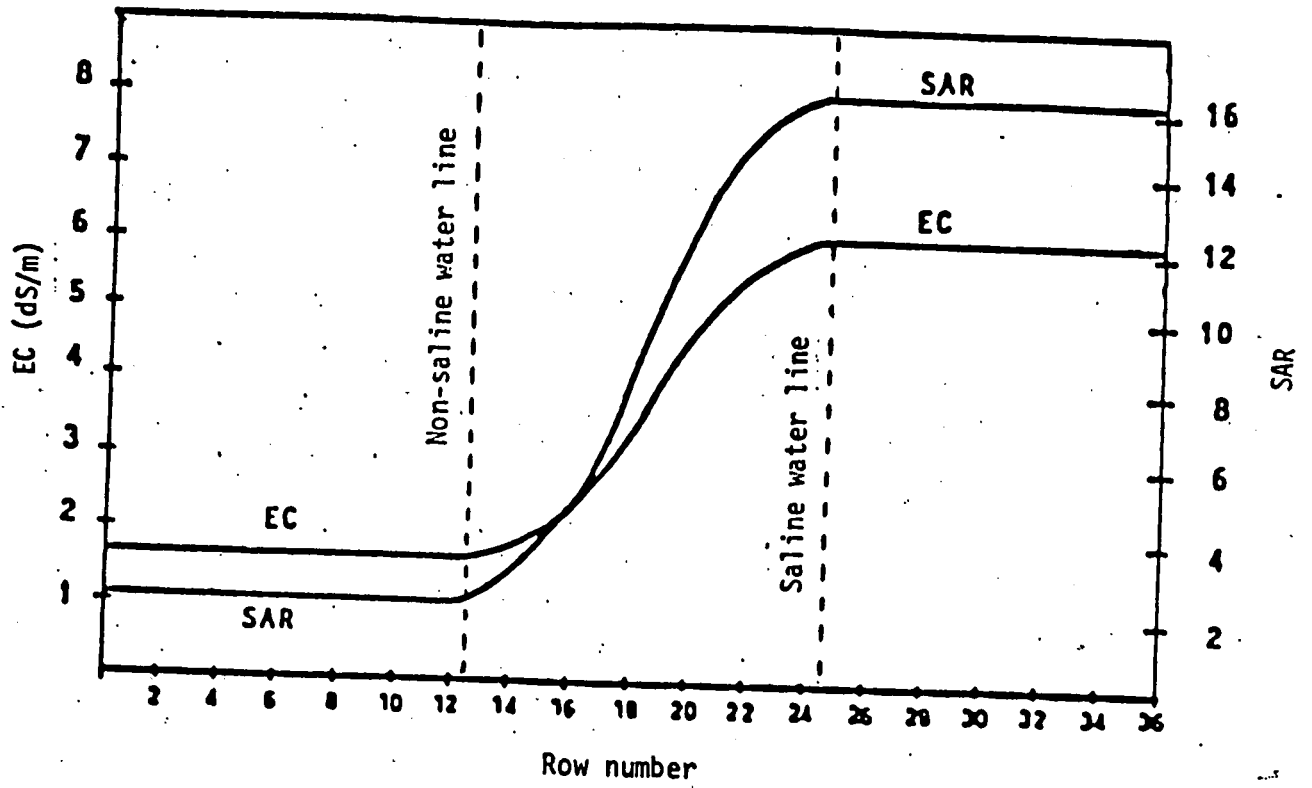


Fig. 18. The distribution of irrigation water salinity (EC) and SAR as a function of row location in relation to the sprinkler lines.

Fig. 19. Sum of irrigation applied over the whole season.

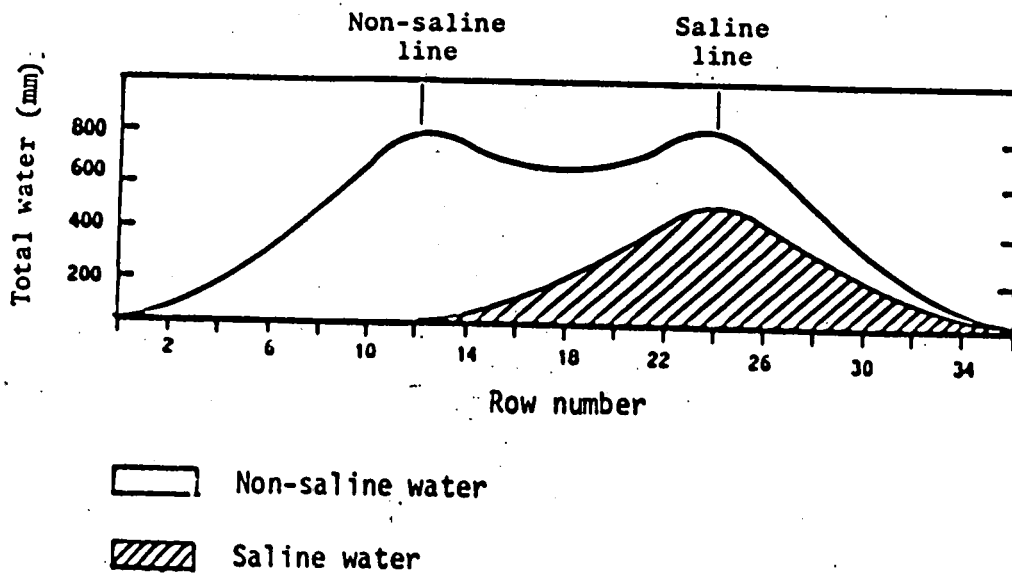


Fig. 20. Soil water content (% by weight) in the 0-30-cm layer as a function of distance from the sprinkler lines at 2 dates after sowing.

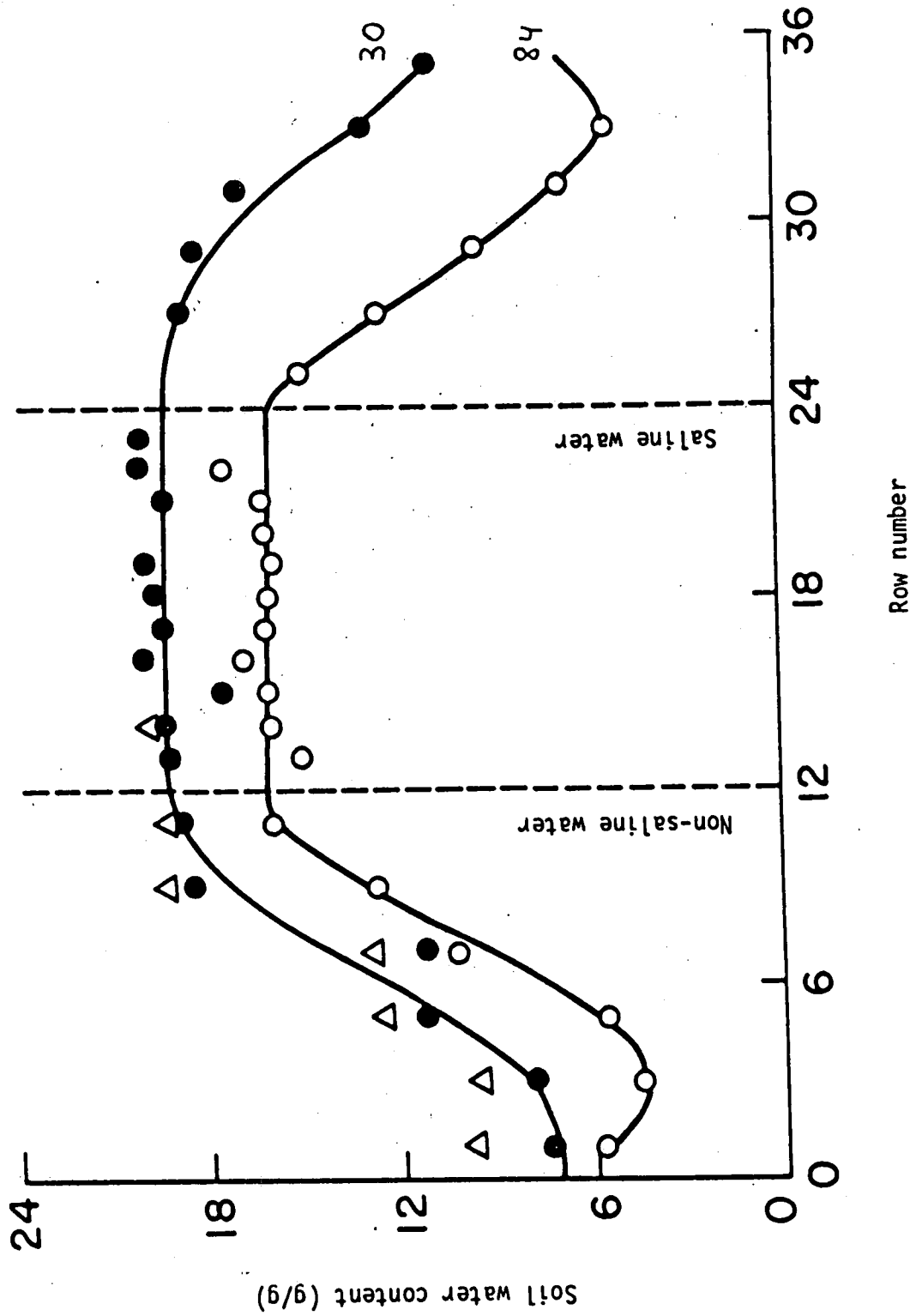


Fig. 21, and this effect was also evident throughout the entire season. In treatment A the rate of water application was low (7.3 mm/hr) while in treatment D it was high (15.0 mm/hr). This difference was expressed in the soil water content throughout the entire profile .

The salt distribution, expressed as the average electrical conductivity at the end of the first growing season in the 0-120-cm soil layer, as a function of distance between the sprinkler lines, is given in Fig. 22. In the vicinity of the low-salinity line (reservoir), the conductivity of a saturated soil paste extract was about 2.0 dS/m, which is 1.5 times greater than the salinity of the irrigation water. Such a ratio is normal in loess soils. Between the two lines the salinity gradually increases from row 12 to row 24. The increase is linear, with a rise of about 0.3 dS/m for each 1-m increment in distance from the low- to the high-salinity line. The maximal salinity level occurs in the two rows adjacent to the high-salinity line. Beyond these rows there is a decrease in soil salinity due to the decreasing quantity of saline water. At a distance of 12 m from the high-salinity line (row 36) the soil salinity is only slightly higher than at an identical distance on the other side of the low-salinity line. The quantity of water reaching these extreme rows is almost nil. The same tendency of salt accumulation is also obtained in respect to the ESP of the soil (Fig. 23) where a linear increase in ESP (mean values of 0-90 cm) was obtained in between the two lines, reaching an ESP of 17.8 near the saline line, compared with SAR 16.1 of the irrigation water.

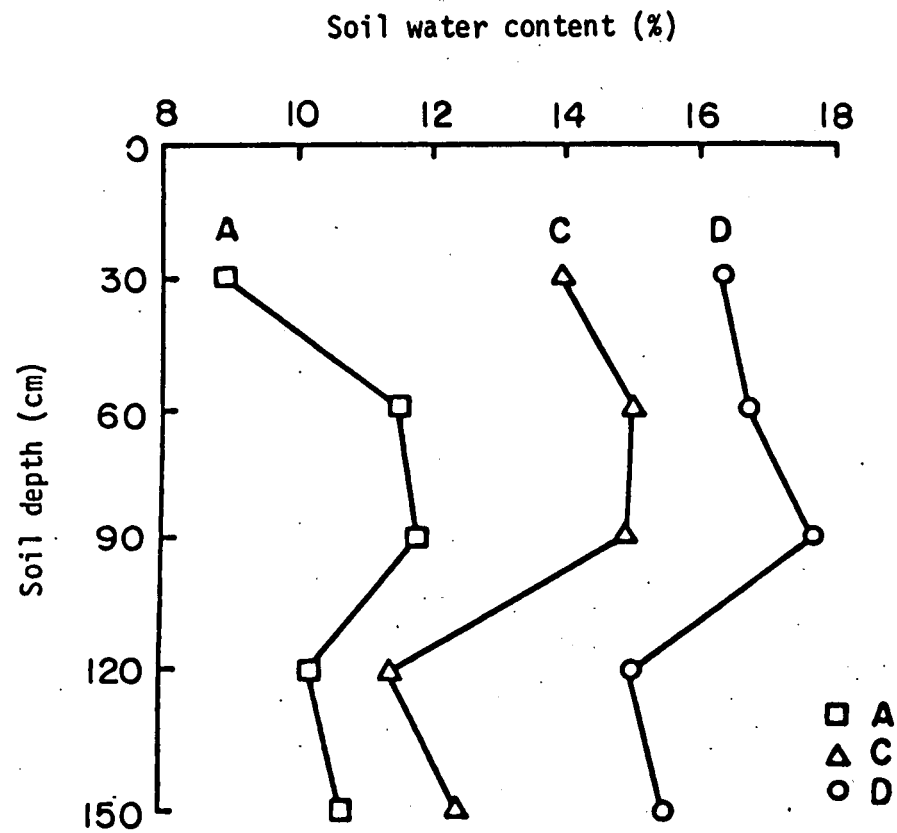


Fig. 21. Effect of sprinkler type on soil water content in row 7.

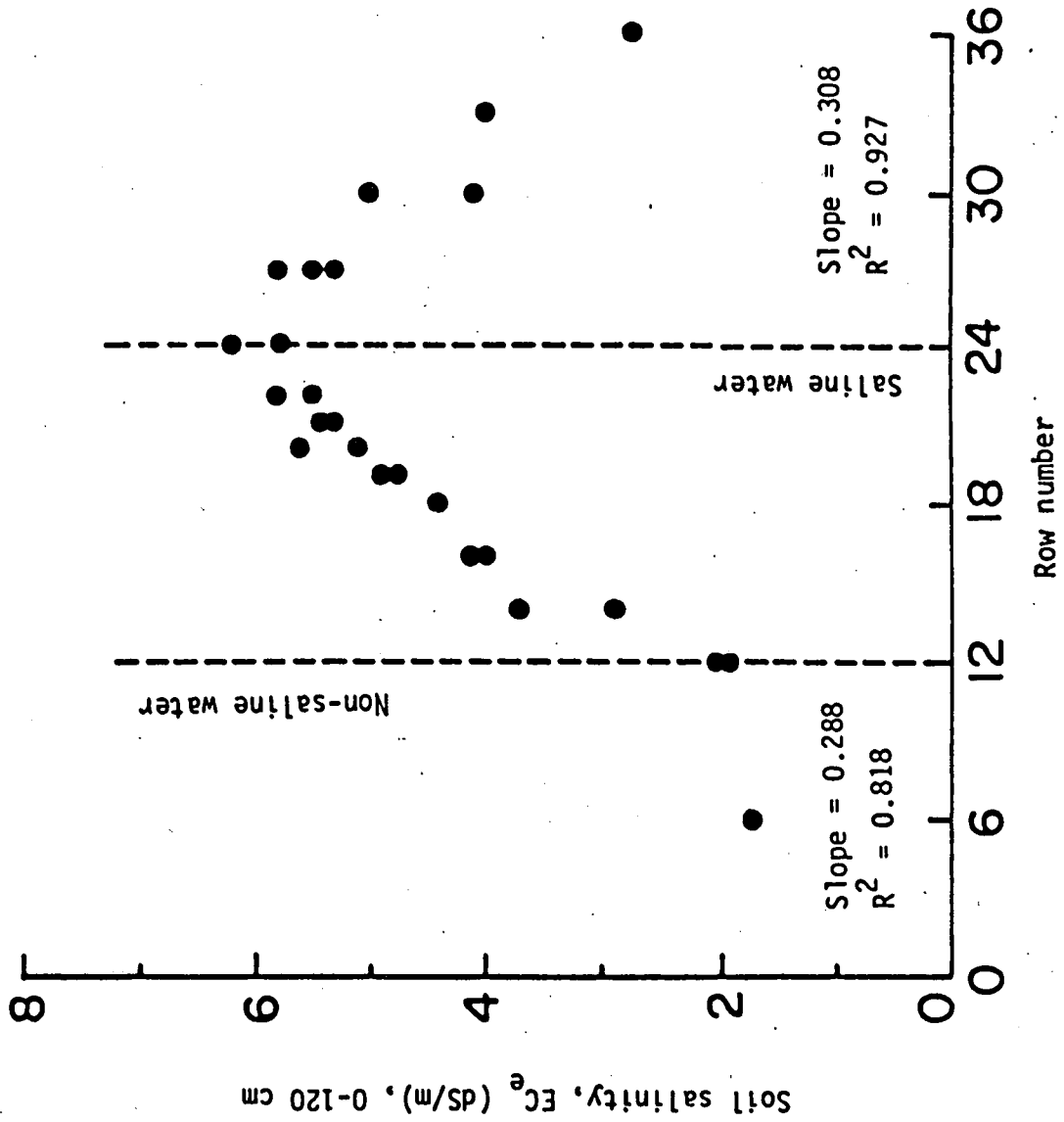


Fig. 22. Soil salinity as a function of distance from the irrigation lines.

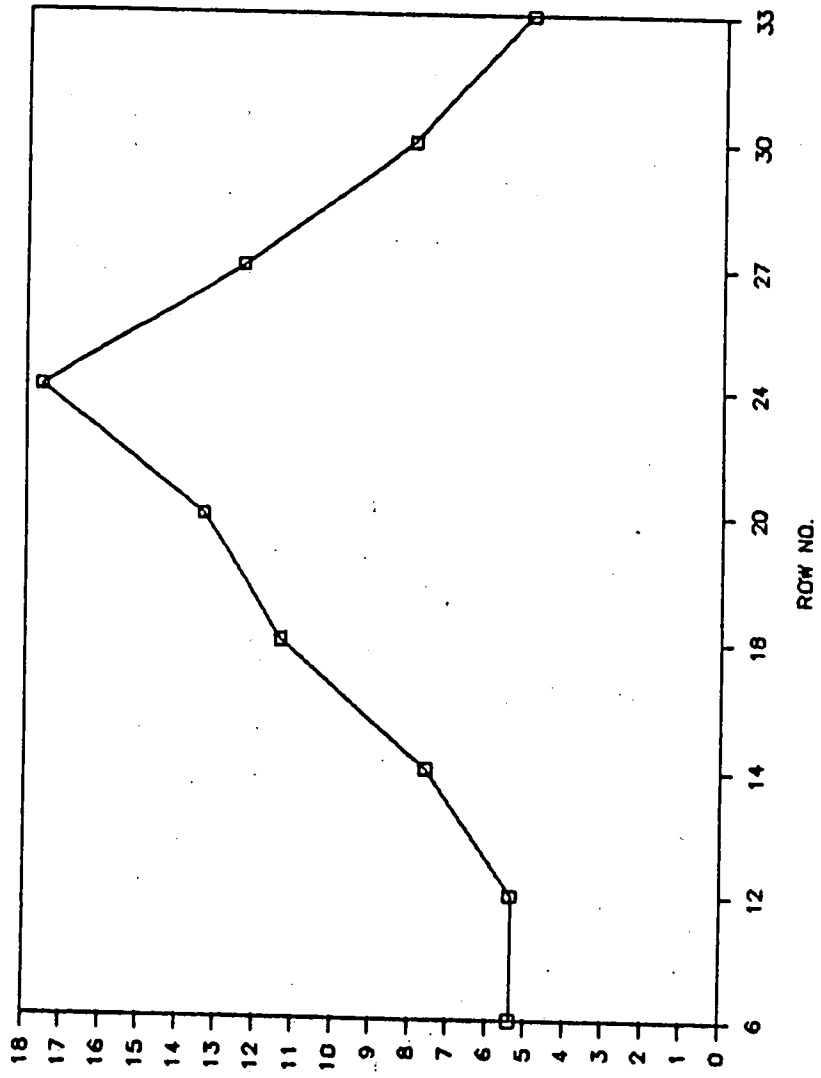


Fig. 23. Mean values of exchangeable sodium percentage (ESP) in the 0-90-cm soil layer as a function of distance.

The average chloride concentration at the end of the first growing season in the 0-120-cm and 0-210-cm layers, minus the concentration in these layers before the beginning of the irrigations, as a function of distance from the sprinkler line (different water amounts and varying salinity) is given in Fig. 24. If we compare the additional chloride found in the 0-120-cm layer with the amount added by the irrigation water the quantities are most similar. On the other hand, the balance in the case of the 0-210-cm layer is not good: the chloride content is much greater than that added by the water, and the standard deviation of the measurement is high. This phenomenon is due to the high initial variability in chloride content in the 120-210-cm layer which is apparently the region where chlorides were deposited during many previous years of irrigation with good quality water from the National Water Carrier. The irrigation treatments reduced the variability in the upper 120 cm so that the agreement was quite good.

As with electrical conductivity, the chloride content also increased from row 12 to row 24, and the salinity reaches a maximum in row 24 (beside the high-salinity line). With increasing distance from the high-salinity line towards row 36 (in the region where the irrigation water is of uniformly high salinity, the chloride content decreases since the quantity of water applied decreases. The increase and decrease in chloride content can be described as linear, and is consistent with the change in quantity of water as a function of distance from the lines.

The contents of chloride and sodium in the corn leaves at the end of the first growing season are shown in Fig. 25. The data are averages of

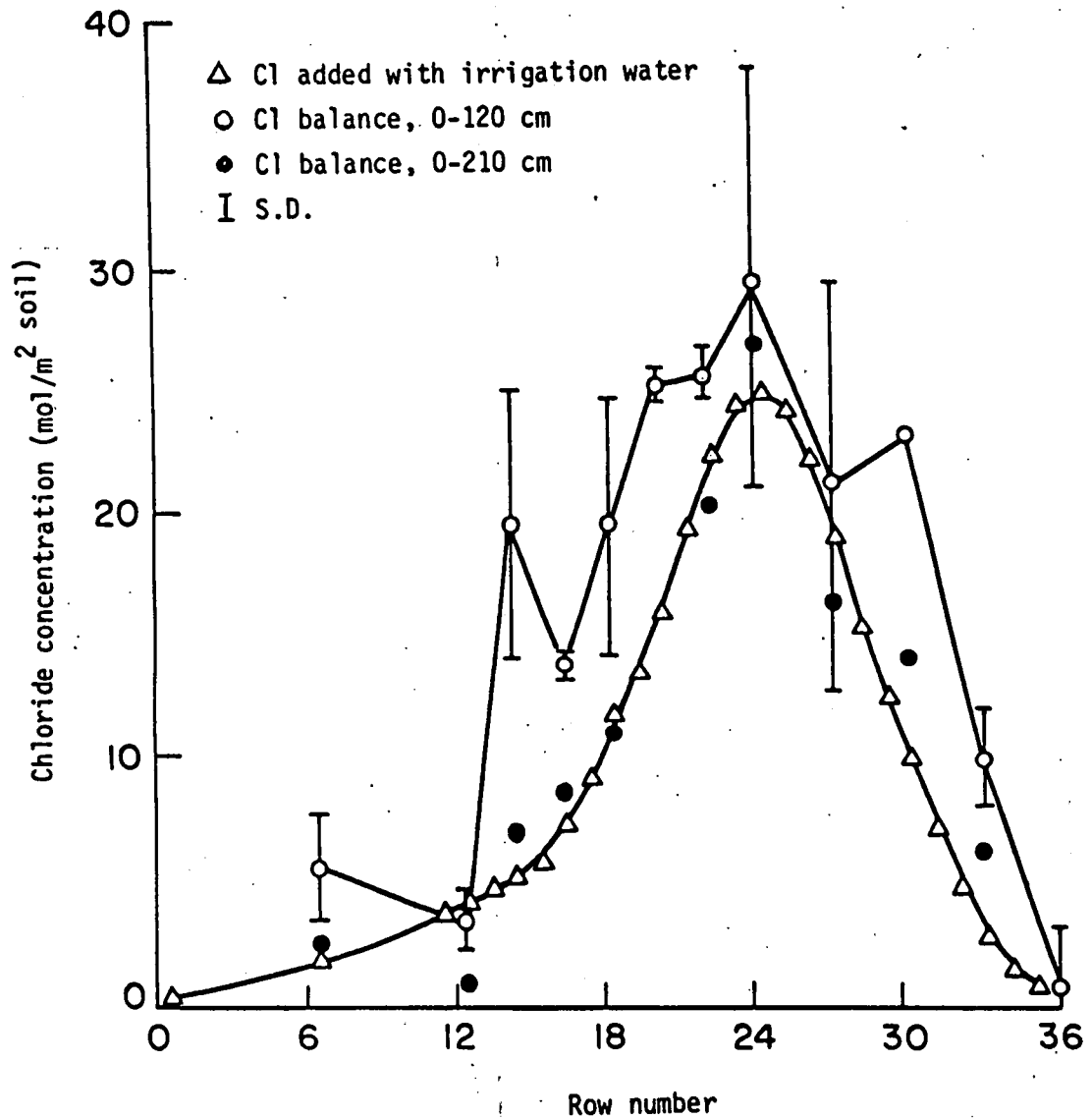


Fig. 24. Amount of chloride in the soil at the end of the experiment, minus the amount of chloride at the beginning of the experiment, as a function of distance from the sprinkler lines and compared with the amount added by the irrigation water.

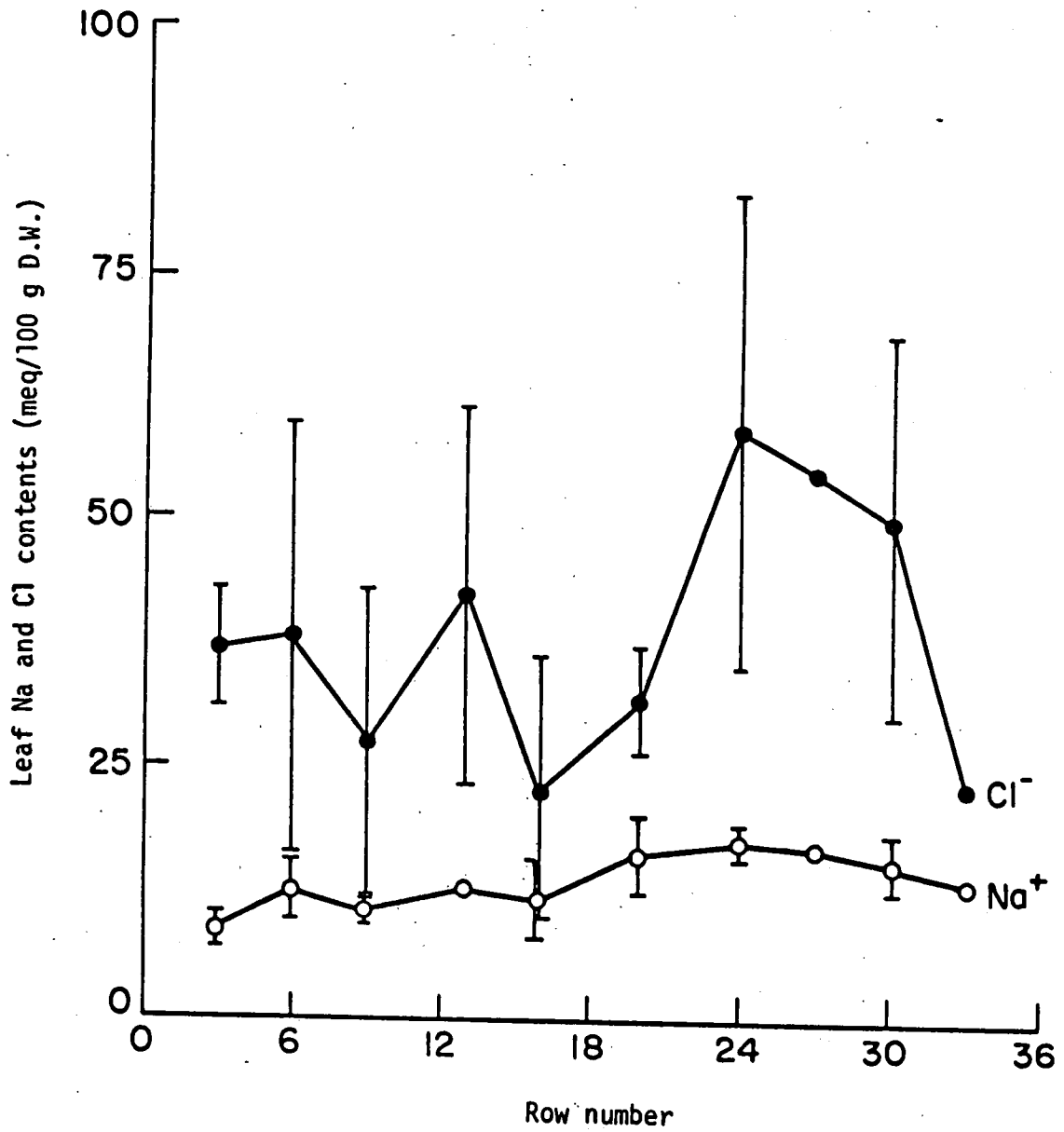


Fig. 25. Chloride and sodium content in the corn leaves at the end of the season. Means of AI-EI.

the high and low water treatments, each from two replications. There was no specific effect of irrigation with saline water on the leaves, and the brief "washing" of the leaves at the end of each irrigation was sufficient to prevent any specific effect. The pattern of sodium and chloride contents in the leaves was similar to that of the soil salinity or the concentration of chloride in the soil solution, and to that of the irrigation water salinity, in terms of distance from the sprinkler lines. The sodium content of the leaves until row 12 (beside the low-salinity line) was constant, with a low standard deviation. Beyond row 12 the content increased, followed by a tendency to decrease beyond row 24 whereupon the quantity of applied high-salinity water gradually decreased. Leaf chloride content behaved similarly, but the absolute content was considerably greater than that of the sodium, and the standard deviation was higher.

The field water balance!

THE water balance is a summary of all gains, losses and changes of storage of water occurring in a given field. Gains of water are due to precipitation or irrigation. Losses include surface runoff, deep percolation below the root zone (drainage), evaporation and transpiration. The total change in storage must equal the difference between the sum of all gains and the sum of all losses. Accordingly we can write the water balance eq(18)

$$P+I-(R+D+E+T)= \Delta S+ \Delta V \quad (18)$$

where

P-precipitation, I-irrigation, R-runoff, D-drainage, E-evaporation, T-transpirat

ion, ΔS -the change in soil water storage and ΔV the change in plant water content.

For the two corn experiments $P=0$ and $R=0$ (The crops were grown during the summer, and we used a tillage practice-dense basin technique-which prevents runoff). V may be assumed to be insignificant in regard to the other terms. Therefore,

$$ET+D=I+\Delta S \quad (19)$$

I and S were measured (see field management), therefore, ET can be determined if D is known.

Drainage volume was calculated by several methods:

I-"Field capacity"-when irrigation or rain occurs, the top soil layer is filled to field capacity first. If there is any excess, the next layer is filled, etc. When the water applied exceeds the amount required to raise the root zone to field capacity, the difference is regarded as drainage.

$$D=I-(W_{fci}-W_i) \quad (20)$$

where D -drainage, I -irrigation, W_{fci} -mean water amount at field capacity to a specified depth (depending on the depth of the root zone, which changes with time) and W_i -amount of water in the soil to depth i . If $I < (W_{fci}-W_i)$ then $D=0$

II-Drainage was also calculated by using the concepts of Davidson, et al (1969) and of Nielsen, et al (1973). The calculation is based on the assumption that the change in soil water content or pressure with soil depth for vertical drainage will be small and will approach zero in a uniform soil profile without appreciable error. Under these conditions, water will drain almost equally from all depths under a unit hydraulic gradient.

The rate of change in soil water content, θ , within a soil profile of length L is approximately

$$\frac{d\theta}{dt} = -\frac{K}{L} \quad (21)$$

where t -time. Eq(21) can be integrated to express the average profile water content with time when a numerical relationship between K and θ which has been commonly used is

$$K = K_s \exp[a(\theta - \theta_s)] \quad (22)$$

where a is a constant.

Substituting and integrating eq(22) from $t=0$ to t , and from $\theta_s - \theta$ yields

$$\theta = \theta_s - \frac{1}{a} \ln(1 + aK_s t/L) \quad (23)$$

Differentiating this eq with respect to t and multiplying by the soil profile depth, L gives the magnitude of the soil water flux at the depth $t=L$.

$$q_L = K_s / (1 + aK_s t/L) \quad (24) \text{ In order to}$$

calculate the constant a or $\theta(t)$ and $q_L(t)$ function we used the following procedure of Brooks and Corey and the $\theta(t)$ method.

$$\theta = (\theta_s - \theta_r) (1 - K_s/L((1-\eta)t))^{(1/(1-\eta))} + \theta_r \quad (24)$$

$$q_L = -K_s/L(\theta_s - \theta_r) ((1 - K_s/L(1-\eta)t)^\eta)^{(1-\eta)} \quad (25)$$

With the assumption that the volume of drainage is not affected by ET, it is possible to calculate it.

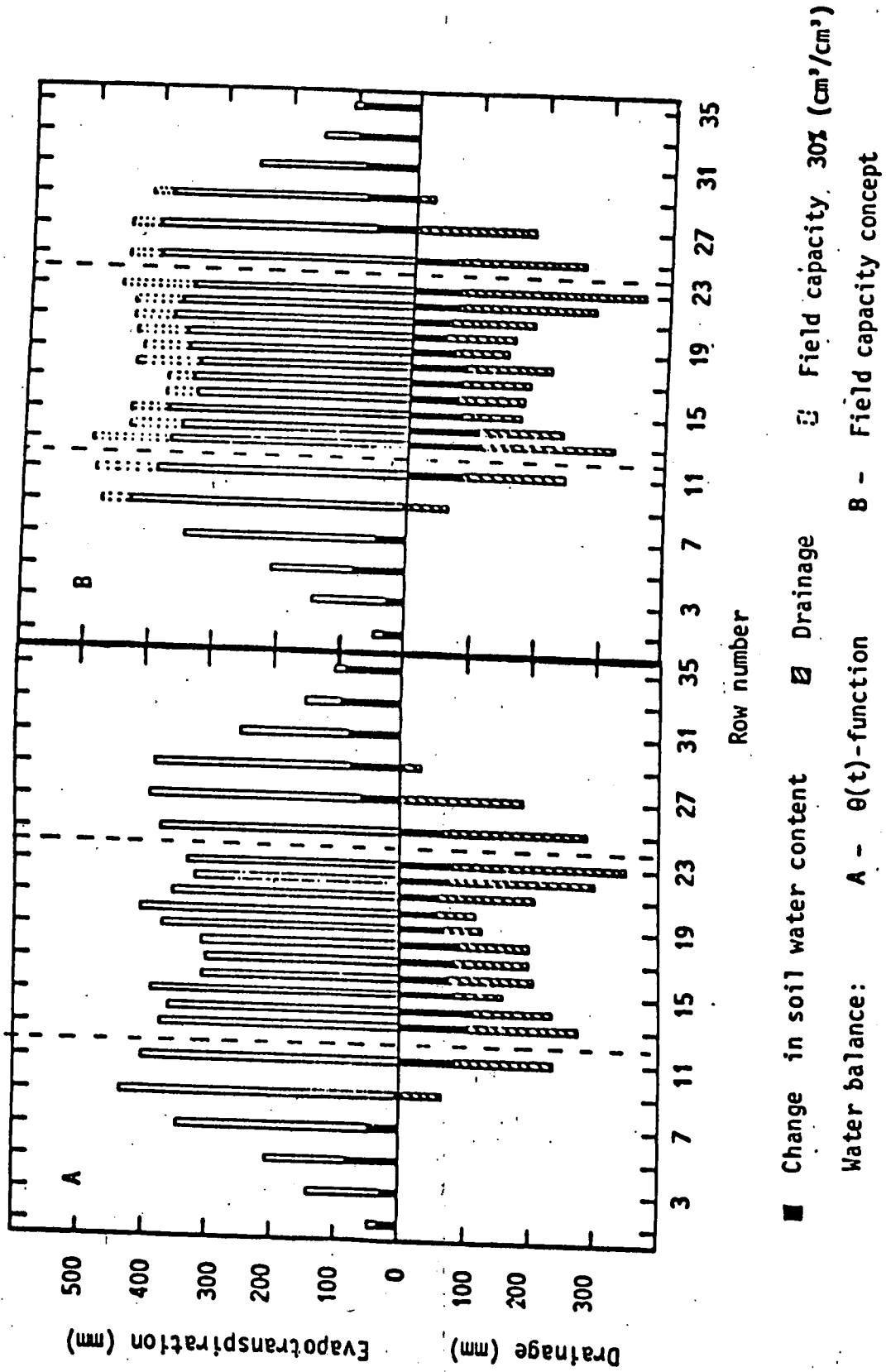
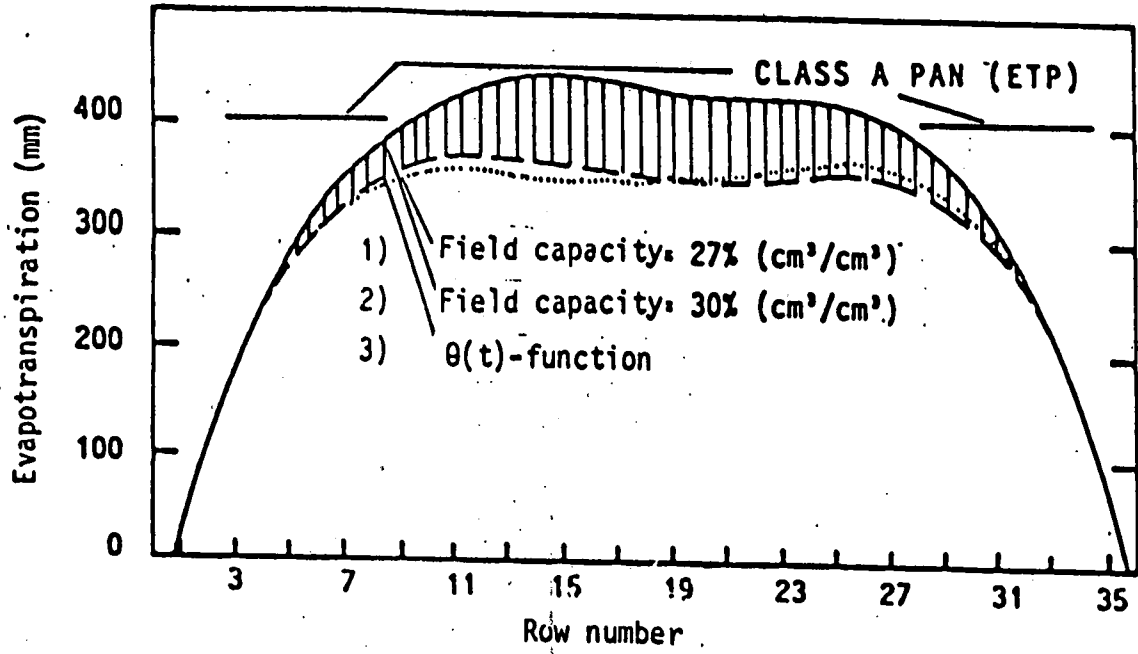


Fig. 26. Soil water balance as a function of row number calculated by field capacity method and $\theta(t)$ -function.



$$\begin{aligned}
 1) ET &= -92,2 + 120,7R - 11,3R^2 + 0,44R^3 - 10^{-3}R^4 + 4,4 \cdot 10^{-5}R^5 & r^2 &= 0,045 \\
 2) ET &= -82,6 + 106,5R - 7,1R^2 + 0,21R^3 - 4,9 \cdot 10^{-4}R^4 - 4,6 \cdot 10^{-5}R^5 & r^2 &= 0,893 \\
 3) ET &= -78,6 + 109,1R - 9,0R^2 + 0,28R^3 - 1,7 \cdot 10^{-3}R^4 - 4,1 \cdot 10^{-5}R^5 & r^2 &= 0,854
 \end{aligned}$$

Fig. 27

Polynomial of evapotranspiration as a function of row number.

Table 14. Water balance and evapotranspiration calculations for Treatments DI and DIII.

R	I	S	ET*	D**	ET*	D**	ET*	D**	Treat- ment
(1)	(2)	(3)	(4)		(5)		(6)		
14	781,9	107,2	304,5	370,2	494,3	180,4	424,5	249,9	D I
17	635,5	103,1	315,7	216,7	451,3	81,1	365,9	166,6	
20	674,7	98,9	276,5	299,3	460,7	115,1	307,9	268,0	
23	879,3	99,4	347,5	432,4	541,5	238,3	431,3	348,2	
14	791,9	102,2	381,3	300,4	495,6	186,1	425,8	256,0	D III
17	635,5	65,0	357,0	213,5	457,5	143,2	350,9	219,4	
20	674,7	76,6	252,9	345,2	453,9	196,3	259,5	338,7	
23	879,3	67,1	342,0	470,2	489,9	323,9	357,5	454,6	

- (1) Row number
- (2) Irrigation, I (mm)
- (3) Changes in water content to a depth of 150 cm during the season, calculated from the weekly water balance by
$$S = \sum_{n=1}^{n=10} (W_n - W_{n+1})$$
 where w = water content in mm (0-150 cm) and n = irrigation number.
- (4) ET and D (FC = 27% in Treatments CI, CIII, DI, and 33% in DIII)
- (5) ET and D (FC = 30% in Treatments CI, CIII, DI, and 33% in DIII)
- (6) ET and D calculated with the $\theta(t)$ -function
- * Evapotranspiration (mm)
- ** Drainage (mm)

Table 14a. Water balance and evapotranspiration calculations
for Treatments CI and CIII.

R	I	S	ET*	D**	ET*	D**	ET*	D**
(1)	(2)	(3)	(4)		(5)		(6)	
1	14,0	- 31,9	51,4	0,0	51,4	0,0	51,4	0,0
3	53,3	- 25,7	147,8	0,0	147,8	0,0	147,8	0,0
5	162,7	- 80,3	213,1	0,0	213,1	0,0	213,1	0,0
9	496,7	- 4,1	434,3	66,5	480,2	20,5	437,2	63,4
11	642,6	83,2	390,3	169,0	487,8	71,5	402,8	156,6
13	657,1	105,6	397,1	211,6	492,0	116,7	375,0	174,9
14	604,5	108,1	351,7	153,2	435,1	69,8	364,0	127,7
15	551,9	79,9	379,4	290,6	435,2	36,3	392,8	79,0
16	512,4	72,9	335,3	101,3	381,0	58,6	309,1	132,2
17	491,3	79,5	343,0	109,2	377,8	74,4	304,7	107,1
18	502,8	82,3	316,0	133,3	426,0	50,6	309,5	110,9
19	497,1	63,8	349,4	83,9	419,9	23,4	374,7	58,6
20	521,6	50,1	352,1	119,5	428,2	43,4	410,8	60,8
21	567,9	53,0	377,3	137,6	435,9	78,9	359,0	155,9
22	623,8	70,4	360,4	212,5	436,6	136,3	321,1	232,7
23	679,8	70,0	345,8	286,9	454,1	178,6	334,3	275,4
25	665,7	65,8	405,5	200,2	445,2	160,5	375,2	224,8
27	514,6	- 69,6	403,0	181,3	448,9	136,2	396,4	187,8
29	334,3	- 79,5	387,1	26,7	413,8	0,0	380,3	33,5
31	168,6	- 82,8	251,4	0,0	251,4	0,0	251,4	0,0
33	55,2	- 97,7	152,9	0,0	152,9	0,0	152,9	0,0
35	14,5	- 93,6	108,1	0,0	108,1	0,0	108,1	0,0

CI

R	I	S	ET*	D**	ET*	D**	ET*	D**
(1)	(2)	(3)	(4)		(5)		(6)	
1	14,0	- 76,2	112,8	0,0	112,8	0,0	112,8	0,0
3	53,3	- 53,8	107,1	0,0	107,1	0,0	107,1	0,0
5	162,7	- 65,4	228,2	0,0	228,2	0,0	228,2	0,0
7	322,7	- 72,9	395,6	0,0	395,6	0,0	395,6	0,0
9	496,7	- 41,0	472,8	64,8	530,0	7,6	518,7	18,9
11	642,6	99,4	392,8	150,4	482,2	61,0	474,0	69,2
13	657,1	123,4	375,3	158,5	487,2	46,6	477,1	56,5
14	604,5	82,4	409,9	112,2	491,3	30,8	476,8	45,3
15	551,9	75,3	422,5	54,0	476,5	0,0	462,2	14,4
16	512,4	60,0	386,7	65,8	448,7	3,8	423,7	28,7
17	491,3	90,7	340,3	60,3	400,6	0,0	374,3	26,6
18	502,8	61,2	365,7	72,9	438,6	0,0	424,7	13,7
19	497,1	82,4	322,7	92,0	414,7	0,0	377,7	36,6
20	521,6	90,3	303,4	128,0	374,6	68,2	375,4	55,8
21	567,9	93,2	336,2	130,5	415,0	70,0	416,3	58,4
22	623,8	105,2	261,0	257,7	461,5	119,1	349,9	170,9
23	679,8	96,0	241,3	342,4	435,5	148,2	356,9	224,8
25	665,7	108,5	291,8	265,5	429,8	12,8	376,6	180,2
27	514,6	- 21,5	389,6	146,5	449,7	86,4	423,5	112,6
29	334,3	- 45,1	318,4	61,0	376,0	3,0	373,0	6,4
31	168,6	- 62,9	231,5	0,0	231,5	0,0	231,5	0,0
33	55,2	- 37,7	92,9	0,0	92,9	0,0	92,9	0,0
35	14,5	- 17,4	31,9	0,0	31,9	0,0	31,9	0,0

CIII

In the preceding paragraph, we dealt with the water balance calculations. According to the procedures described we calculated I, S, ET and D. The results are summarized in Table 14. Fig 26 also, shows the various parameters calculated by these procedures.

Both the "field capacity" and the $\theta(t)$ methods show the same trend for ET and D and the results are very similar. It is also clear that in rows 1-9 and 27-35 water is depleted from the soil during the growing season. ET is greater for the non-saline side compared with the saline side. ET_{max} appears in the rows beside the sprinkler lines. In order to see if ET values calculated are in accordance with the water application (Fig-19) a 5th-order polynomial regression analysis was carried out on ET as a function of row number (Fig.27) (irrigation and salinity). Curve 1 was calculated using the "field capacity" method, using $FC=27\%(\text{cm}^3/\text{cm}^3)$; curve 2 is the same as curve 1 but $FC=30\%(\text{cm}^3/\text{cm}^3)$ and for curve 3 ET was calculated using the $\theta(t)$ function. From this figure it is clear that ET_{max} appears in the row close to the sprinkler line on the non -saline side. However drainage volume is larger on the saline side.

Drainage depth was related to the depth of irrigation water and to water quality (Table 14 and Fig 26). For illustration one may compare the depth of drainage water in the C and D treatments. It is evident that the depth of drainage water is significantly higher in treatment D. The reason is that $ET_p = ET_{max}$ near the sprinkler line in treatment C, and because treatment D received a greater amount of irrigation water (if we take treatment C to equal 1, then treatment D received on the average ≈ 1.2 times more water)

In Fig.28 where ET was calculated for rows 1-14 (fresh water) and for rows 22-35 (saline water) ET was related to I-ΔS assuming

$$ET = I - \Delta S \quad ; D=0 \quad (27)$$

It is clear from this Figure that ET increases linearly with available water independent of water salinity, and only at high amounts of water is there a difference between the saline and fresh water.

For example, the mean ET for treatment C rows 9-17 = 437mm ±49.3, whereas in rows 23-29 mean ET = 372mm ±32.7. The reduction in ET is a function of the different soil salinity e.g row 13 (C) $EC_e = 2.6$ dS/m whereas in row 23(C) $EC_e = 3.8$ dS/m. After the last irrigation the water content in those rows was 16 and 18.4%(g/g) respectively. ET calculated for treatment-C- for the different rows by the $\theta(t)$ procedure, as a function of time from sowing is given in Fig,29. Also given are the Class A pan values (Table 15) and Class A pan evaporation times the crop factor used. In rows 7,9 and 11 ET was similar to the crop factor times E_{pan} throughout the season, whereas rows 1,3 and 5 were much below.

Another comparison of ET obtained in the experiment can be made by using the work of Hillel and Guron (1973). They determined cumulative ET of corn grown in 1966-1970 at the Gilat farm. Since the conditions of both places, Gilat and Reim, are similar, we compared the ET at these locations. The results of Hillel and Guron are presented in Fig 30. In all cases ET_{max} in their experiment was between 64-75% of E_{pan} . If we use this value, then at Reim ET will be between 380-410 mm. This corresponds very well with ET calculated by the methods using $FC = 27\% (cm^3/cm^3)$ and the $\theta(t)$ function (Fig.27).

Table 15. Class A pan.

Days after sowing	Ep* mm/d	\sum Ep** mm
1 - 18	7,00	126,0
19 - 25	7,33	177,3
26 - 32	6,78	224,8
33 - 39	7,55	277,6
40 - 46	6,65	324,2
47 - 53	6,85	372,3
54 - 60	6,73	419,3
61 - 67	6,61	465,5
68 - 74	6,34	509,9
75 - 81	5,97	551,7
82 - 88	5,96	593,4
89 - 95	5,50	631,9
96 - 99	4,43	649,7

* Mean daily pan evaporation

** Total evaporation

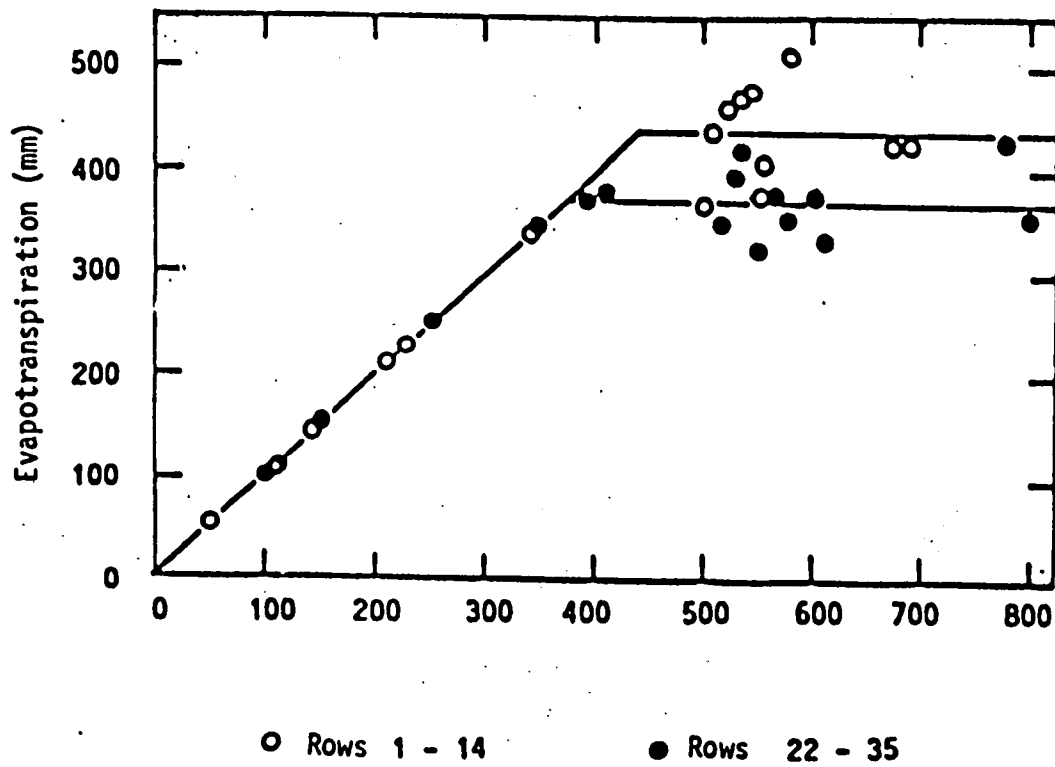


Fig. 28

Irrigation - S (changes in soil water content)

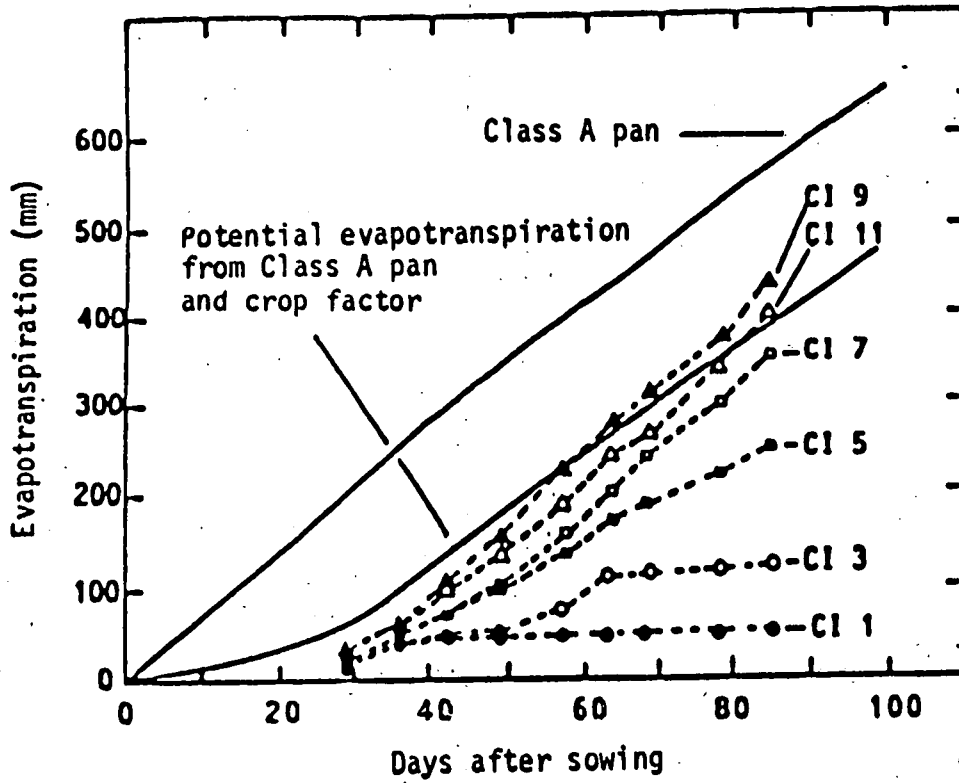


Fig. 29

Cumulative evapotranspiration in Treatment CI as a function of row number and days after sowing.

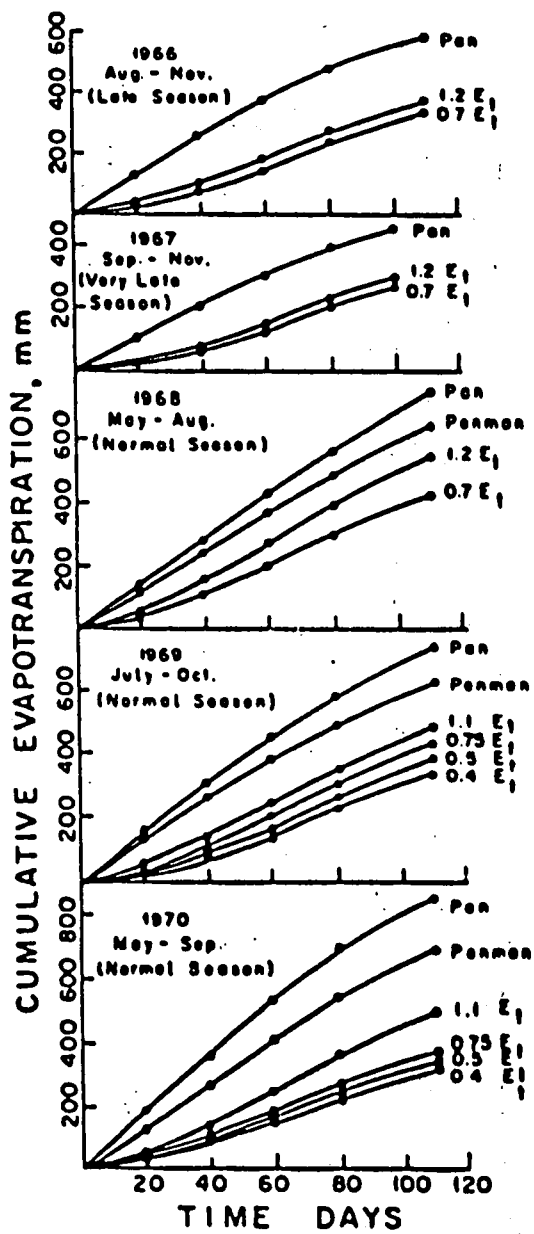


Fig. 30

Evapotranspiration for five years of corn (Hillel and Guron, 1973).

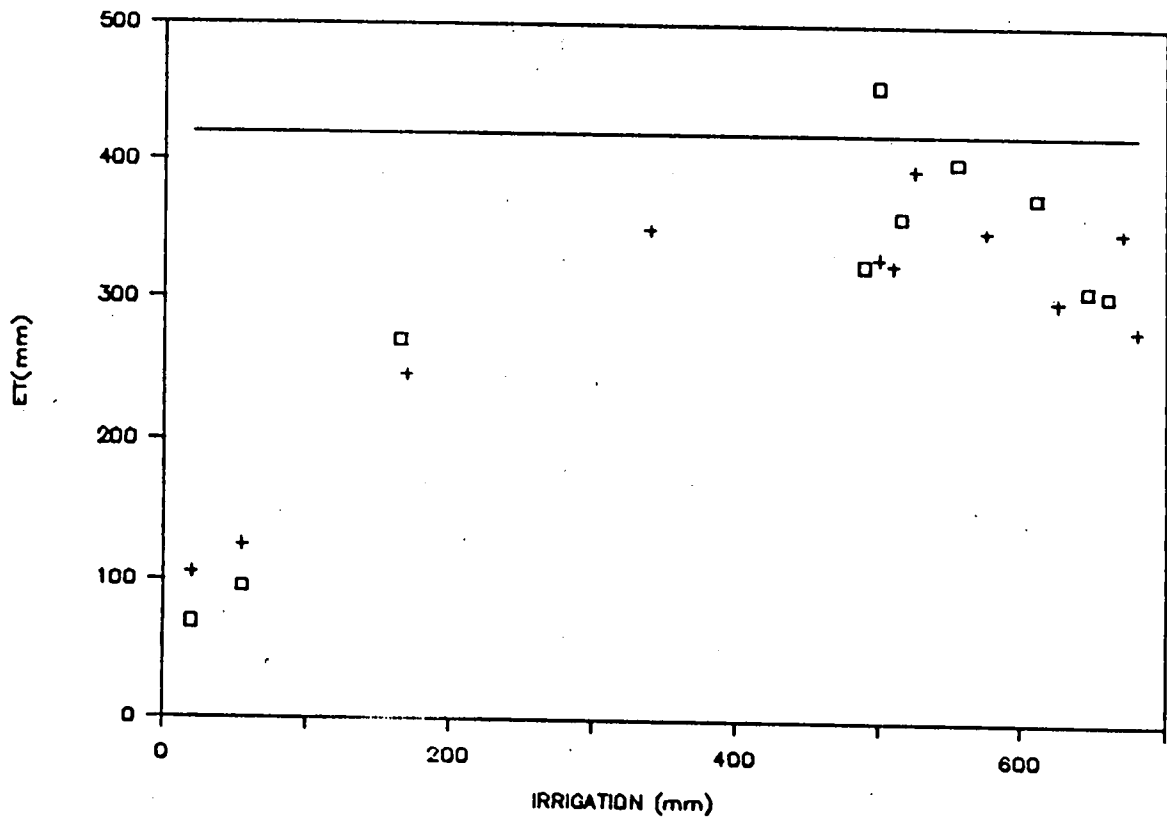


Fig. 31. Calculated ET as compared with ET(pot)

The other procedure we used in our study to calculate ET is based on the model developed by Childs and Hanks (1975). The result of the computation using this model is shown in Fig.31. ET_p according to the model is equal to 420 mm (using $ESTART=20, ESTOP=40, AK1=AK2+0.9$). This value is in agreement with the values obtained by the other methods discussed.

Many researchers quantify yield as a function of evapotranspiration by means of a linear regression equation. Shalhevet, et al.,(1976) point out the strong relation between yield and ET for many crops. Stewart et al., (1977) have shown this for corn, as have Hillel and Guron (1975). Stewart et al.,(1977) described a very simple yield - ET relation of the form

$$Y/Y_m = 1 - \beta_0 + \beta_0 ET/ET_m \quad (28)$$

where y is actual dry matter yield, y_m is maximal dry matter yield where $ET=ET_m$, ET is actual seasonal evapotranspiration, ET_m is maximal seasonal evapotranspiration, ET_d is evapotranspiration deficit and it is equal to $1 - ET/ET_m$, β_0 is the slope of the relative yield (Y/Y_m) vs the ET relation (ET/ET_m). This equation requires that ET be measured or estimated. The relationship between relative yield and relative ET using the equation of Stewart (1977) is shown in Fig.32. regardless of the type of stress causing decreased yield, ET was decreased proportionally. Under the saline treatments soil water depletion by plants was lower than in similar treatments without salinity stress (Table 14). These results are in agreement with those reported by Stewart, et al.(1977), who collected data from three different location with different climates, soils and salinities. This resulted in different values of ET_m and Y_m . It is interesting to note that the value of β_0 corn grown under those variable conditions was between

1-1.3. Our β_0 for the corn was 1.0 for non saline conditions and 0.98 for the saline conditions. This support the fact that the β_0 coefficient is not strongly site or year related, meaning that this approach is transferable to other locations.

In all three crops, as a result of the water application pattern, and the irrigation water salinity pattern (Fig.18), the mean yield of both corn crops and of wheat increased with distance from the edge of the field toward the irrigation line. Maximal mean yield was obtained in the vicinity of the low-salt line. This can be seen in Figs 33-35 where total yield for corn, and grain yield for wheat, is given as a function of distance from the lines. A fifth - order polynomial was fitted to the corn and wheat yield values as given in Fig's 33 - 35, with correlation coefficients of 0.982, 0.980 and 0.985 for Halamees and Jubilee corn, and wheat, respectively (the figures for the other treatments are given in the Appendix). Total yields as a function of irrigation amounts for the low and high salinity for all treatments are given in Fig's 36 - 39, and the relationship with irrigation amounts (only the linear parts of the data shown in Fig;s 36 - 39) are given in Fig's 40 - 42. Also, the relationship between total fresh yield and ear yield for Jubilee is given in Fig 43.

Between the two irrigation lines yield decreased in the direction from low salinity line to the high salinity line. Each curve in this figure is a combination of the mean yields obtained in a specific row (between the lines) over all the irrigation treatments (A, B, C, D and E). For the same amount of irrigation water, EC_e increases from row 14 to row 24.

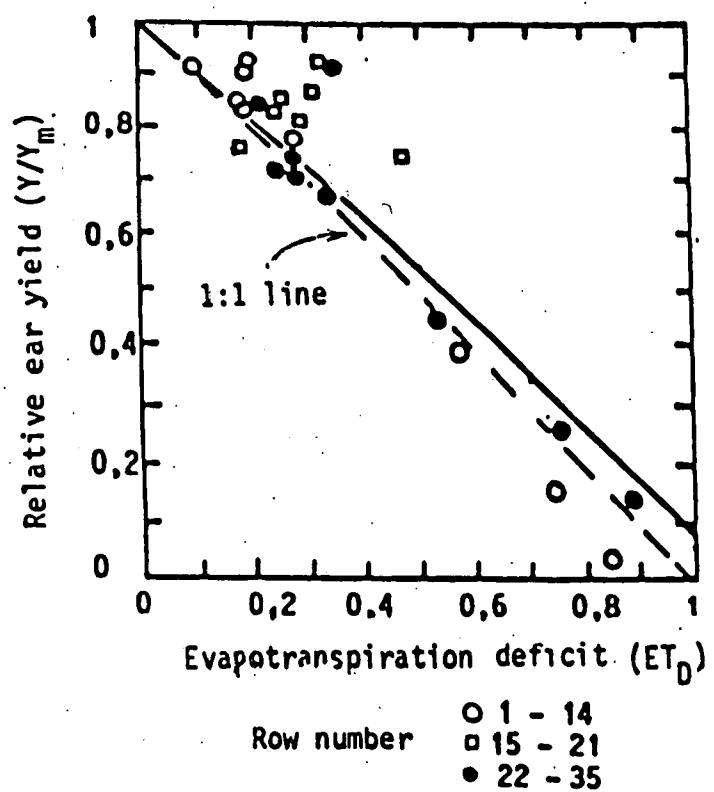
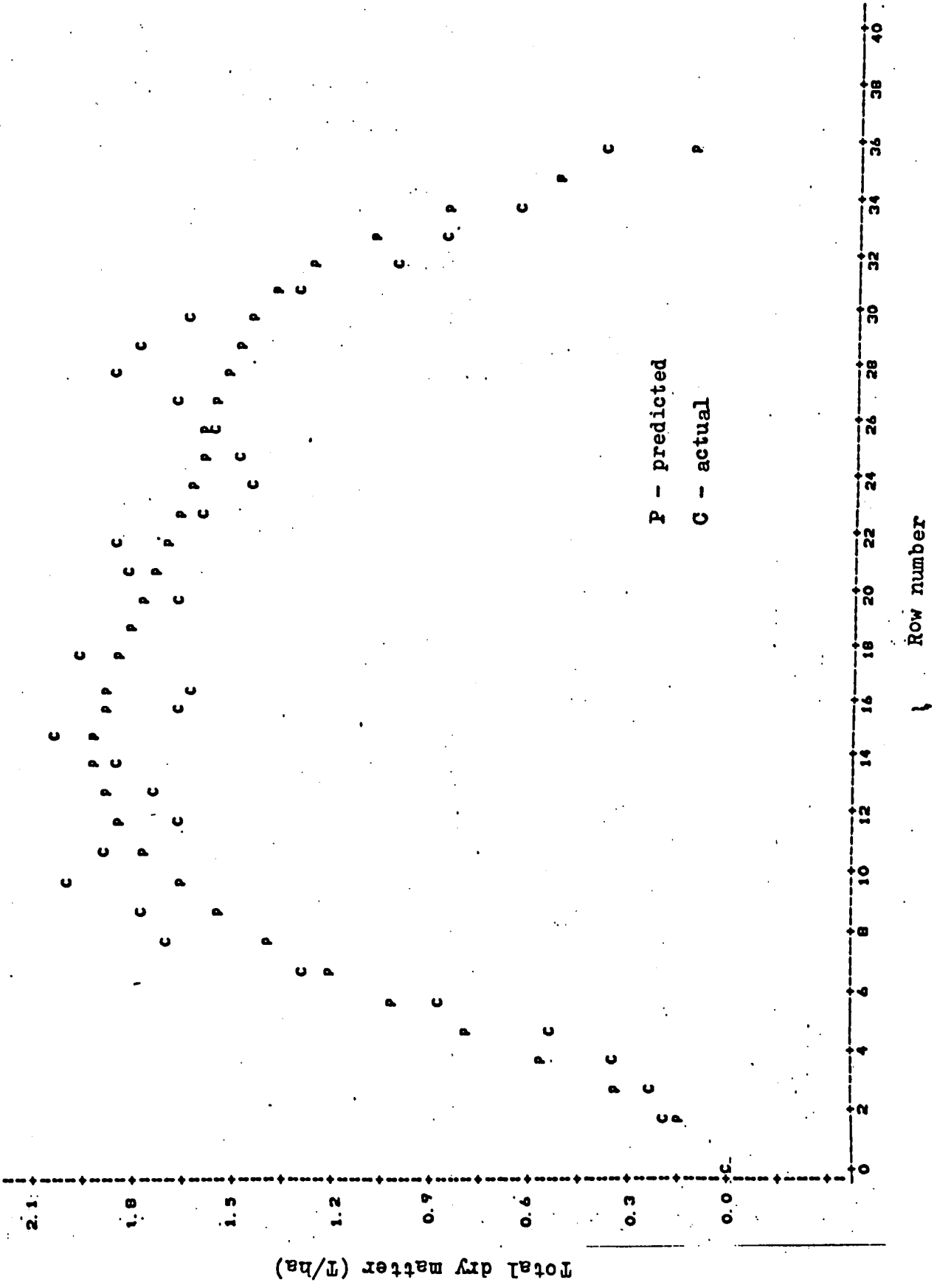


Fig. 32

Relative ear yield as a function of evapotranspiration deficit.

Fig. 33. Dry matter yield of corn (Halameesh) as a function of row number.



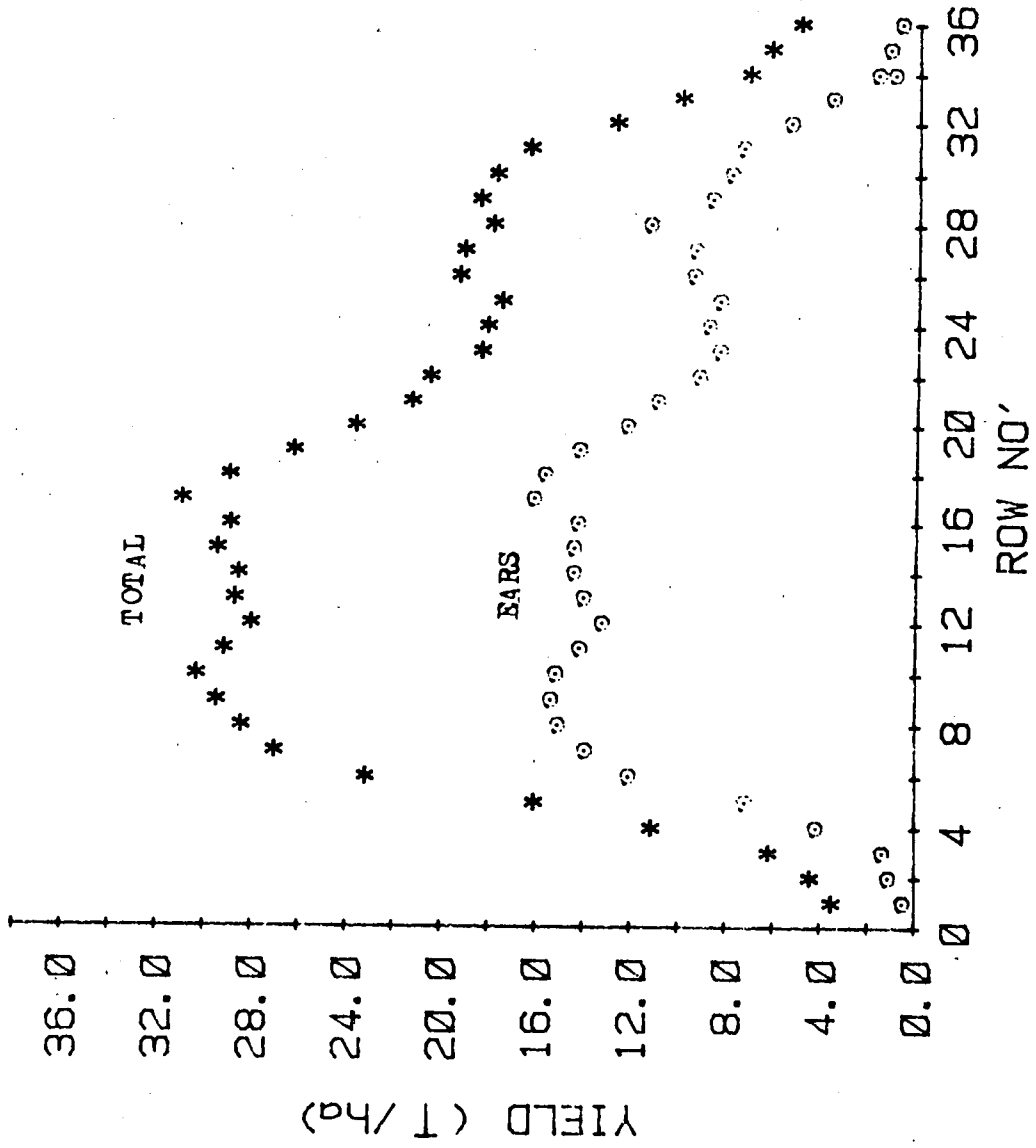


Fig. 34. Fresh yield of corn (Jubilee) as a function of row number.

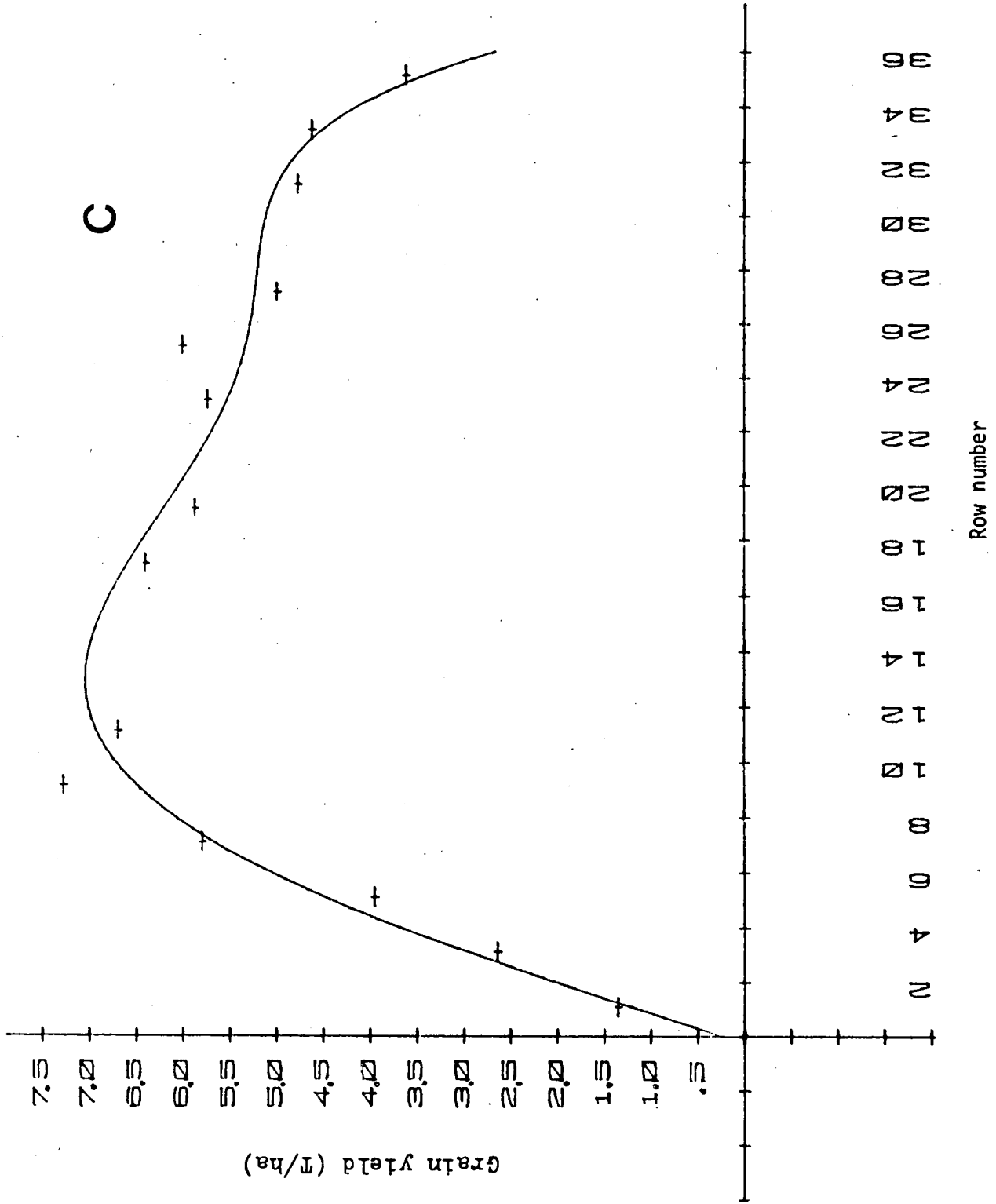


Fig. 35. Wheat grain yield as a function of row number.

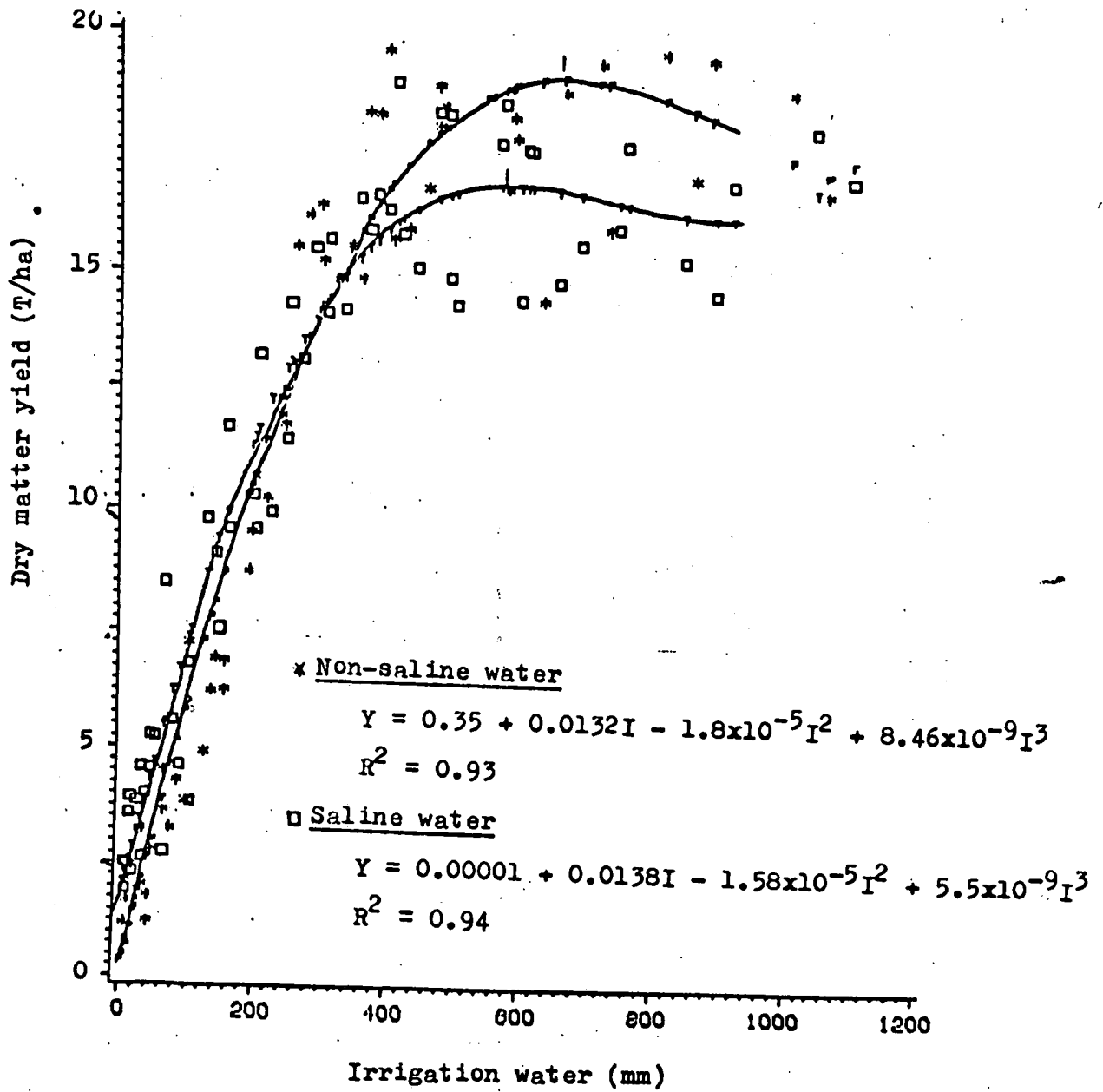


Fig. 36. Total dry matter yield of corn (Halameesh) as a function of amount of water applied, in all the treatments.

Fig. 37. Total fresh weight of Jubilee corn as a function of irrigation water amount, in all the treatments.

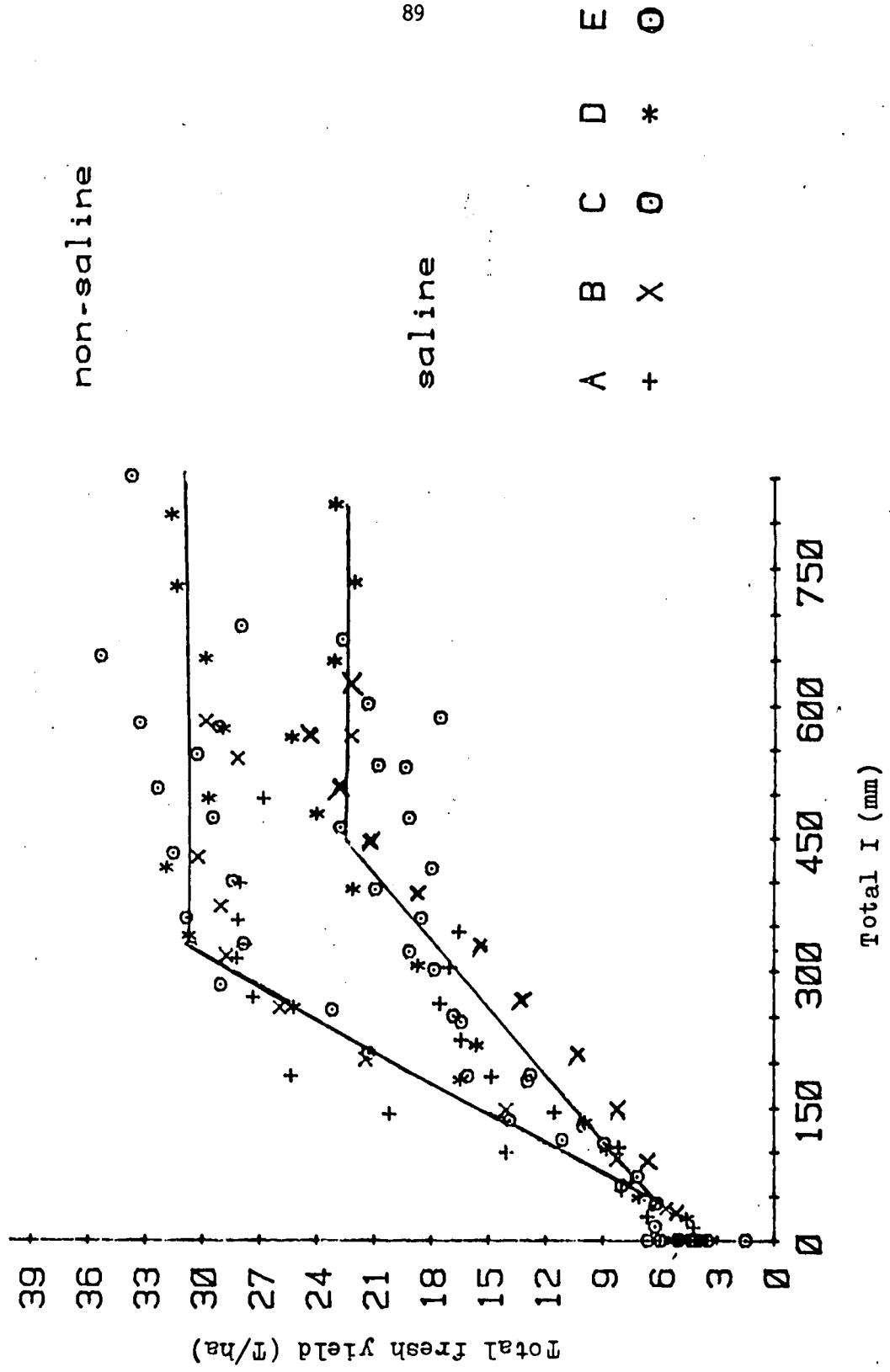
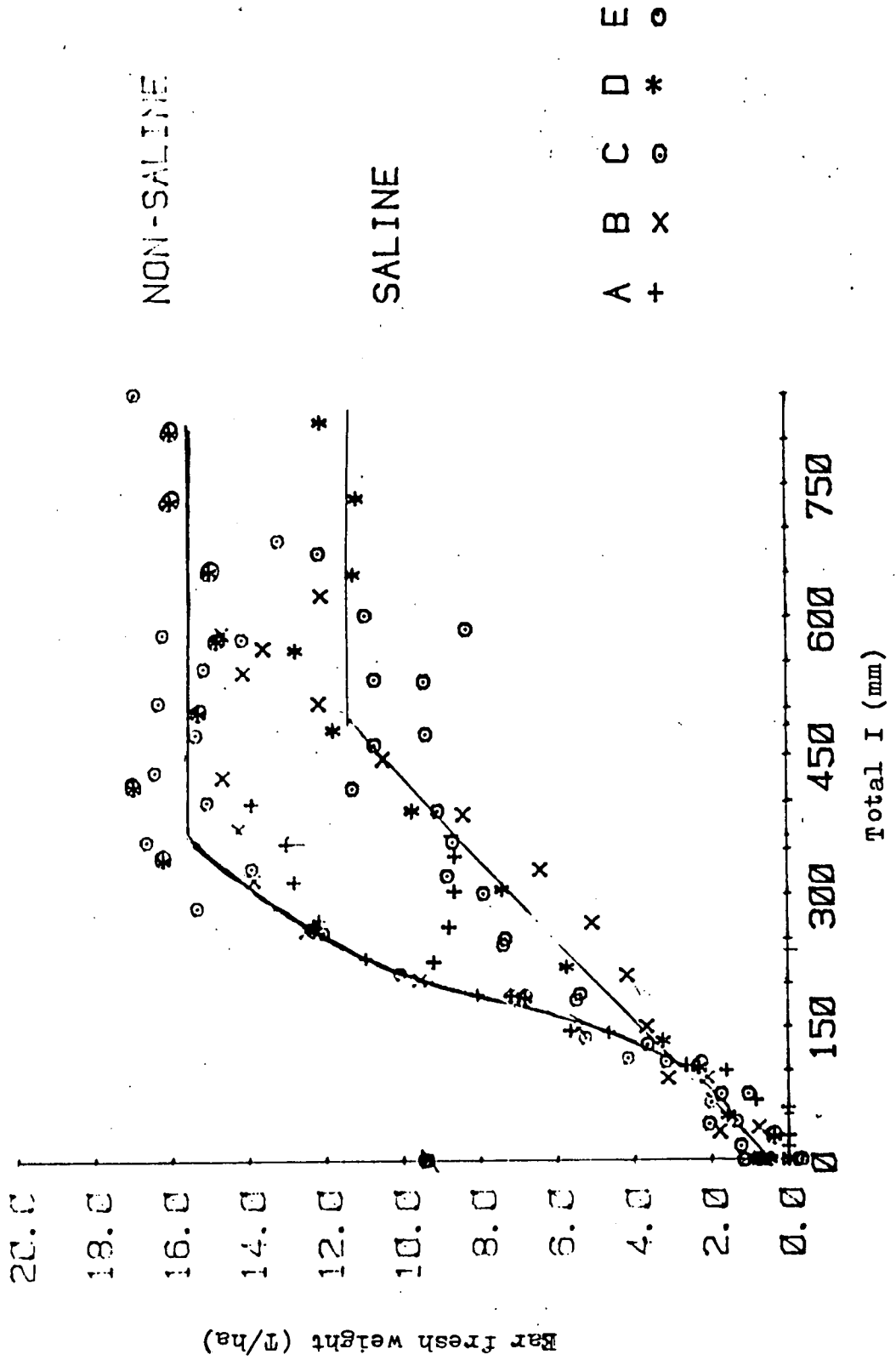


Fig. 38. Fresh weight of ears of Jubilee corn as a function of irrigation water amount, in all the treatments.



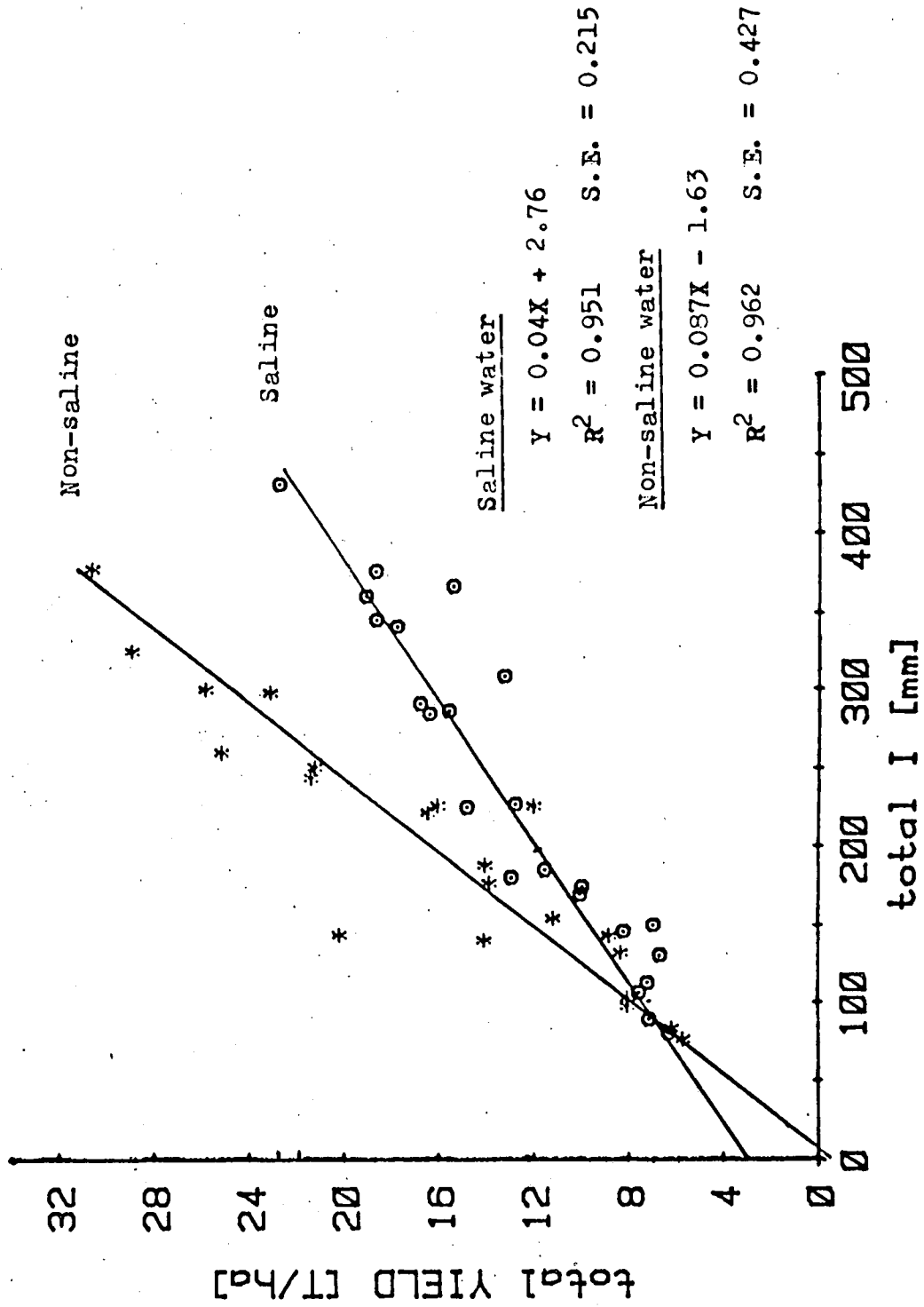


Fig. 39 . Total fresh yield of corn (Jubilee) as a function of irrigation amount. (Linear part of the curve in Fig. 36.)

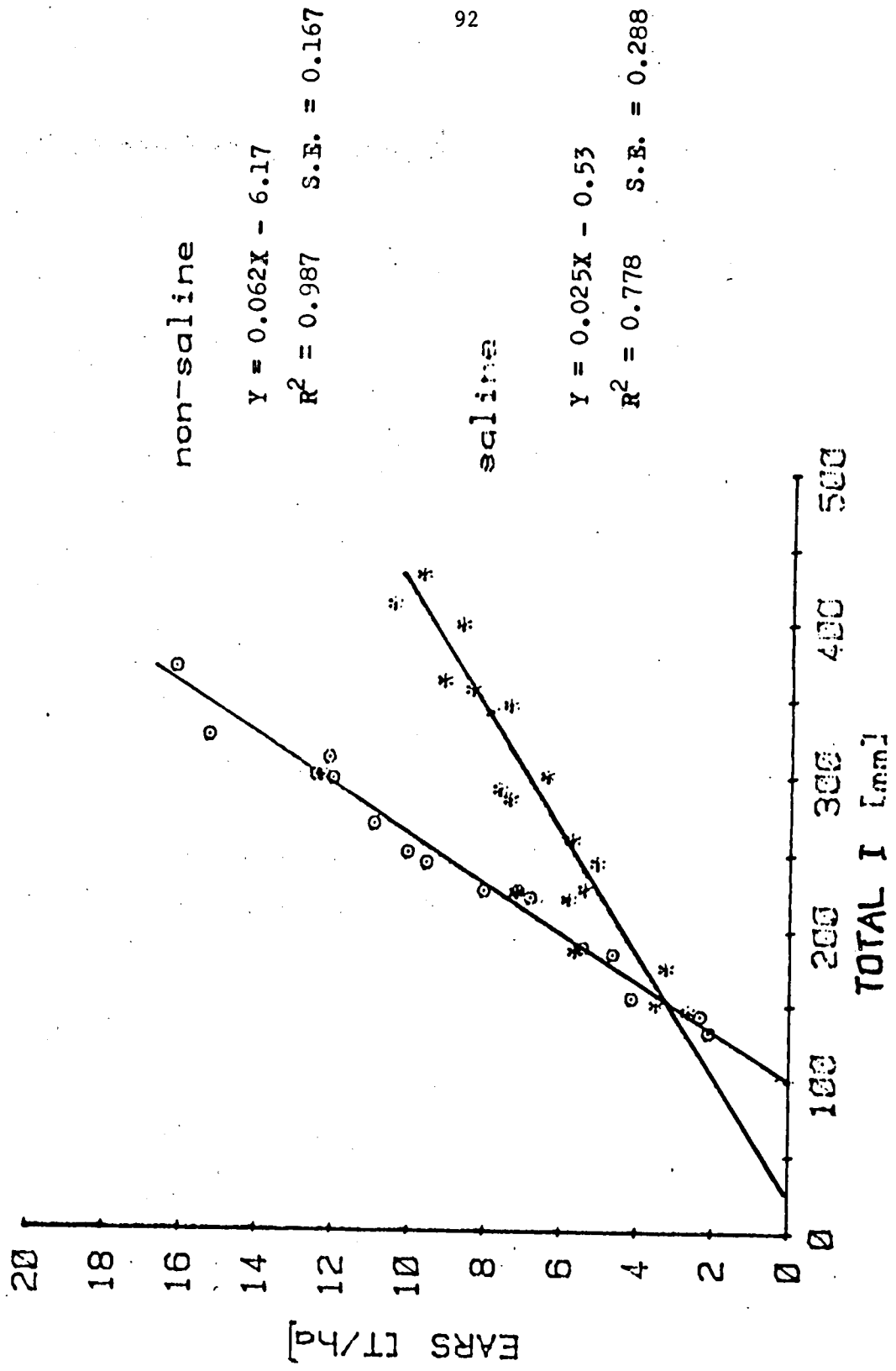


Fig. 40. Yield of corn ears (Jubilee) as a function of irrigation amount. (Linear part of the curve in Fig. 38.)

Fig. 41. Wheat grain yield as a function of evapotranspiration
(Non-saline water).

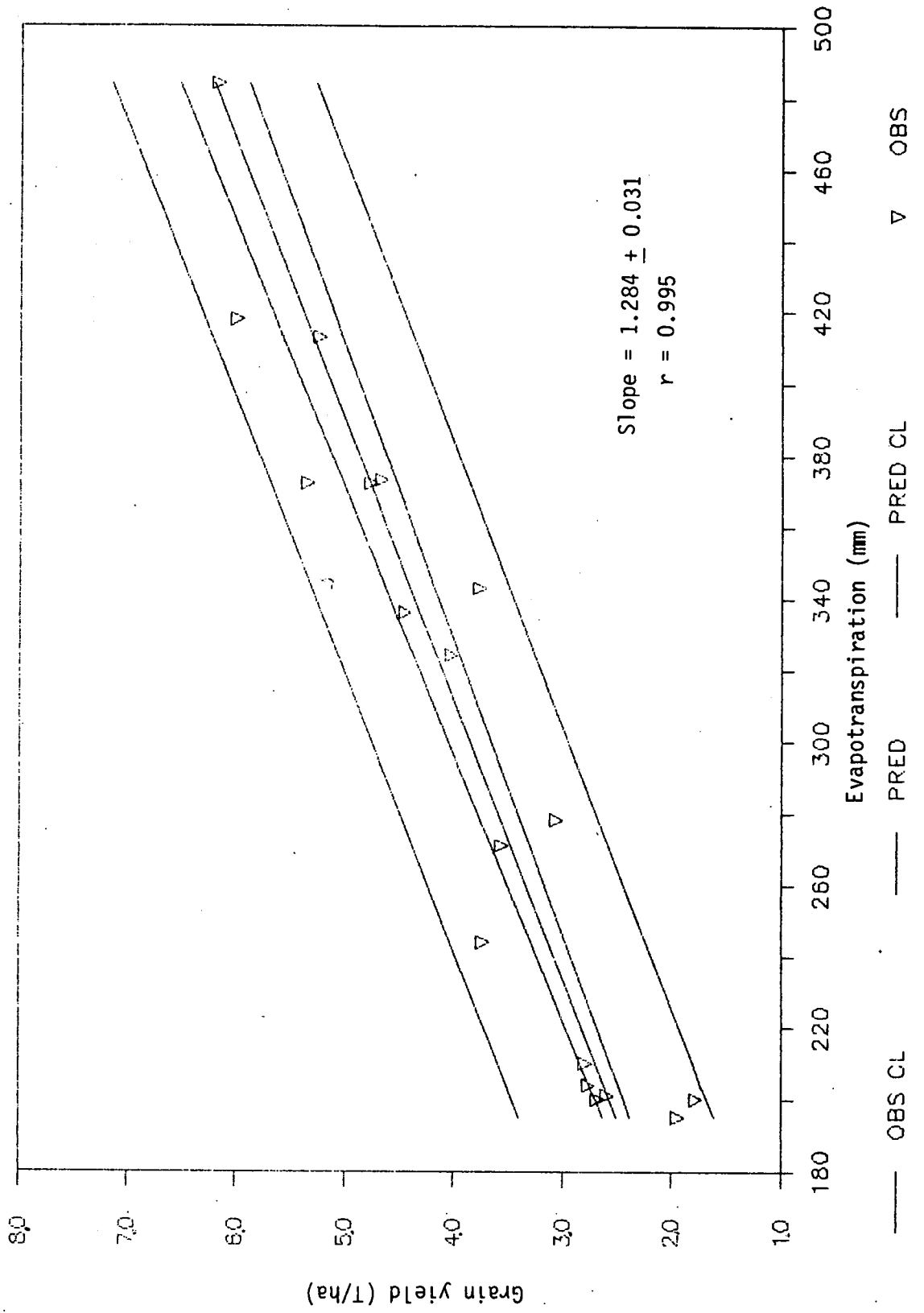
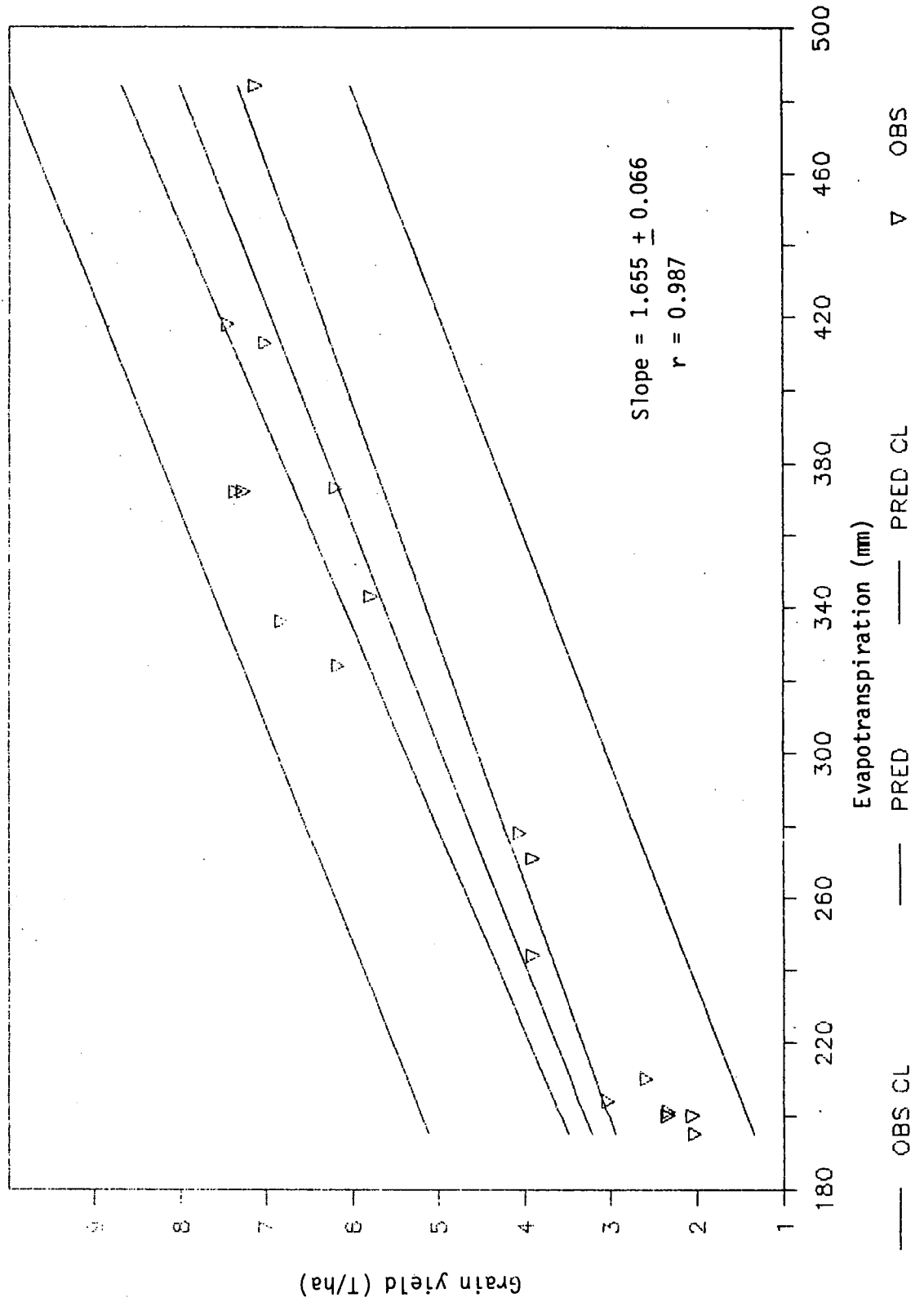


Fig. 42. Wheat grain yield as a function of evapotranspiration (Saline water).



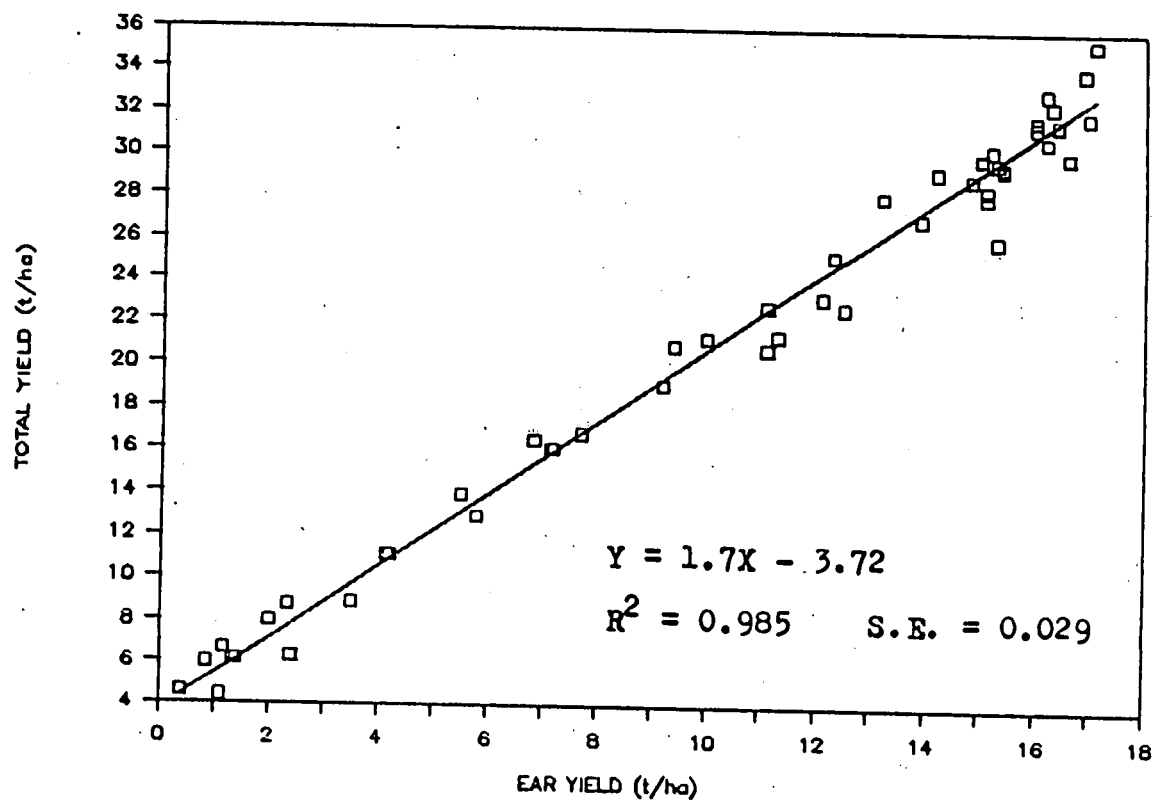


Fig. 43. Relationship between total fresh yield and ear yield of corn (Jubilee).

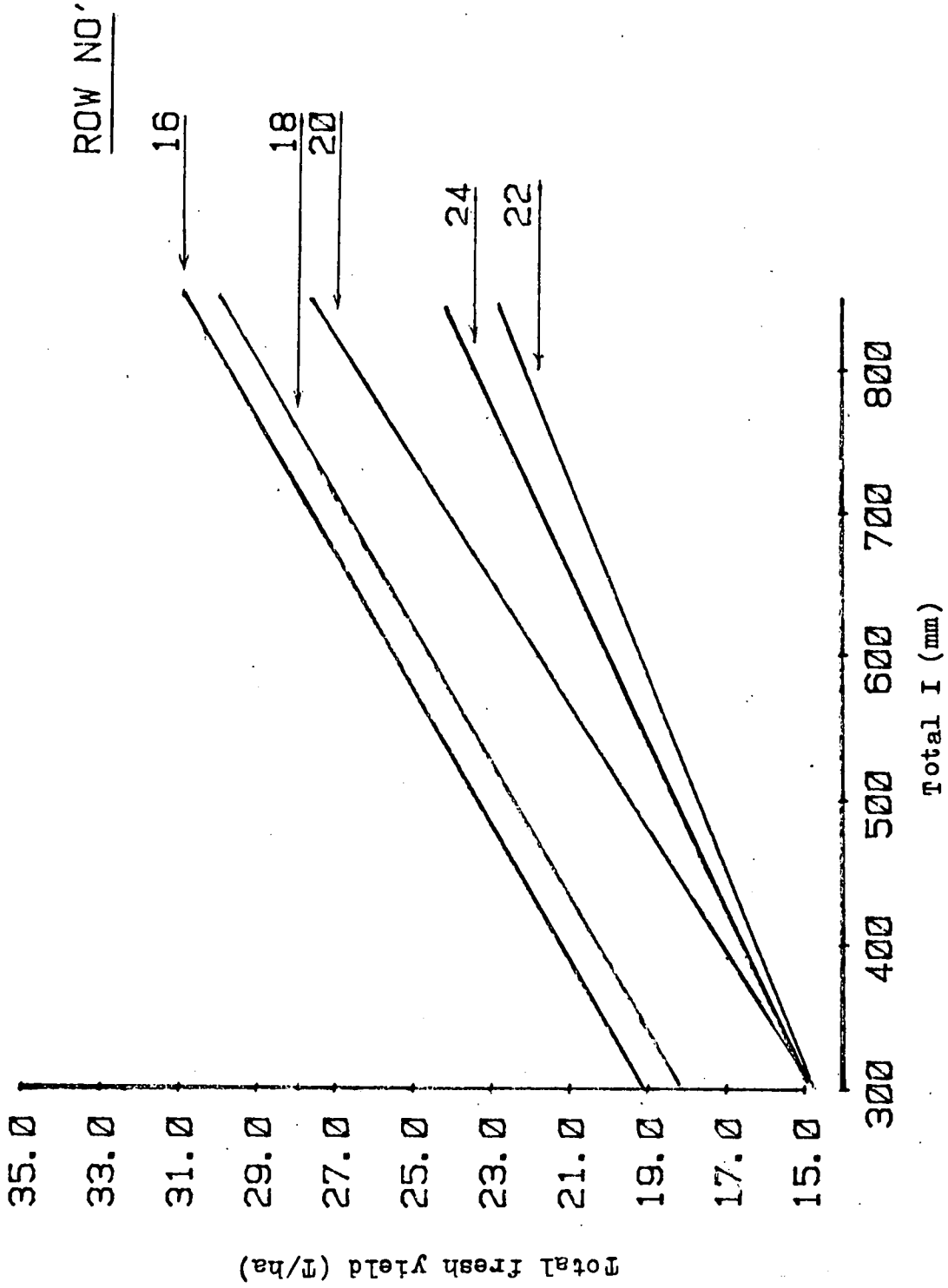


Fig. 44. Total fresh weight of Jubilee corn as a function of irrigation water amount. E_ce increases with row number from Row 16 to Row 22.

Literature Cited

- Banin, A. and Amiel, A. (1960) A correlative study of the chemical and physical properties of a group of natural soils of Israel. *Geoderma* 3: 185-198.
- Black, C.A., Evans, D.D. White, J.L., Ensminger, L.E. and Clark, F.E. (Eds.) (1965) *Methods of Soil Analysis, Part I*. *Agronomy* 9: 854.
- Brooks, R.H. and Corey, A.T. (1964) Hydraulic properties of porous media. *Hydrology Papers No. 3*: 27. Colorado State Univ., Fort Collins, Colo.
- Burdine, N.T. (1953) Relative permeability calculations from pore size distribution data. *Petr. Tran. Am. Inst. Mining Metal Eng.* 198: 71-77.
- Childs, S. W. and Hanks, R.J. (1975) Model of soil salinity effects on crop growth. *Soil Sci. Soc. Am. Proc.* 36: 617-622.
- Davidson, J.M., Stone, L.R., Nielsen, D.R. and Larue, M.E. (1969) Field measurement and the use of soil water properties. *Water Resources Res.* 5: 1312-1321.
- Frenkel, H., Nadler, A. and Shainberg, I. (1983) Effect of entrapped air on EC_e vs. EC_w calibration curves as measured in a soil column. *Soil Sci. Soc. Am. J.* 47: 1036-1038.
- Frenkel, H., Goertzen, G.R. and Rhoades, J.D. (1978) Effects of clay type and content, exchangeable sodium percentage and electrolyte concentration on clay dispersion on soil hydraulic conductivity. *Soil Sci. Soc. Am. J.* 42: 32-39.
- Hanks, R.J. and Ashcroft, G.L. (1980) *Applied Soil Physics*: 159. Springer Verlag, Berlin/Heidelberg.
- Hanks, R.J., Keller, J., Rasmussen, V.P. and Wilson, G.I. (1976) Line source sprinkler for continuous variable irrigation-crop production studies. *Soil Sci. Soc. Am. Proc.* 40: 425-429.
- Hillel, D. (1980a) *Fundamentals of Soil Physics*: 413. Academic Press, New York.
- Hillel, D. (1980b) *Applications of Soil Physics*: 385. Academic Press, New York.
- Hillel, D. and Guron, Y. (1973) Relation between evapotranspiration rate and maize yield. *Water Resources Res.* 9: 743-748.
- Lauer, D.A. (1983) Line-source sprinkler systems for experimentation with sprinkler-applied nitrogen fertilizers. *Soil Sci. Soc. Am. J.* 47: 124-128.
- Maas, E.V. (1985) Crop tolerance to saline sprinkling water. *Plant and Soil* 89: 273-284.

- McBride, R.A. and MacIntosh, E.E. (1984) Soil survey interpretations from water retention data. I.: Development and validation of a water retention model. *Soil Sci. Soc. Am. J.* 48: 1338-1343.
- Mualem, Y. A. (1976) A new model for predicting the hydraulic conductivity of unsaturated porous media. *Water Resources Res.* 12: 513-522.
- Nielsen, D.R., Biggar, J.W. and Erh, K.T. (1973) Spatial variability of field measured soil water properties. *Hilgardia* 42(7): 215-259.
- Richards, L.A. (1965) Physical condition of water and soil. In: Black, et al. (Eds.): *Methods of Soil Analysis, Part I. Agronomy* 9: 128-151.
- Russo, D. and Bresler, E. (1980a) Field determination of soil hydraulic properties for statistical analysis. *Soil Sci. Soc. Am. J.* 44: 697-702.
- Russo, D. and Bresler, E. (1980b) Soil water suction relationships as affected by soil solution concentration and composition. In: Banin, A. and Kafkafi, U. (Eds.): *Agri-chemicals in Soils*: 287-297. Pergamon Press, New York.
- Shaykewich, C.F. (1970) Hydraulic properties of disturbed and undisturbed soils. *Can. J. Soil Sci.* 50: 431-437.
- Shalhevet, J., Mantell, A., Bielorai, H. and Shimshi, D. (Eds.) (1976) *Irrigation of Field and Orchard Crops Under Semi-Arid Contions*. Int. Irrig. Inf. Center, Publ. 1. Bet Dagan.
- Soil Survey Staff (1975) *Soil Taxonomy*. Agriculture Handbook No. 436. Soil Cons. Serv., U.S. Dept. Agr., Washington, D.C.
- Stark, J.C., Jarrell, W.M. and Letey, J. (1982) A modified line source sprinkler technique for continuous-variable leaching studies. *Soil Sci. Soc. Am. J.* 46: 441-443.
- Stewart, J.I., Hagan, R.M. and Pruitt, W.O. (1974) Function to predict optimal irrigation programs. *J. Irr. Drain., ASCE* 100 (IR2): 179-199.
- Stewart, J.I., Misra, R.D. and Pruitt, W.O. (1975) Irrigation of corn and grain sorghum with a deficient water supply. *Tran. Am. Soc. Civ. Eng.* 18(2): 270-280.
- Stewart, J.I., Danielson, R.E., Hanks, R.J., Jackson, E.B., Hagan, R.M., Pruitt, W.O., Franklin, W.T. and Riley, J.P. (1977) Optimizing crop production through control of water salinity levels in the soil. Utah Water Research Lab. PR 151-1, Logan, Utah, 191 pp.

- U.S. Salinity Laboratory Staff (1954) Diagnosis and Improvement of Saline and Alkali Soils. U.S. Dept. Agriculture Handbook No. 60. Washington, D.C.
- Van Genuchten, M. Th. (1980) A closed-form equation for predicting the hydraulic conductivity of unsaturated soils. Soil Sci. Soc. Am. J. 44: 892-898.
- Warrick, A.W. and Nielsen, D.R. (1980) Spatial variability of soil physical properties in the field. In: Hillel, D.: Applications of Soil Physics: 319-344. Academic Press, New York.
- Yaron, B., Bresler, E. and Shalhevet, J. (1966) A method for uniform packing of soil columns. Soil Sci. 101: 205-209.
- Youngs, E.G. (1964) An infiltration method for measuring the hydraulic conductivity of unsaturated porous materials. Soil Sci. 97: 307-311.

BASIC program for calculating the soil water retention curve by
the Brooks and Corey method and the simplified Van Genuchten method.

```

100 HOME
120 PRINT "THIS PROGRAM CALCULATES THE PRESSURE HEAD / HYDRAULIC CONDUCTIVITY - WATER CONTENT FUNCTION USING:"
140 PRINT "-THE BROOKS AND COREY METHOD"
160 PRINT
180 PRINT "-A SIMPLIFIED VAN GENUCHTEN METHOD JACKSON METHOD"
200 PRINT
220 PRINT "THE PRESSURE HEAD - WATER CONTENT RELATIONSHIP IS ESTIMATED BY A LINEAR REGRESSION USING THE EFFECTIVE SATURATION  $S_e$  WHICH IS DEFINED AS  $S_e = (W - W_r) / (W_s - W_r)$  (WR=RESIDUAL WATER CONTENT, WS=SATURATED WATER CONTENT, WC=ACTUAL WATER CONTENT)
240 PRINT "WR IS ESTIMATED BY THE BEST FITTING OF THE REGRESSION LINE"
260 PRINT
280 PRINT "TO CONTINUE PRESS 1"
300 INPUT ZP
320 HOME
340 PRINT
360 PRINT
380 PRINT "HOW MANY INCREMENT SHOULD THE PROGRAM USE FOR CALCULATING HYDRAULIC CONDUCTIVITY?"
400 INPUT RM
420 DIM W(RM), WC(RM), H(RM), S(RM)
440 PRINT
460 PRINT
480 Z = 0
500 PRINT "NUMBER OF POINTS?"
520 INPUT N
540 PRINT
560 PRINT
580 PRINT "PRESSURE HEAD = ? WATER CONTENT = ?"
600 PRINT
620 PRINT
640 DIM H(1), WC(1), S(1)
660 FOR I = 1 TO N
680 PRINT "POINT NO. AND VALUE OF POINT:"
700 INPUT H(I), WC(I)
720 NEXT I
740 PRINT
760 PRINT
780 PRINT "INPUT OF SATURATION WATER CONTENT"
800 PRINT "1.?"
820 INPUT WS
840 PRINT "INPUT LOWER AND UPPER
R RESIDUAL WATER CONTENT"
860 PRINT "MINIMUM WR="
880 INPUT IR
900 PRINT "MAXIMUM WR="
920 INPUT MR
940 RI = IR
960 RM = MR
980 PRINT
1000 PRINT
1020 PRINT
1040 PRINT "ANY CORRECTIONS?"
1060 PRINT "IF YES PRESS 1"
1080 INPUT ME
1100 IF ME = 1 THEN 2000
1120 PRINT
1140 PRINT
1160 PRINT "B.C. OF SIMPLIFIED VAN GENUCHTEN METHOD?"
1180 PRINT "0=B.C.2=V.G."
1200 INPUT C
1220 STE = .5
1240 T = 0
1260 Z = 0
1280 FOR WR = RI TO RM STEP STE
1300 IF C = 0 THEN 1360
1320 GOSUB 3780
1340 IF C = 2 THEN 1500
1360 FOR I = 1 TO N
1380 O = (Y(I) - WR) / (WS - WR)
1400 IF O < 0 THEN 1460
1420 IF O > 0 THEN 1480
1440 Y(I) = LOG(O) / LOG(10)
1460 IF X(I) = 0 THEN 1480
1480 X(I) = LOG(X(I)) / LOG(10)
1480 NEXT I
1500 J = 0
1520 K = 0
1540 L = 0
1560 M = 0
1580 P2 = 0
1600 FOR I = 1 TO N
1620 J = J + O(I)
1640 K = K + O(I)^2
1660 L = L + O(I)^3
1680 M = M + O(I)^4
1700 P2 = P2 + O(I) * Y(I)
1720 H(I) = 1
1740 P = O(I) * P2 - J * J / N
L = L + 2 * P
1760 A = O(I) - P * J / M
1780 J = E * (P2 - J * K / M)
1800 H = H + A * 2 * N
1820 I = H - J
1840 P2 = J * H
1860 IF T = 1 THEN 2140
1880 IF P2 < 2 THEN 1960

```

```

1900 Z = R2
1920 PRINT INT (100 * NR + .5) /
100; TAB( 10); INT (1000 * R
2 + .5) / 1000
1930 CALL - 198
1940 NEXT NR
1960 IF STE = .J THEN 2080
1980 STE = .J
2000 FI = NR - .5
2020 IF (NF - .5) < 0 THEN FI =
.J
2040 RH = NR + .5
2060 GOTO 1240
2080 NR = NR - .1
2100 T = 1
2120 GOTO 1300
2140 FOR I = 1 TO N
2160 PRINT X(I); TAB( 7); Y(I);
TAB( 14); INT (1000 * X(I) *
.5) / 1000; TAB( 20); INT (1
000 * Y(I) + .5) / 1000
2180 NEXT I
2200 PRINT "F(X)=";A1;"+";B1;"*X)
2220 IF C = 0 THEN 2320
2240 AL = 10 * (A / B)
2260 PRINT "ALFA = " ; INT (10000
* AL + .5) / 10000
2280 PRINT "EXPON. N=" ; INT (100
00 * B + .5) / 10000
2300 IF C = 2 THEN 2380
2320 HB = 10 * (A / ABS (B))
2340 PRINT "BUBBLING PRESSURE HB
=" ; HB
2360 PRINT "LAMBDA = " ; B
2380 PRINT "RESIDUAL WATER CONTE
NT=" ; NR
2400 PRINT "SATURATION WATER CON
T. WS=" ; WS
2420 PRINT
2440 PRINT "COEFF. OF DETER. (R^
2)=" ; R2
2460 PRINT "COEFFICIENT OF CORRE
LATION = " ; SQ (R2)
2480 IF (1 - R2) = 0 THEN 2520
2500 PRINT "STANDARD ERROR OF ES
TIMATE = " ; SQ (ABS (1 - (1
- R2)))
2520 PRINT R12, R12
2540 PRINT
2560 PRINT "INTERPOLATION: (ENTE
R = 0 TO CONTINUE PROGRAM)"
2580 INPUT "Y = " ; Y
2600 IF Y = 0 THEN 2620
2620 PRINT "I = " ; (A + B * Y)
2640 PRINT
2660 NONE
2680 PRINT
2700 PRINT
2720 PRINT
2740 GOTO 2580
2820 NONE
2840 PRINT
2860 PRINT
2880 PRINT "0 CALCULATING HYD
RAULIC CONDUCTIVITY"
2900 PRINT
2920 PRINT "1 CHANGING MAX AND
D MIN WAT. CONT."
2940 PRINT
2960 PRINT "2 END PROGRAM"
2980 PRINT
3000 PRINT "3 CORRECTIONS OF
POINTS"
3020 PRINT
3040 PRINT "4 CHANGING SATURA
TION WAT. CONT."
3060 PRINT
3080 PRINT "5 USING DIFFERENT
METHOD OF CALC-"
3090 PRINT " ULATION THE WAT
ER RET. CURVE"
3092 PRINT
3094 PRINT
3096 PRINT "WHICH" ;
3100 INPUT C
3120 IF C = 0 THEN 3480
3140 IF C = 2 THEN 3760
3160 IF C = 3 THEN 3320
3180 IF C = 4 THEN INPUT WS
3200 IF C = 4 THEN 940
3210 IF C = 5 THEN 940
3220 PRINT
3240 PRINT
3260 PRINT
3280 PRINT "NEW INPUT OF MIN AND
MAX RES. WATER CONT."
3300 GOTO 860
3320 PRINT "CORRECTION OF X,Y VAL
UES, INPUT NUMBER OF POINT" ;
3340 INPUT G
3360 PRINT "INPUT OF X,Y VALUE" ;
3380 INPUT X; G; Y; (G)
3400 PRINT "ANOTHER ONE? (1=Y, 2
=1)" ;
3420 INPUT F
3440 IF F = 1 THEN 3320
3460 GOTO 940
3480 NONE
3500 PRINT "CHOOSE METHOD" ;
3520 PRINT
3540 PRINT "0 END PROGRAM"
3560 PRINT
3580 PRINT "1 FROM S. L. COPEL
METHOD"
3600 PRINT
3620 PRINT "2 SIMPLIFIED USING
CROUCHER-JACKSON METHOD"
3640 PRINT
3660 PRINT "WHICH?" ;
3680 INPUT FI
3700 IF FI = 1 THEN GOTO 860

```

```

3720 IF FI = 2 THEN GOSUB 4620
3740 GOTO 2020
3760 END
3780 REIN INTERPROGRAMM
3800 FOR I = 1 TO II
3820 O = (Y(I) - WR) / (WS - WR)
    ) ^ ( - 1) - 1
3840 IF O < 0 THEN 3900
3860 Y(I) = LOG(O) / LOG(10)
3880 X(I) = LOG(X(I)) / LOG(
10)
3900 NEXT I
3920 RETURN
3940 LAM = ABS (E)
3960 FI = FI
3980 PRINT "INPUT SAT. HYD. COND.
UC.":
4000 INPUT KS
4020 NI = (WS - WR) / LI
4040 WC(I) = WS - NI
4060 W(KI) = W(I) - (NI * YI)
4080 PRINT W(I)
4100 FOR I = 2 TO (KI - 1)
4120 J = I - 1
4140 W(I) = W(J) - NI
4160 NEXT I
4180 PRINT "I": TAB( 4) "WC": TAB(
11) "H": TAB( 18) "S": TAB(
23) "KR": TAB( 31) "K"
4200 FOR I = 1 TO KI
4220 IF W(I) < WR THEN 4440
4240 S = (W(I) - WR) / (WS - WR)
4260 IF S = 0 THEN 4420
4280 H = HE * S ^ (1 / ( - LAM))
4300 KP = S ^ (3 + 2 / LAM)
4320 Y = KS + KR
4340 H = INT (H + .5)
4360 KR = INT (100000 * KR + .5)
    / 100000
4380 W(I) = INT (10 * W(I) + .5)
    / 10
4390 S = INT (100 * S + .5) / 10
4400 PRINT I: TAB( 4) "WC": TAB(
11) "H": TAB( 18) "S": TAB(
23) "KR": TAB( 31) "K"
4420 NEXT I
4440 FI = I - 1
4460 PRINT "POROSITY COEFF. = "
    H
4480 PRINT "BUBBLING PRESS. = "
    HMF
4500 PRINT "SATURATION WGT. CONT.
    = "
    HMC
4520 PRINT "RESIDUAL WGT. CONT. =
    "
    HMR
4540 PRINT "SATURATION HYD. COND.
    = "
    HKS
4545 INPUT FC
4560 PRINT
4580 PRINT
4600 RETURN
4620 REIN CALCULATING HYDRAULIC C
ONTENT FUNCTION USING VAN GEN
UCHTEN (SIMPLIFIED) METHOD
4640 NE = ABS (E)
4650 KI = KN
4660 NI = (WS - WR) / KI
4680 KI = KI - 1
4700 W(I) = WS - NI
4720 W(KI) = W(I) - (NI * KI)
4740 FOR I = 2 TO (KI - 1)
4760 J = I - 1
4780 W(I) = W(J) - NI
4800 NEXT I
4820 FOR I = 1 TO KI
4840 IF (W(I) - WR) = < 0 THEN
    4920
4860 S = (WS - WR) / (W(I) - WR)
4880 IF (1 / AL) * (S - 1) ^ (1
    / NI) > 1.7E + 38 THEN 4920
4900 H(I) = (1 / AL) * (S - 1) ^
    (1 / NE)
4965 S(I) = INT (100 / S + .5) /
    100
4910 NEXT I
4920 KI = I - 1
4940 PRINT "MATCHING FACTOR?"
4960 INPUT M
4980 PRINT "SATURATION HYD. COND.
    ?"
5000 INPUT KS
5040 FOR I = 1 TO KI
5060 WC(I) = W(I) + NI
5080 W(I) = INT (100 * WC(I) +
    .5) / 100
5100 NEXT I
5120 D = 0
5122 SU = 0
5124 B1 = 0
5126 B2 = 0
5140 FOR L = 1 TO KI
5160 IF H(L) = 0 THEN 5300
5200 IF H(L) > 1.3E + 19 THEN 53
    00
5220 IF (H(L) - 2) = 0 THEN 5300
5240 B1 = (2 * L - 1) / H(L) + 2
5260 SU = B1 + B2
5280 B2 = SU
5300 NEXT L
5320 PRINT B2
5340 PRINT
5360 PRINT "I": TAB( 4) "WC": TAB(
10) "H": TAB( 18) "S": TAB(
23) "KR": TAB( 31) "K"
5380 PRINT
5400 I = 0
5420 J = 0
5440 FOR I = 1 TO II
5460 FOR J = 1 TO I
5480 HZ = 2 * J + I - 2 * J

```

```

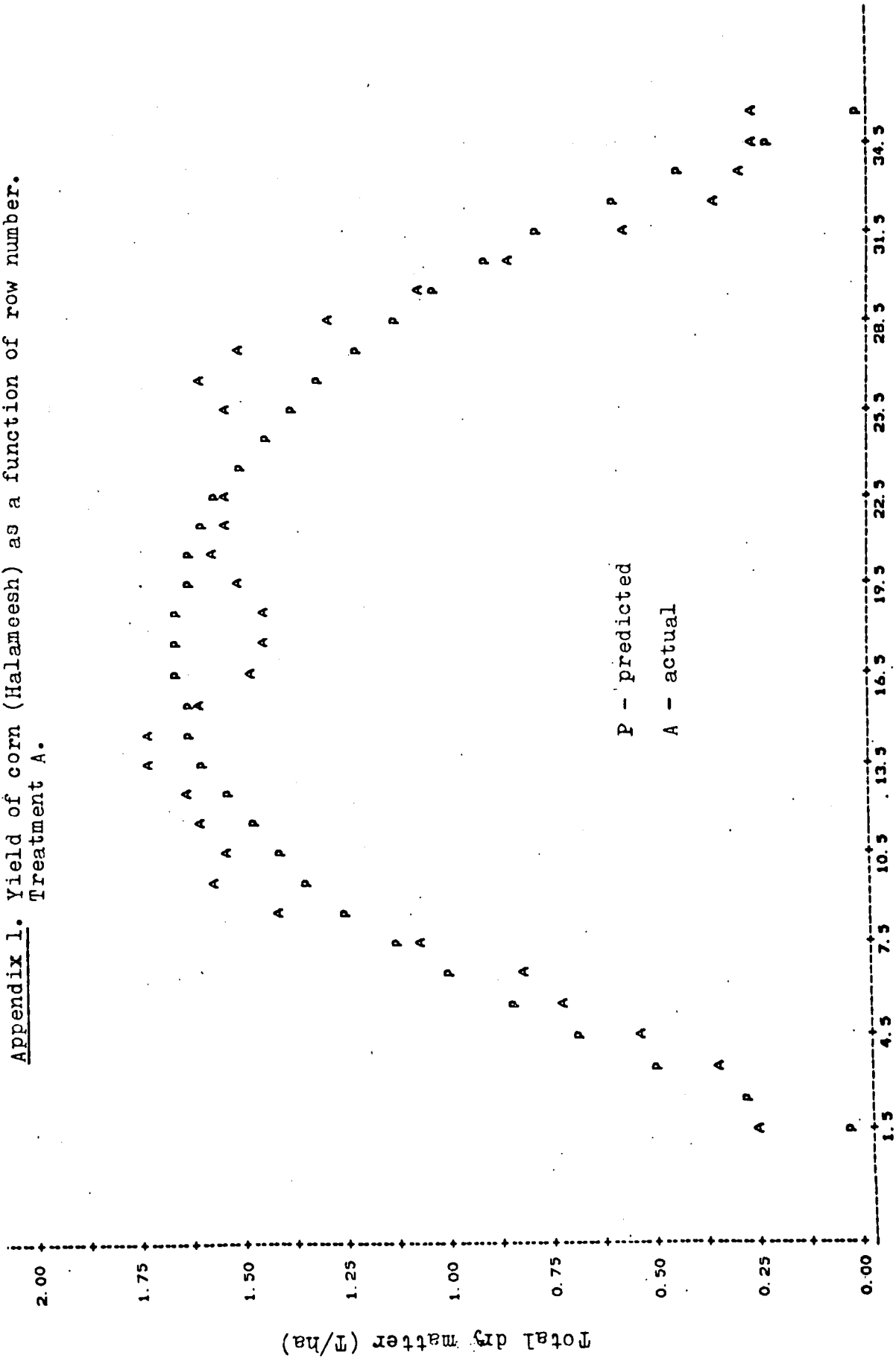
5500 IF (H(J) - 2) > 1.7E + 38 THEN
5540
5520 IF (H(J) - 2) = 0 THEN 5640

5540 IF H(J) < = 0 THEN 5640
5560 AC = N2 / (H(J) ^ 2)
5580 AC = 10000000 + AC
5600 C = AC + D
5620 D = C
5640 NEXT J
5660 D = D / 10000000
5680 D1 = D / B2
5700 IF = D1 * (MC(1) / ME - 1)
IF
5720 I = IF * KS
5740 IF = INT (10000 * IF + .5) /
10000
5760 H-1 = INT (1 + H(1) + .5) /
1
5780 PRINT I; TAB( 4); MC(1); TAB(
11); H(1); TAB( 18); S(1); TAB(
25); IR; TAB( 33); K
5800 NEXT I
5820 PRINT
5840 PRINT "MATCHING FACTOR, ALFA
. EXP. 1"
5860 PRINT II; TAB( 4); INT (1000
0 * AL + .5) / 10000; TAB( 1
4); INT (10000 * NE + .5) /
10000
5880 PRINT "RESIDUAL AND SAT. WA
T. CONT: " ; IR; " " ; IS
5900 PRINT "SAT. HYD. COND. KS="
; KS
5920 PRINT
5940 PRINT
5950 INPUT TR
5960 RETURN

```

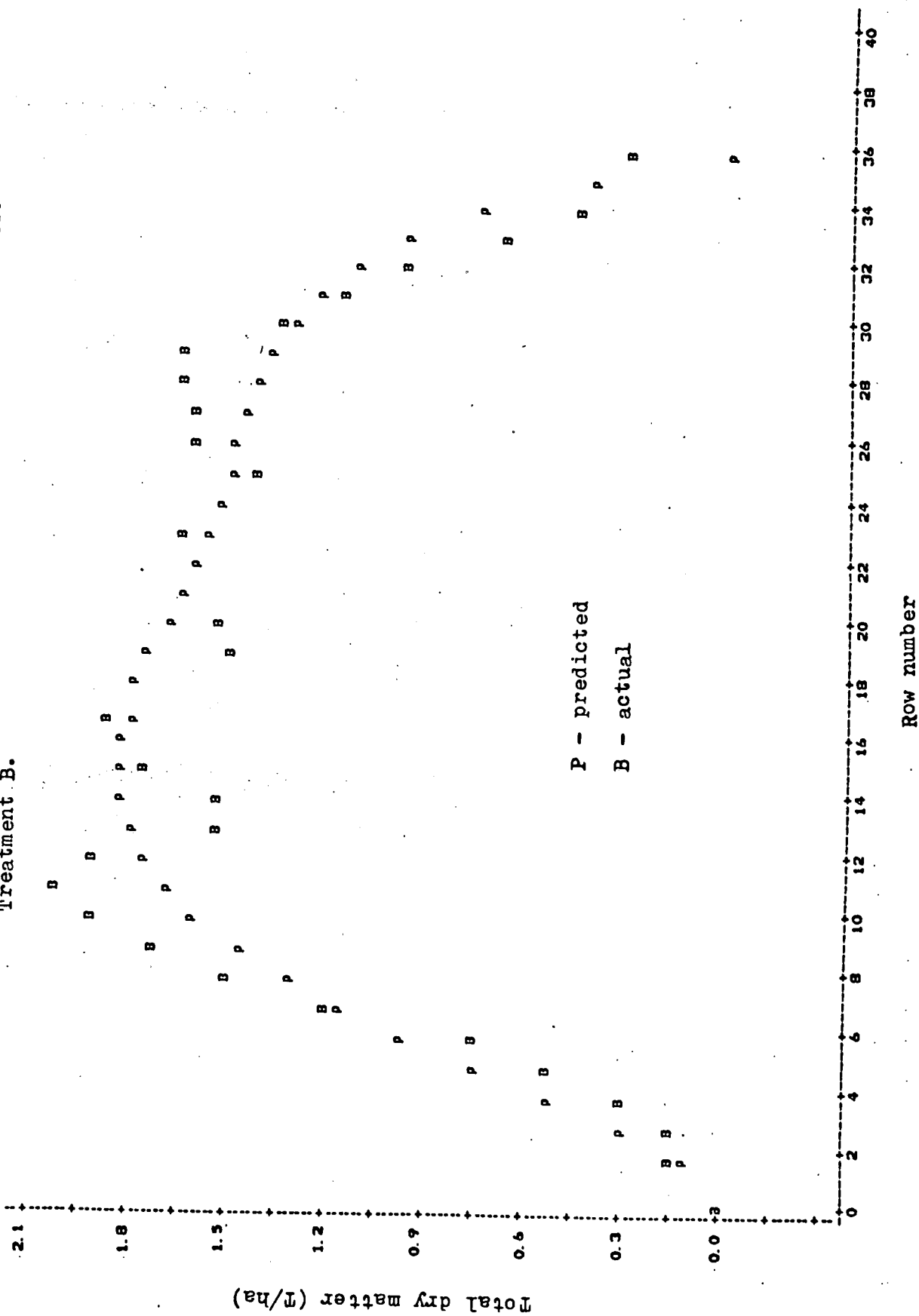
)

Appendix 1. Yield of corn (Halameesh) as a function of row number.
Treatment A.

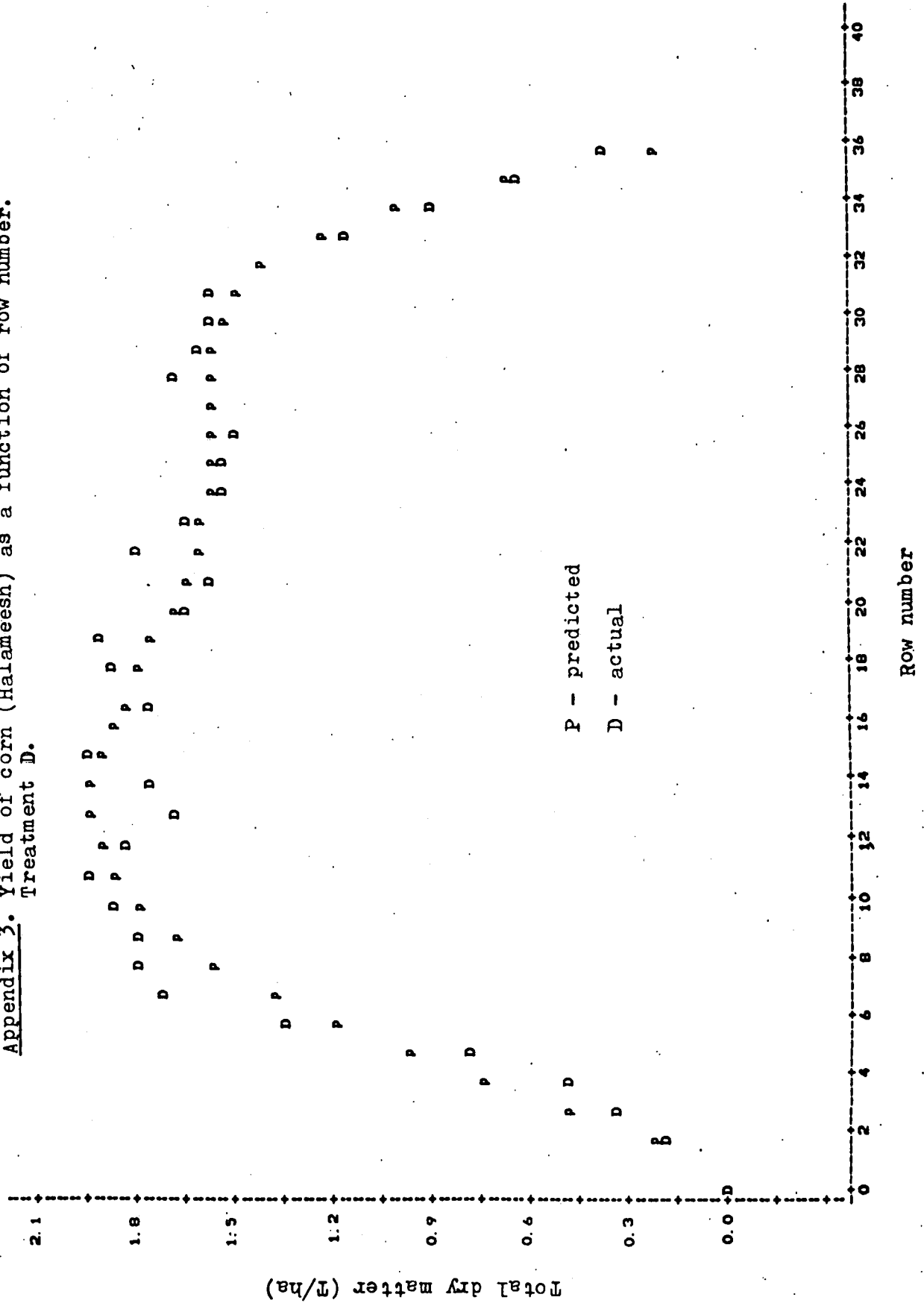


Row number

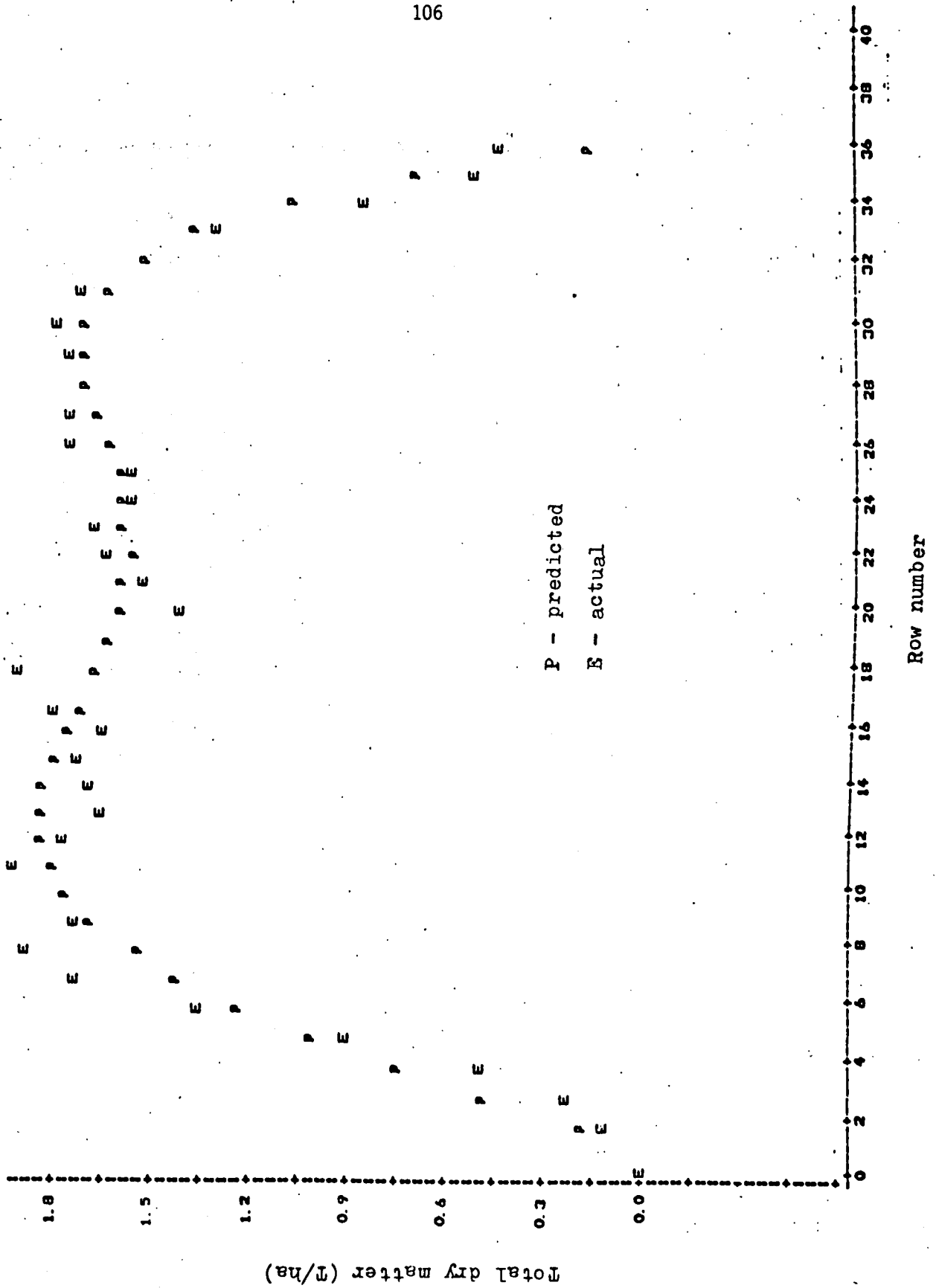
Appendix 2. Yield of corn (Halameesh) as a function of row number.
Treatment B.

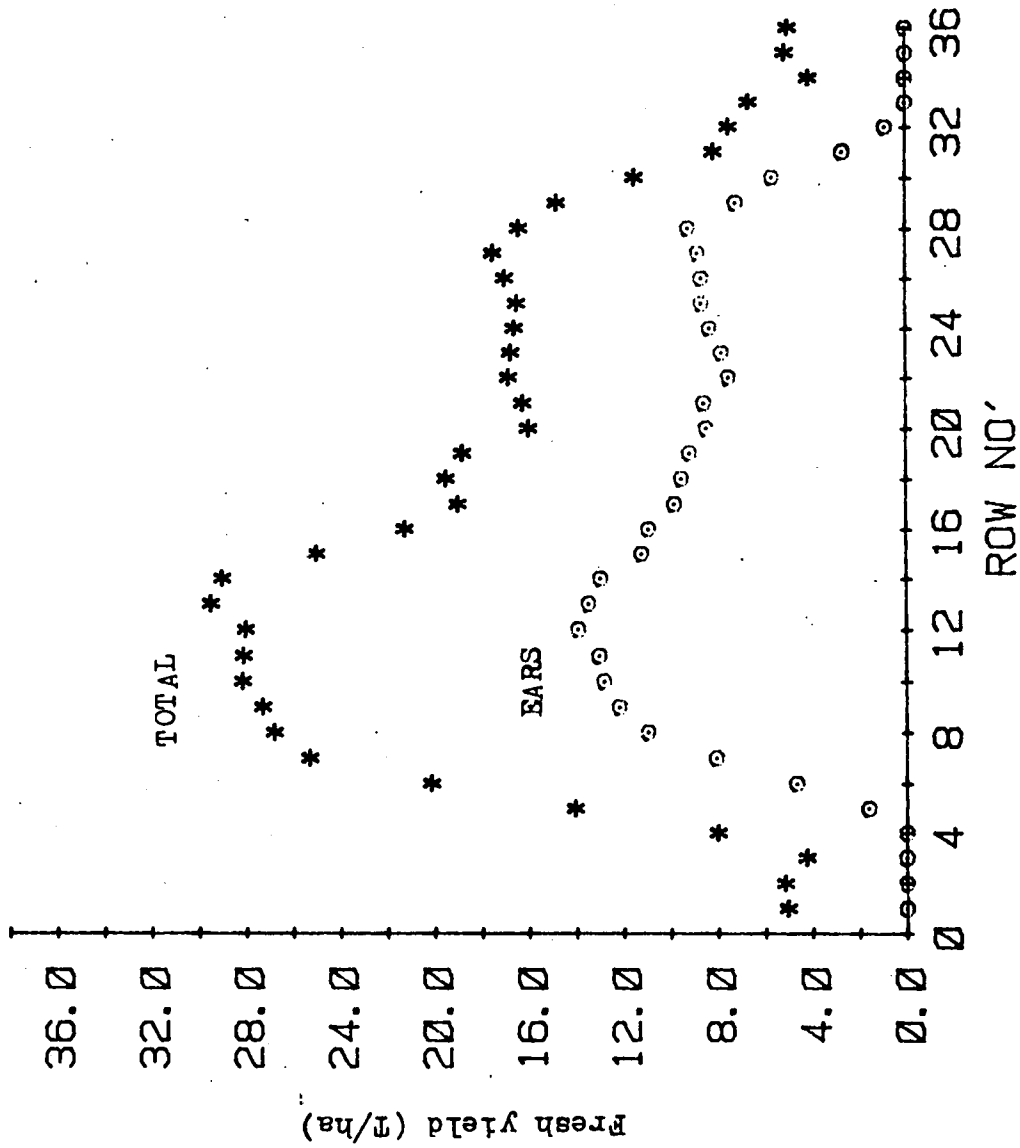


Appendix 3. Yield of corn (Halameesh) as a function of row number.
Treatment D.

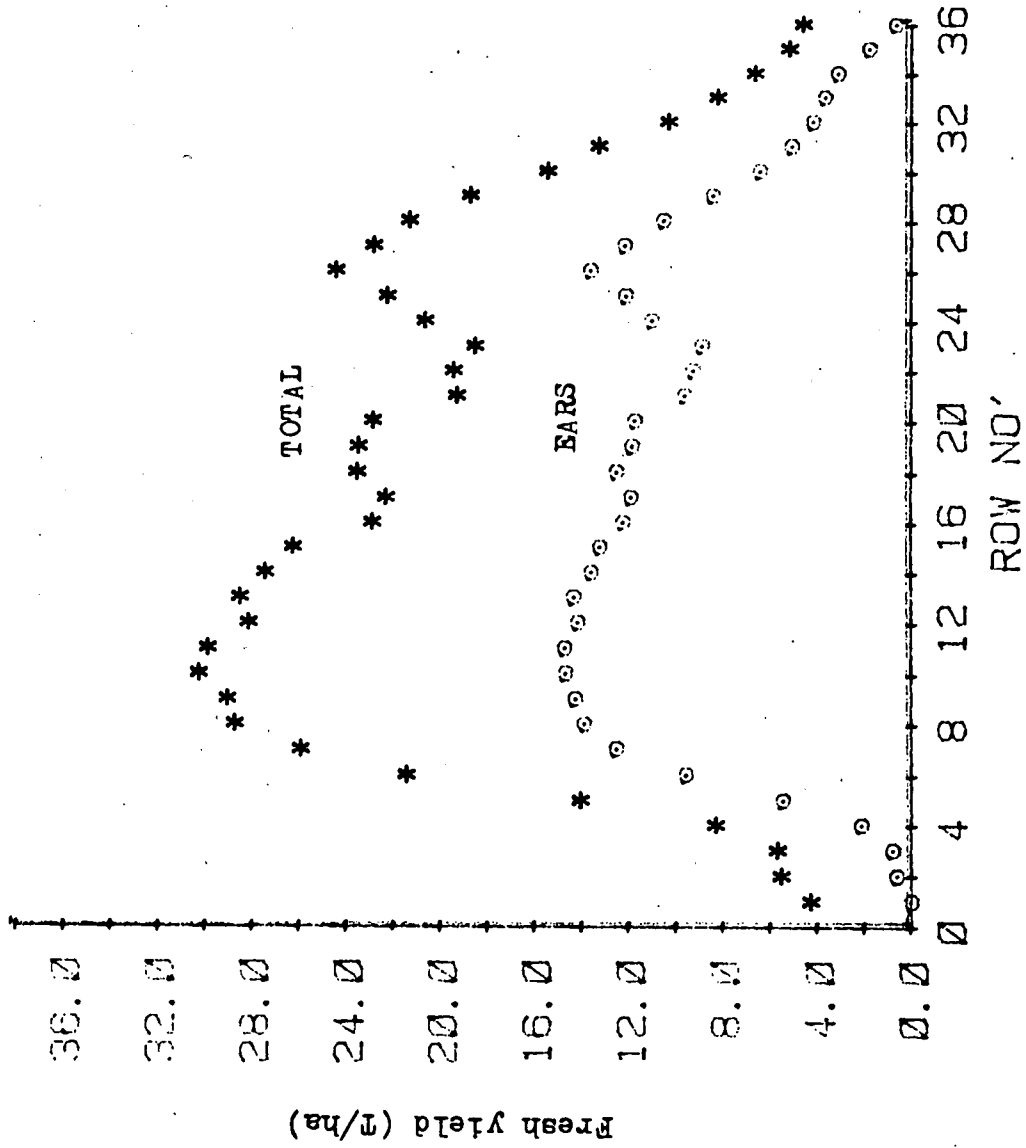


Appendix 4. Yield of corn (Halameesh) as a function of row number.
Treatment E.

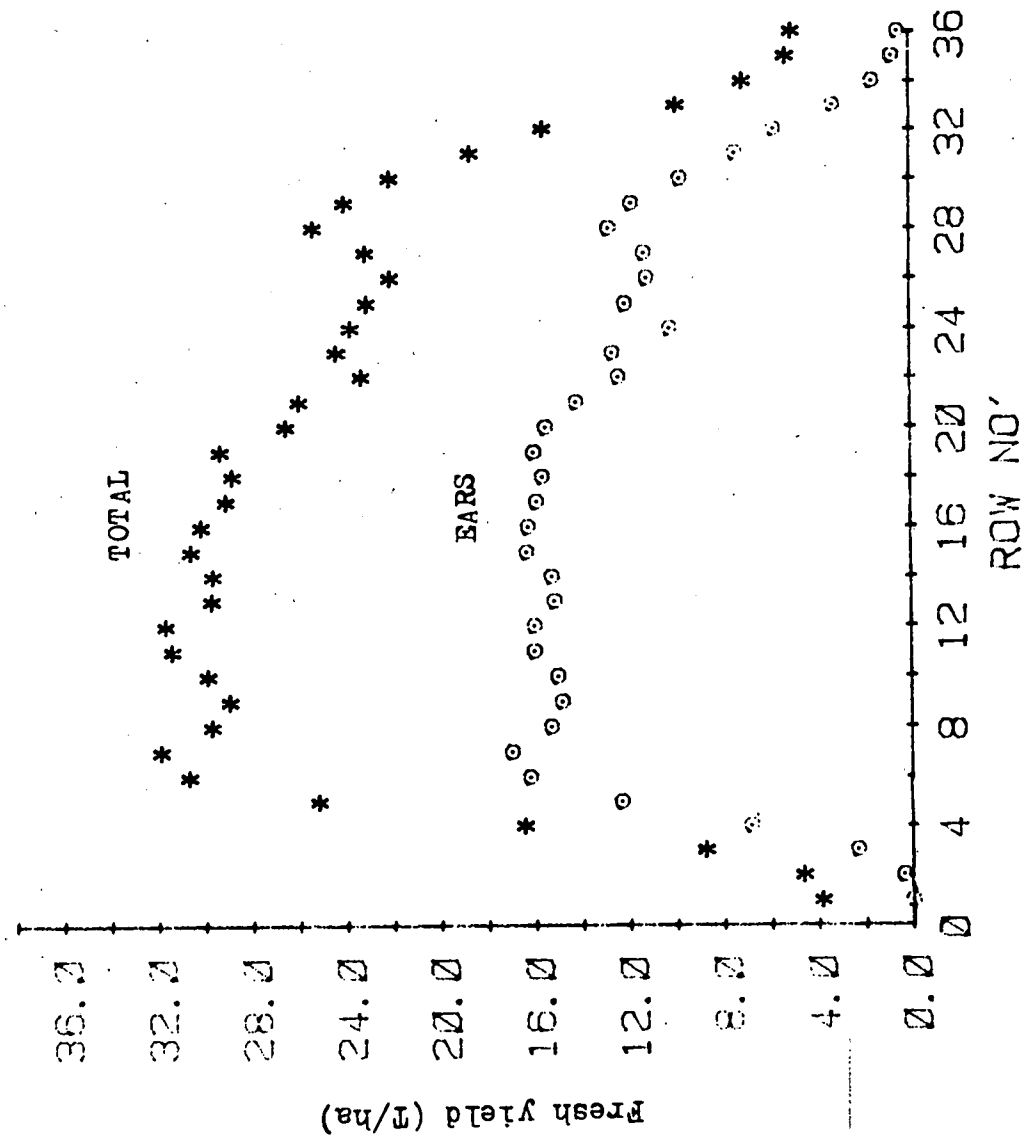




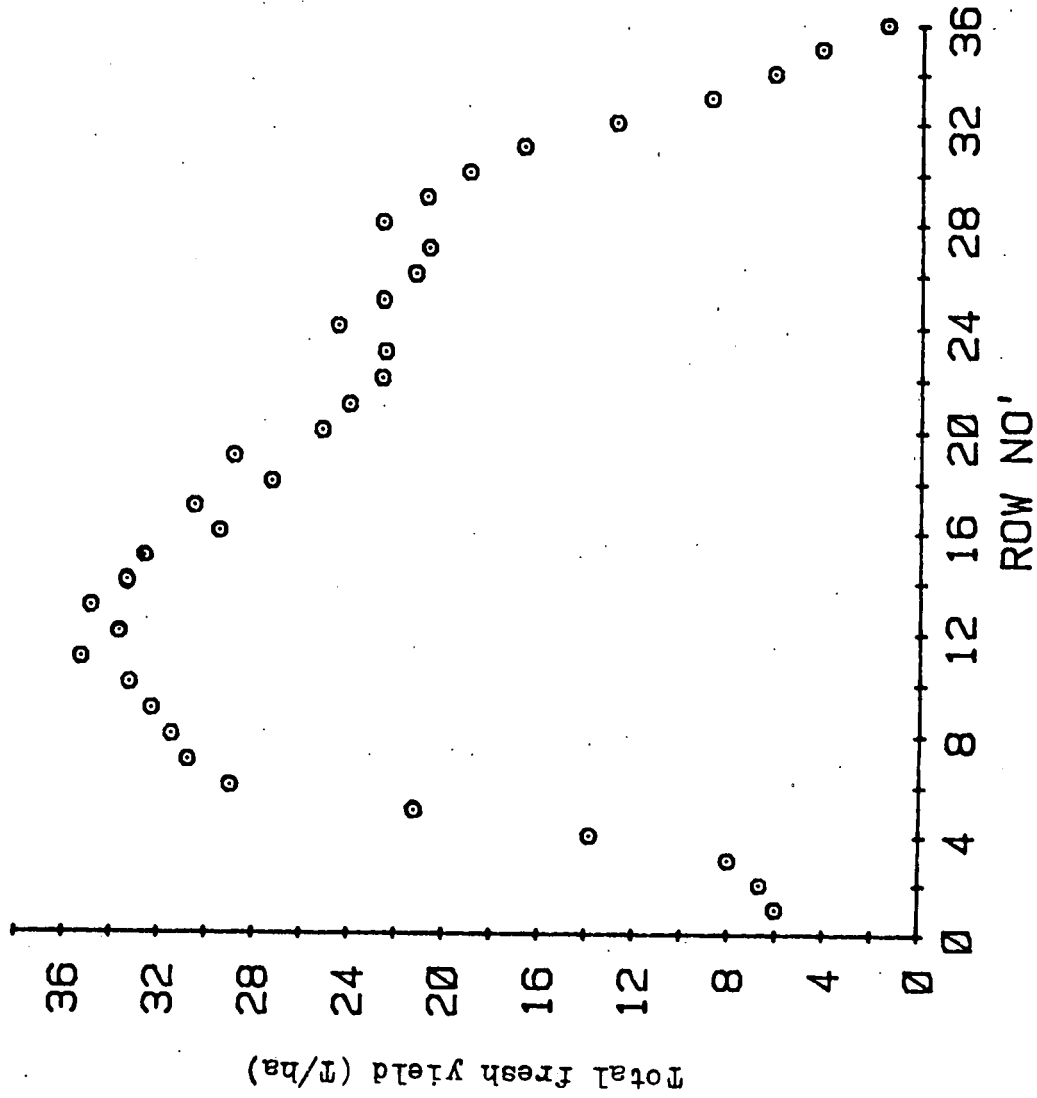
Appendix 5. Yield of corn (Jubilee) as a function of row number.
Treatment A.



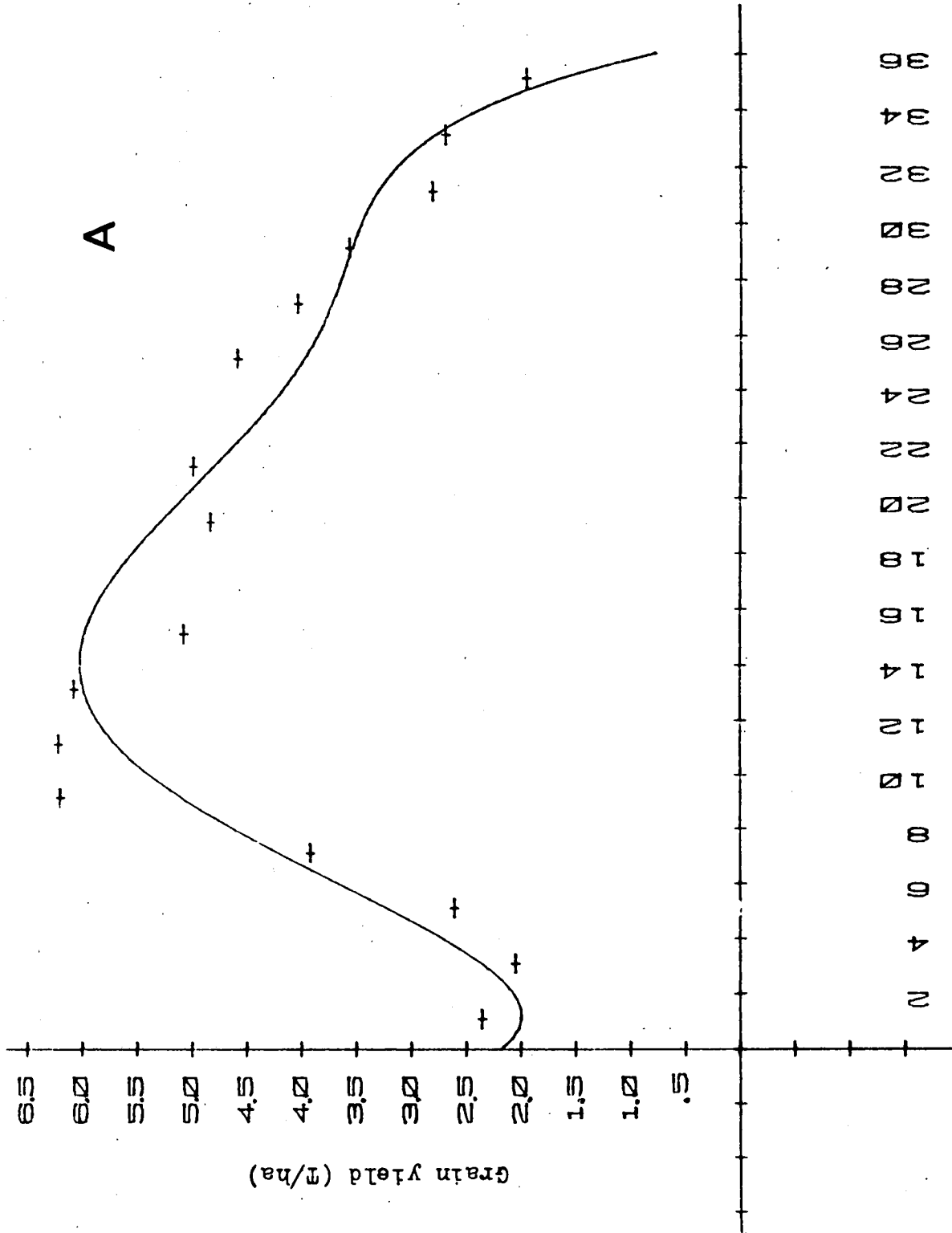
Appendix 6. Yield of corn (Jubilee) as a function of row number.
Treatment B.



Appendix 7. Yield of corn (Jubilee) as a function of row number. Treatment D.

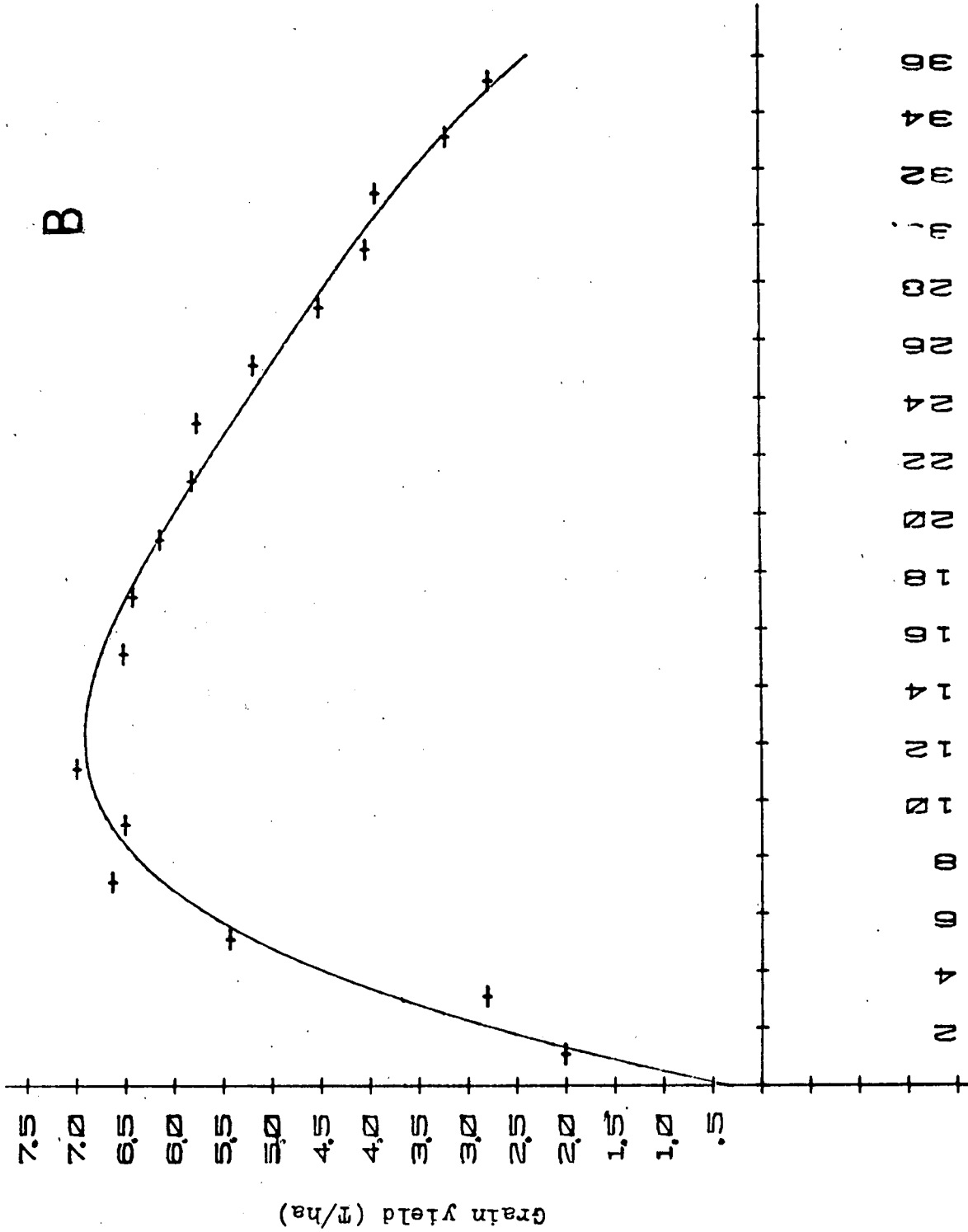


Appendix 8. Yield of corn (Jubilee) as a function of row number.
Treatment B.

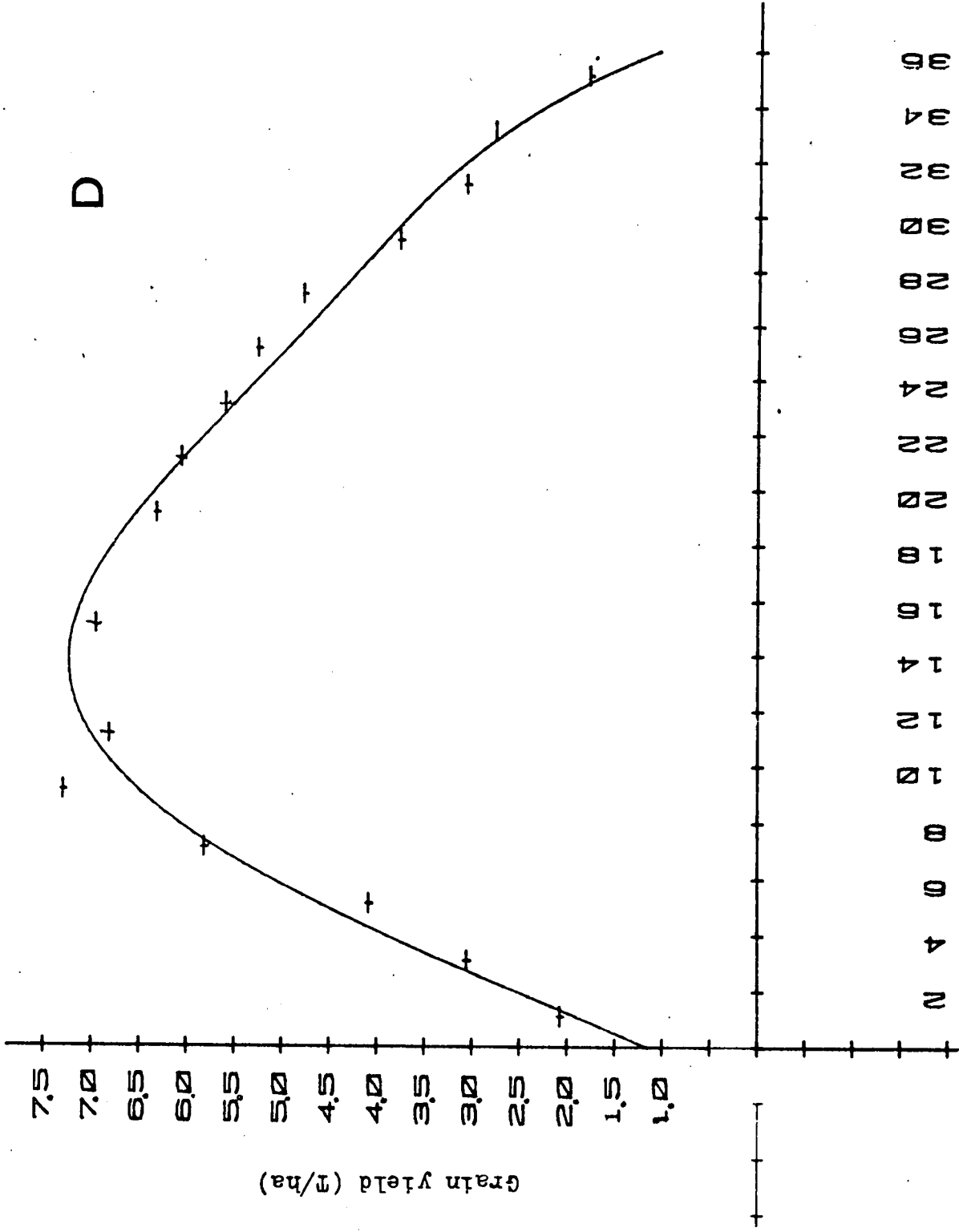


Row number

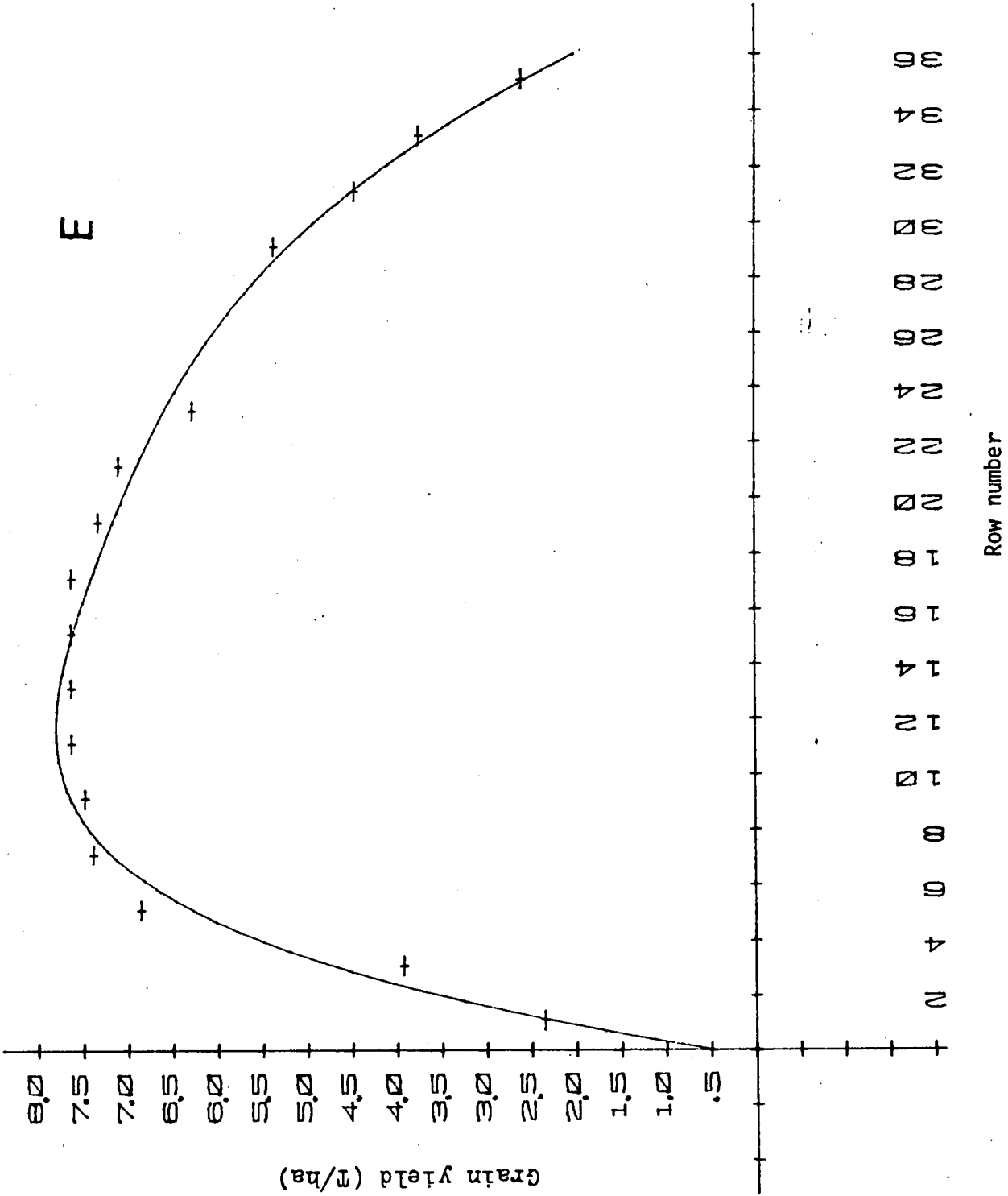
Appendix 9. Wheat grain yield as a function of row number.
Treatment A.



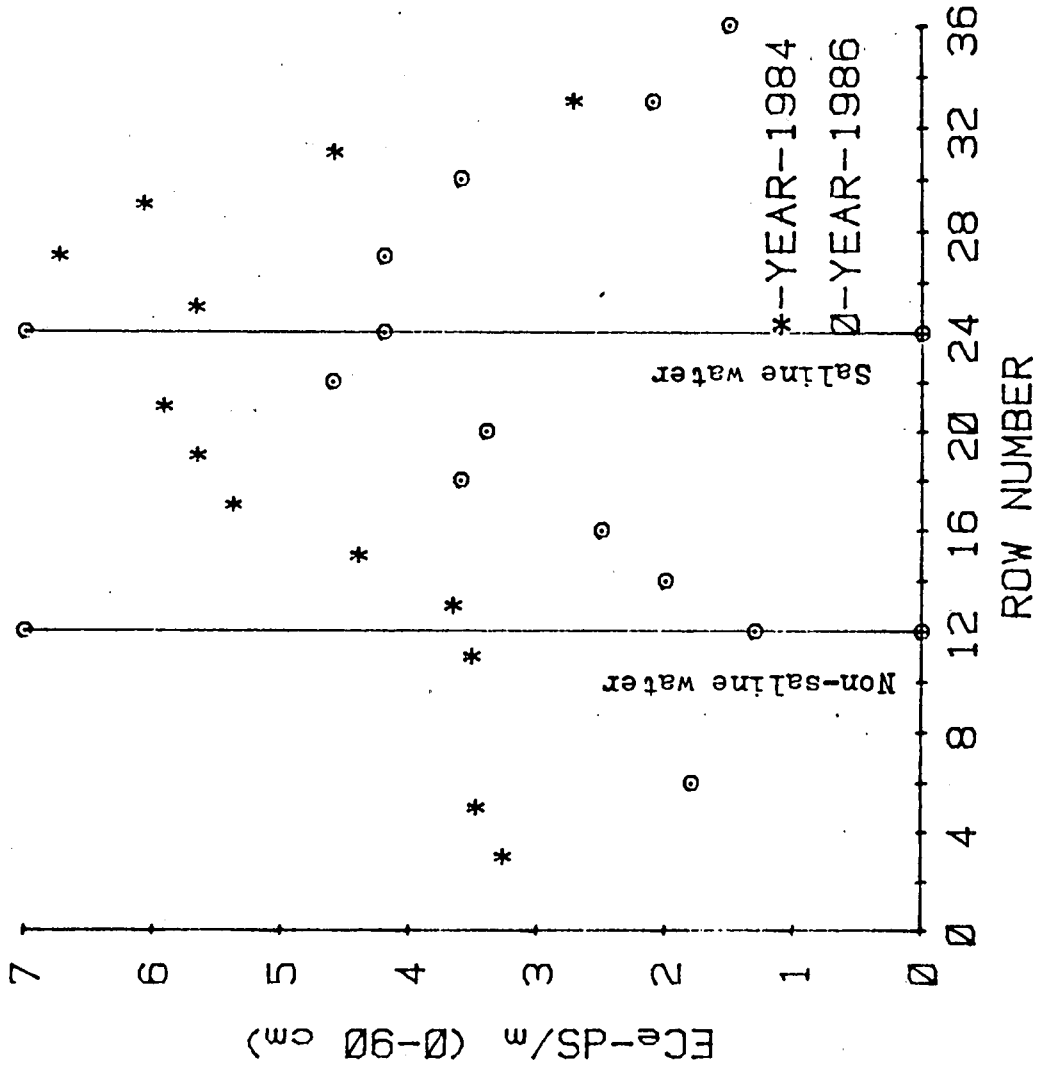
Appendix 10. Wheat grain yield as a function of row number.
Treatment B.



Appendix 11. Wheat grain yield as a function of row number.
Treatment D.

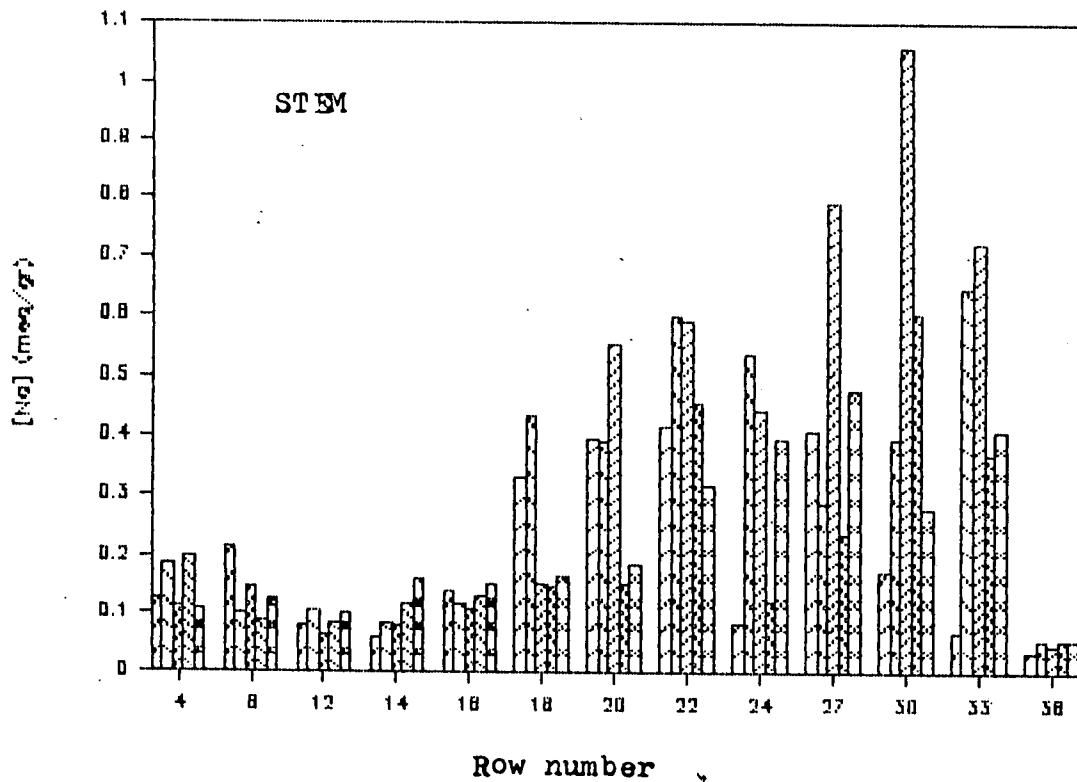
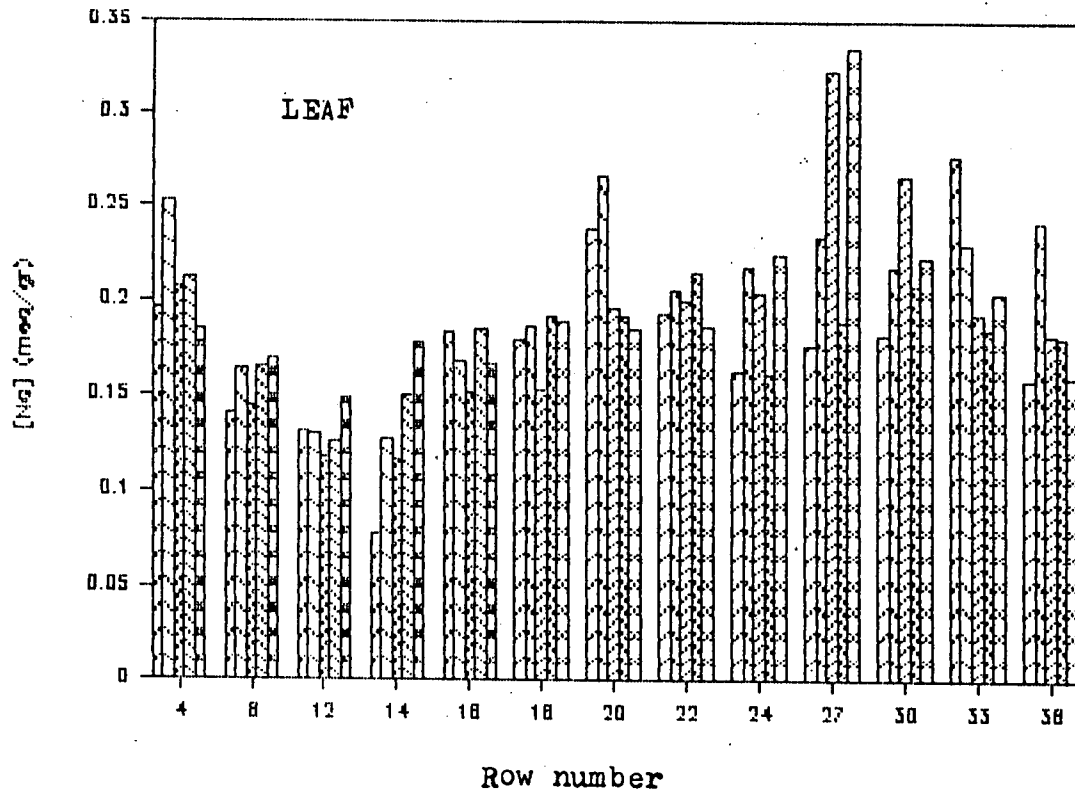


Appendix 12. Wheat grain yield as a function of row number.
Treatment B.



Appendix 13. ECe (0-90 cm) as a function of distance from the irrigation lines after the first and third years.

Appendix 14. Na concentration in the leaf and stem of Jubilee corn.



E C e

ROW	A			B			C			D			E		
	0 - 90	0 - 120	0 - 180	0 - 90	0 - 120	0 - 180	0 - 90	0 - 120	0 - 180	0 - 90	0 - 120	0 - 180	0 - 90	0 - 120	0 - 180
4	5.20	4.28	3.61	2.76	2.30	2.11	2.40	2.20	2.14	2.65	2.43	2.19	3.32	2.91	2.82
6	4.19	3.50	2.90	2.92	2.44	2.08	3.22	2.77	2.61	3.40	3.30	2.78	3.60	3.26	2.84
12	3.99	3.73	3.22	3.73	3.45	3.19	3.88	3.27	2.89	2.67	2.62	2.43	3.28	2.88	2.42
14	5.47	4.95	4.64	4.04	3.66	3.36	2.74	2.60	2.35	3.22	2.86	2.85	2.81	2.59	2.32
16	6.64	5.75	5.05	5.21	4.74	4.26	3.77	3.43	3.09	3.12	3.07	2.87	3.25	3.14	2.89
18	6.13	5.61	4.90	6.14	5.50	4.59	5.92	5.25	4.33	3.80	3.79	3.58	4.93	4.50	3.91
20	7.87	7.27	6.34	6.25	5.57	4.79	5.28	4.69	4.20	3.49	3.48	3.39	5.42	5.07	4.69
22	6.68	6.19	5.49	6.18	5.93	4.96	5.94	5.80	5.40	5.66	5.58	4.67	5.15	4.84	4.51
24	5.36	5.38	4.94	5.82	5.28	5.01	5.16	5.10	4.76	5.38	5.11	4.53	4.89	4.61	4.20
26	6.19	5.86	5.35	7.61	6.93	5.85	7.14	6.73	5.97	5.90	5.52	5.16	6.04	5.43	5.05
28	7.45	6.46	5.68	6.06	5.57	5.12	7.52	7.17	6.61	6.96	6.29	5.58	5.70	5.57	5.40
30	4.84	4.48	3.82	4.84	3.98	3.64	7.65	6.61	5.51	6.87	6.85	6.36	6.21	6.20	5.73
32	3.79	3.25	2.92	4.57	4.57	4.57	4.56	3.97	3.90	4.40	4.02	3.72	5.62	5.38	5.38
34	2.24	1.93	1.65	2.84	2.84	2.84	3.13	2.84	2.76	2.56	2.25	2.04	2.85	2.51	2.39

Appendix 16. BCE (ds/m) values of the various treatments as a function of row number (1986).

E C e (ds/M); Average values

ROW	0 - 50	0 - 120	0 - 180
4	3.26	2.82	2.57
6	3.47	3.05	2.64
12	3.51	3.19	2.83
14	3.66	3.33	3.10
16	4.40	4.03	3.63
18	5.38	4.93	4.24
20	5.66	5.22	4.68
22	5.92	5.67	5.01
24	5.32	5.10	4.69
26	6.57	6.09	5.48
28	6.74	6.21	5.68
30	6.08	5.62	5.01
32	4.59	4.24	4.10
34	2.72	2.47	2.33

VALIDATION OF A MODIFIED STEADY STATE MODEL OF
CROP RESPONSE TO SALINE WATER IRRIGATION
UNDER TRANSIENT CONDITIONS

A J A Vinten*
H Frenkel**
and J Shalhevet**

* Edinburgh School of Agriculture, West Mains Road, Edinburgh EH9 3JG.
The experimental part of this work was carried out when the author
was a Research Associate at the Institute of Soils and Water, PO
Box 6, Bet Dagan, Israel.

** Institute of Soils and Water, Departments of Soil Physical Chemistry
and Environmental Physiology, respectively.

Summary

A recently published semi-empirical model of crop response to irrigation with saline water is tested using data from three field experiments under non-steady state conditions with respect to root zone salinity. Difficulties in applying the model under these circumstances occur (Fig. 3), when global input parameters are chosen. This situation is improved, particularly in the case of a trickle irrigation experiment, when local parameters are used. A modification which calculates effective seasonal root zone salinity using a simple salt balance and a piston flow approximation of solute transport is proposed. For the two experiments where this modified approach was tested predictions were improved somewhat (Figs. 4, 5 and 6). Predicted leaching requirements were much reduced compared with the original steady state model (Fig. 1) in the case where the root zone is initially non-saline. This is relevant to attempts to minimising salt burdens to soils, ground water and return flow by reducing leaching fractions applied to crops irrigated with saline water, especially where winter rainfall is sufficient to leach a large proportion of the residual salts.

Introduction

Effective use of the extensive saline ground and surface water resources that exist in many arid or semi-arid regions of the world requires that efficient use is made of the water and that further salinisation of these resources by deep percolation or return flow from irrigated land is minimised. One way to achieve these aims is to minimise the amount of irrigation water applied for leaching of excess salts. This reduces both the volume and the total salt burden of drainage water percolating to ground water or returning to surface water systems (Rhoades, 1972). However such minimal leaching must be managed carefully to ensure that yields are not impaired by gradual salinisation of the root zone both within a single season and cumulatively over a lengthy period of irrigated agriculture, and to ensure that the sodium hazard of the drainage water does not become unacceptable. A valuable aid to this management is the use of semi-empirical models of crop response to irrigation with saline water, which help accurate scheduling of irrigation requirements to be done.

Letey and Dinar (1986) recently published a semi-empirical simulation model for prediction of crop water response functions when irrigated with saline water. The model assumes that the salt distribution in the root zone is that which would occur under steady state water uptake. However they showed reasonable agreement also under non-steady state conditions when a weighted mean irrigation water salinity was used. Such simple semi-empirical models have practical advantages over mechanistic models, but the validity of this model under non-steady state conditions is questionable on both theoretical and practical grounds. Moreover, in most practical irrigation situations,

steady state situations with respect to salinity do not occur. Therefore the model has been tested using data from independent experimental work (Vinten et al., 1986; Shalhevet et al., 1985; Frenkel et al., unpublished) and a modification to allow for transient conditions is introduced.

Theoretical considerations

The principal components of the model of Letey and Dinar (1986) are described here briefly. An empirical relationship relates yield to applied water, when non-saline irrigation water is used:

$$Y_{ns} = S(AW - AW_t) \text{ for } AW_t < AW < ET_{max} \quad (1a)$$

$$\text{or } Y_{ns} = Y_{max} \text{ for } AW_t > ET_{max} \quad (1b)$$

where ET_{max} = evapotranspiration at maximum yield (cm)

Y_{ns} = yield with non-saline water (kg/m^2)

S = slope of production function ($kg/m^2 \text{ cm}$)

AW = applied water (cm)

AW_t = applied water at zero yield (cm)

The slope of the response function (S) depends on crop type and the local climatic conditions. At some minimum applied water (AW_t) yield is zero. When irrigating with saline water with an amount AW_1 , a yield deficit (YD) occurs at any given application amount resulting in unused water which is lost by deep percolation (D). The yield deficit which occurs depends on the mean root zone salinity estimated from the saturated paste electrical conductivity $(\overline{EC_e})_x$ averaged over the root zone.

$$YD_s = \frac{Y_{ns}}{100} B(\overline{EC}_e - C) \quad (2)$$

where B = slope of response function to root zone salinity (kg/m dS)

C = threshold of response function to root zone salinity (dS/m)

Y_{ns} = yield with non saline water for a given AW (kg/m²)

YD_s = yield deficit compared with non-saline water (kg/m²)

The average root zone salinity is estimated assuming an exponential root uptake function (Raats, 1974) using a value of α of 0.20 (Hoffmann and van Genuchten, 1983) and assuming steady state conditions.

$$(\overline{EC}_e)_x = \frac{\overline{EC}_i}{2} \left[\frac{1}{L} + \frac{0.2}{L} \left\{ L + (1 - L) \exp(-5) \right\} \right] \quad (3)$$

where $(\overline{EC}_e)_x$ = depth averaged root zone salinity (dS/m)

L = leaching fraction (dimensionless)

\overline{EC}_i = average irrigation water salinity (ds/m)

The value of L is given by:

$$L = \frac{D}{AW} = \frac{YD}{AW S} \text{ for } AW_t < AW < ET_{max} \quad (4a)$$

$$\text{or } L = 1 - \frac{ET}{AW} \text{ max} + \frac{YD}{AWS} \text{ for } AW > ET_{max} \quad (4b)$$

where D = deep percolation (cm)

Under non-steady state conditions the value of EC_i can be calculated from a weighted mean value:

$$\overline{EC}_i = \frac{I_p EC_{ip} + I_A EC_{iA}}{S_i - S_f + I_p + I_A} \quad (5)$$

where $(S_i - S_f)$ = change in soil water storage in the root zone from beginning to end of the experiment (cm)

I_p = Irrigation prior to initiation of saline irrigation (cm)

I_A = Irrigation after initiation of saline irrigation (cm)

EC_{ip}, EC_{iA} = electrical conductivity of respective irrigation waters (dS/M)

The use of $(S_i - S_f)$ allows use of water from soil moisture storage to be accounted for. It is assumed that the profile is initially non saline. When estimating potential yield from water application the change in storage should also be included.

As Letey and Dinar point out, when they consider situations where EC_i varies, this model is not strictly valid under non steady state conditions. There are several reasons for this and we shall deal chiefly with two:

- (A) The model has limitations when applying the global parameter estimates (ie values purported to be non site specific) to new sites because the water lost at zero yield (AW_t) will be sensitive to method and frequency of irrigation. For example, drip irrigation will give low AW_t because little water loss by evaporation occurs during crop establishment. Local estimates of the model parameters may, however, be difficult to obtain. In this paper we compare local estimates of model parameters based on experimental data which we are using to test the model, with Letey and Dinar's global values. It would also be difficult to apply the model to an already saline profile because the root zone salinity under non-steady state conditions is estimated

using only the average irrigation water salinity and the leaching fraction (eq. 3).

- (B) The model assumes that the distribution of salts in the root zone is that of the steady state estimation of Raats (1974), with EC_i given by eq. (5). This will not always be the case, particularly when irrigation with saline water on initially non-saline soil occurs.

In this paper we propose an alternative for estimating the time and depth averaged root zone salinity which should be more valid under non-steady state conditions, and deal with the case of an initially salinised profile by making the following assumptions:

- (1) Piston displacement of the water and salt initially present in the soil profile by irrigation water occurs.
- (2) The initial salt concentration (EC_{e_i}) is uniform throughout the root zone.
- (3) The effective seasonal root zone salinity is the arithmetic mean of the average root zone salinity at the beginning (\overline{EC}_{e_i}) and at the end of the season (\overline{EC}_{e_f}).

Using assumptions (1) and (2) the final root zone salinity can be determined by estimating the proportion of the salt initially present within the root zone which is leached and calculating the amount of salt applied with the irrigation water, assuming none of the latter is leached.

Assuming piston displacement the proportion (L_s) of solute initially

present in the soil displaced by the seasonal leaching fraction (eq. 4a or 4b) is:

$$L_s = \frac{AW L}{Z\theta_i} \quad (6)$$

where θ_i = initial root zone water content (cm^3/cm^3)

Z = root zone depth (cm)

as long as $AWL < Z\theta_i$. This inequality will usually hold unless excessive leaching fractions are used.

The final root zone salinity can then be calculated by a simple salt balance:

$$\overline{EC}_e = \frac{\overline{EC}_i AW}{Z \theta_s} + \overline{EC}_{e_i} (1 - L_s) \quad (7)$$

where θ_s = saturated paste water content (cm^3/cm^3)

And the mean root zone salinity over the season is then simply:

$$\overline{EC}_e = \frac{\overline{EC}_{e_f} + \overline{EC}_{e_i}}{2} \quad (8)$$

By substituting for L from eq. 4(a) or 4(b) into eq. (8) and from eq. (8) for \overline{EC}_e into eq. (1) a value of YD_s can be estimated, as for the steady state case.

This approach requires knowledge of several additional parameters (\overline{EC}_{e_i} , Z , θ_i and θ_s) but meets the objection raised above to the use of the steady state model under transient state conditions.

Fig. 1 shows the influence that the proposed non-steady state approximation has on the production function of yield against applied water compared with the steady state assumptions. The parameters used are the local values for the forage corn in Table 2 (below). Values of $(S_i - S_f = 0, \overline{EC}_{e_i} = 0.9 \text{ dS/m}, \theta_i = 0.20, \theta_s = 0.50$ and $Z = 150 \text{ cm}$ were chosen. There are several notable differences between the predicted production functions. Firstly, much higher maximum yields are predicted, and with considerably less water, with the higher salinity water using the transient state modification. Secondly, the transient state model predicts very similar production functions with low and high salinity irrigation waters, when deficit irrigation is practised. Thirdly, the transient state model shows a maximum in the response curve to water, not a plateau. This is due to the additional salt which accumulates in the root zone when large amounts of water are applied. The extra water displaces soil water with a low solute concentration. Fig. 2 shows a similar comparison except \overline{EC}_{e_i} is now 6.0 dS/m. In this case the steady state model over-predicts yields at the low EC_i value, compared with the modification proposed here. At high EC_i there is little difference between two curves.

Clearly it is necessary to determine which of these two models better describes yield response to irrigation when irrigating with saline water under non-steady state conditions. This is done for three field experiments described below.

Materials and Methods

The experimental data used to test this model come from three field experiments using saline and non-saline water at a wide range of

application rates. Experimental details are given in Table 1. The applied water was estimated from day zero, including any soil water storage change measured from the start of differential irrigation to the end of the experiment. It was assumed that all irrigation water applied prior to the start of differential irrigation was lost by evapotranspiration before the first differential irrigation, ie:

$$AW = I_A + I_p + (S_i - S_f) \quad (9)$$

I_A = Irrigation from start of differential irrigation (cm)

I_p = Irrigation from sowing to start of differential irrigation (cm)

$(S_i - S_f)$ = Water used from storage between just prior to start of differential irrigation and harvest (cm)

In these experiments seasonal crop evapotranspiration was estimated using one of three methods. In Gilat, where irrigation intervals varied between $3\frac{1}{2}$ days and 3 weeks, ET was estimated from changes in moisture content between irrigations for all intervals other than $3\frac{1}{2}$ days assuming drainage between successive measurements was zero. In Ramat Hanegev ET was estimated similarly but a grid of neutron access tubes was used to characterise the water content distribution with lateral distance from the emitter. In Reim ET was estimated using pre-irrigation water contents only, assuming all water applied in excess of 'field capacity' was lost immediately through deep percolation. Local estimates of pan evaporation, maximum yield and S were also obtained. These parameter estimates are listed in Table 2, along with the global estimates given by Letey and Dinar, adjusted to local maximum yield and pan evaporation. More detailed descriptions

of methods used are given in the papers referred to in Table 1.

Results and Discussion

Fig. 3 shows the relative yield measured in each experiment (Y_{RM}) plotted against the applied water divided by local pan evaporation (AW/E_p). Five salinity treatments were used in the Gilat experiment (Fig. 3a), two in the Reim experiment (Fig. 3b) and three in the Ramat Hanegev (Fig. 3c) experiment (though three were used in Ramat Hanegev no values of $(S_i - S_f)$ were obtained for the third salinity level so AW could not be estimated). Only a representative selection of yield data from Reim are used, being those where values of $(S_i - S_f)$ and ET are also available.

Production functions predicted by the original model of Letey and Dinar are also plotted in Fig. 3 using the global parameter estimates provided in their paper. The numbers on the curves are the average irrigation water salinities calculated from eq. (5) for S1, S3 and S5 (sweet corn) or for S1 and S2 (forage corn and tomatoes). In all three cases important discrepancies occur which can be attributed to several causes. Firstly, using a single value for the average irrigation water salinity is incorrect as \overline{EC}_i depends on amount of water applied. Correction of this will using eq. (5) tend to bring the production functions closer together when deficit irrigation occurs. This correction has been made for all the comparisons that follow. Secondly, the global estimates (especially of AW_t) may be inappropriate. This is most evident in the case of the tomatoes which were trickle irrigated but may also be a problem with the sweet corn. Thirdly, the steady state model assumes a time invariant root zone salinity, whereas in all three cases considered here, this is

not the case. Correction of this will also tend to bring the production functions closer together when deficit irrigation occurs (see Fig. 1). The relative importance of the last two effects can be investigated by comparing predicted and observed yields using the unmodified and modified versions of the model and the following combinations of global and local parameters (see Table 2):

- (A) global parameters for both eq. (1) and eq. (2);
- (B) local parameters for both eq. (1) and eq. (2);
- (C) local parameters for eq. (1) and global parameters for eq. (2);
- (D) local parameters for eq. (2) and global parameters for eq. (1).

Local parameter estimates for eq. (2) were available only for Gilat, but these values were also used for Reim as they agreed well with the figures of Maas and Hoffmann (1977) and Bresler, McNeal and Carter (1983). The variety of forage corn used at Reim was considered locally to be a salt tolerant variety, so even the smaller value of B used (9.1 for total yield) may have been an overestimate. Accurate values of AW_t and S were difficult to obtain for the sweet corn because the spread of observed yields and ET estimates was small. Therefore there was a large difference between the linear regression of yield on ET and the linear regression of ET on yield. The latter regression was used (in this case only) as it gave a positive intercept on the ET axis and a more reasonable value of S . Comparison between measured and predicted yields are shown in Fig. 4, using the original, unmodified model.

Agreement between measured and predicted yields was assessed in three ways, as suggested by Letey et al. (1985). These three methods were:

(1) the correlation coefficient, (2) the mean deviation between measured (Y_M) and predicted yields (Y_p) and (3) the ratio between mean predicted and mean measured yields (Y_M/Y_p). Values of these statistical comparisons are given in Table 3. Correlation coefficients were high (> 0.85) in all cases but the values of the mean deviation and Y_p/Y_M were quite variable. For example the global parameters clearly did the best overall job for predicting the sweet corn yields, though Fig. 3 suggests this is fortuitous (Fig 4Ia) but were very poor for the tomatoes (Fig 4IIa). The latter problem is chiefly due to the fact that the tomatoes were trickle irrigated, so that much lower quantities of water were used for evaporation. Thus when local parameter estimates of AW_t and S were used (Fig. 4IIb) good agreement was obtained with an average of 9.2% error in estimating the true yield and an overall 6% underprediction of yield. These deviations are larger than obtained by Letey et al. (1985) but their experimental conditions were closer to steady state. There appears to be no systematic difference in agreement for high and low salinity results, implying that the global values of B and C in equation (2) and the steady state model are adequate. For the sweet corn data there is a systematic difference between the salinity treatments. Deviations between measured and predicted yields occur at the low salinity level, when global parameter estimates are used (Fig. 4Ia). When local parameters are used (Fig. 4Ic), yields with the high salinity irrigation water are underpredicted. When a combination of global and local parameters are used (Fig. 4Ib) yields are systematically overpredicted. These difficulties suggest that the initial soil salinity ($\overline{EC}_{e_i} = 3dS/m$) and transient conditions need to be accounted for. The use of the local estimates may be more correct though as it stands all plot yields at higher salinity levels were underpredicted using local values.

For the Reim data (Fig. 4II) agreement between predicted and measured yields is best when the local values of B and C are used and the global estimates of Awt and S are used (Fig. 4IIb). However there is some deviation when yields approach Y_{max} . This is because of the inefficient way in which water was applied during one of the irrigations of this experiment. A large excess of non-saline water was applied to both saline and non-saline treatments, resulting in large losses by deep percolation. This highlights the problem with assuming that all applied water is used for evaporation when yield with non-saline water is less than Y_{max} . Yields with saline water are systematically underpredicted when deficit irrigation occurs. This is again likely to be due to the steady state assumption in the original model.

Introducing now the modified transient state model, with local parameters, predicted yields were recalculated (Fig. 5). The statistical tests for this transient model are shown in brackets next to the values for the steady state model in Table 3. For the sweet corn, predictions are improved considerably (Fig. 5a). Mean deviation between measured and predicted results goes down from 24.6% to 9.0% and (Y_p/Y_M) approaches much closer to unity. For the forage corn the deviation between measured and predicted yields at high water application rates is due to inefficient water application, so it would not be expected to obtain good predictions of these results. However when deficit irrigation occurs, better prediction of yield with saline water occurs than with the original. There is no systematic difference between high and low salinity treatments.

Fig. 6 shows a comparison between the time and depth averaged root

zone salinities ($\overline{EC_e}$) predicted by the steady state model (eq. 3) and those actually measured for the sweet corn and forage corn experiments. Overprediction of $\overline{EC_e}$ occurs in the case of the forage corn (Fig. 6b) and also at high salinity levels and large irrigation intervals for the sweet corn (Fig. 6a). No comparison of this kind is possible for the tomato experiment, because drip irrigation was used so a meaningful value of average root zone salinity is hard to obtain. This confirms why the steady state model tends to underpredict yields when high salinity irrigation water is used (see Figs. 4Ic and 4Iic). When similar plots are made (with local parameters) using the transient state modification (Figs. 6c and 6d) considerable improvement occurs.

To summarise, the overall effects of the proposed modifications are given in Fig. 7. This shows predictions for each crop as production functions overlaying the yield data of Fig. 3 when all the above corrections are made. Compared with Fig. 3 model predictions are markedly improved due in part to each of the three modifications (ie corrected EC_i values, local parameters and transient conditions). Note that in the case of the tomatoes no correction for transient state conditions has been made, because the assumptions involved are invalid for trickle irrigation.

The transient state modification to Letey and Dinar's model, when appropriate, has implications when planning irrigation schedules for saline water because if the root zone at the beginning of the season is non-saline, leaching fractions required to maintain yields for that season will be much less than the steady state model of Letey and Dinar's predicts. This will save water, diminish rates

of salinisation of the soil and diminish salt burdens in drainage water. However it is important that sufficient winter rainfall occurs to ^{leach} most of the salts left behind. Otherwise over the course of several years salts will accumulate in the root zone, unless allowance for this is made in scheduling of successive irrigation seasons.

The validity of the assumption, in the transient state modification, that piston displacement of salt initially present in the soil occurs will depend on the dispersive properties of the soil at both pore and field scale (Bresler, McNeal and Carter, 1982) and on the irrigation method and intensity. It is quite unlikely, unless excessive irrigation is practised or the soil is initially very dry, that under the piston displacement assumption, any salts applied in irrigation water during the season will be leached below the rooting depth, at least for relatively deep rooting crops such as those used here.

Conclusion

In conclusion therefore the following statements can be made in assessing the use of Letey and Dinar's model under non-steady state conditions.

- (1) Adaptations need to be made to correct the average irrigation water salinity when non-saline water is used for establishment or is stored in the profile. Allowance must also be made for salts initially present in the soil profile.
- (2) It is important if possible to have good local estimates of salt tolerance and crop water use (ET), especially where trickle irrigation is used when a local value of AW_t , particularly,

is necessary. However in the results presented here it is difficult to decide unequivocally which parameters are more suitable.

- (3) When local parameters are used the steady state model overpredicts yield losses when irrigating with saline water (see Figs. 4Ic and 4IIc) under transient state conditions. Under transient conditions the predicted yields under deficit irrigation are nearly independent of irrigation water salinity (Fig. 1). By including a simple piston displacement assumption for solute transport and calculating the mean root zone salinity using a seasonal salt balance, predictions of mean root zone salinity (Fig. 6) and yields (Fig. 5) over the full range of salinities and irrigation amounts are improved somewhat. The only additional information this approach requires is the initial water content, initial soil salinity and the saturated paste water content.
- (4) The importance of the use of this transient state modification will decline when irrigation over many seasons occurs, especially where winter rainfall is low. Here the steady state model will become increasingly more appropriate as time goes on.

Acknowledgements

This paper presents results of experiments supported by grants from the US-Israel Binational Agricultural Research and Development Fund and the US Agency for International Development as part of the Co-operative Arid Lands Agricultural Research Program. The use of the program for the steady state model of Letey and Dinar is acknowledged.

List of References

- Bresler, E., McNeal, B.L. and Carter, D.L. (1982) Saline and Sodic Soils. Adv. Series in Agric. Sci. 10. Springer-Verlag, Heidelberg (236 pp.).
- Frenkel, H., Mantell, A., Vinten, A.J.A. and Meiri, A. A double line source sprinkler system for determining the separate and interactive effects of water and salinity on crop growth. (Unpublished).
- Hoffmann, G.J. and van Genuchten, M.T. (1983) Soil properties and efficient water use: water management for salinity control. In: Taylor, H.M., Jordan, W.R. and Sinclair, T.R. (eds.). Limitations to efficient water use in crop production. American Society of Agronomy, Madison, WI.53711, pp. 73-85.
- Letey, J. and Dinar, A. (1986) Simulated crop-water production functions for several crops when irrigated with saline water. *Hilgardia* 54, 1-32.
- Letey, J., Dinar, A. and Knapp, K.C. (1985) Crop-water production functions model for saline irrigation waters. *Soil Sci. Soc. Am. J.* 49: 1005-1009.
- Maas, E.V. and Hoffmann, G.J. (1977) Crop salt tolerance - current assessment. *J. Irrig. Drainage Div. ASCE* 103, No 1R2 Proc. Paper 12993, pp. 115-34.
- Raats, P.A.C. (1974) Steady flows of water and salt in uniform soil profiles with plant roots. *Soil Sci. Soc. Amer. Proc.* 38, 717-22.
- Shalhevet, J. (1984) Management of irrigation with brackish water. In: I. Shainberg and J. Shalhevet (eds.) *Soil Salinity and Irrigation. Ecological Studies* 51. Springer-Verlag, Heidelberg, pp. 298-318.
- Shalhevet, J., Vinten, A.J.A. and Meiri, A. (1985) Irrigation interval as a factor in sweet corn response to salinity. *Agron. J.* 78, 539-545.
- Vinten, A.J.A., Shalhevet, J., Meiri, A. and Peretz, J. (1986) Water and leaching requirements of industrial tomatoes irrigated with brackish water. *Irrig. Sci.* 7: 13-25.

Table 1

A. Details of experimental water use

<u>Site</u>	<u>Year</u>	<u>Crop</u>	<u>Irrigation</u>	<u>Range of AW/Ep</u>	<u>Soil type</u>	<u>Ref</u>
Gilat	1982	Sweet corn	Minisprinkler	0.65-0.87	Calcic Haploxeralf (silt loam)	Shalhevet et al. (1986)
Ramat Hanegev	1983	Processing tomatoes	Trickle	0.40-0.72	Xeric Torripsamment (sandy loam)	Vinten et al. (1986)
Reim	1984	Forage maize	Overhead sprinkler	0.18-1.05	Calcic mollic Haploxeralf (silt loam)	Frenkel et al. (unpubl.)

B. Salinity treatments

<u>Site</u>	<u>Salinisation initiation day</u>	<u>Harvest day</u>	<u>EC_i of irrigation water / (dS/M) / after initiation</u>
Gilat	37	87	S1 1.5-1.9
			S2 3.8-4.3
			S3 4.9-5.7
			S4 7.5-8.4
			S5 9.5-10.1
Ramat Hanegev	48	111-127	S1 1.1
			S2 3.9
Reim	22	87	S1 1.1
			S2 5.2

Table 2 Global and local values of model parameters

A. GLOBAL PARAMETERS ADJUSTED TO LOCAL Y_{max} , E_p

Site	Item	Y_{max} (Kg/m ²)	ET_{max} (cm)	AWt (cm)	S (Kg/m ² cm)	E_p (cm)	B (dS/m)	C (%/dS/m)
Reim	Ears	0.72	45.2	4.7	0.0178	65.0	1.7	12.0
	Total	2.28	45.2	4.7	0.0563	65.0		
Gilat	Ears	0.87	45.0	4.7	0.0216	64.7	1.7	12.0
	Total	1.83	45.0	4.7	0.0454	64.7		
Ramat Hanegev	Ripe fruit (FW)	11.3	79.0	40.5	0.294	106.0	2.5	9.9

B. LOCAL PARAMETER ESTIMATES

Reim	Ears	0.72	50.6	4.1	0.0155	65.0	1.7	9.0*
	Total	2.28	52.3	6.4	0.0496	65.0	1.8	9.1*
Gilat	Ears	0.87	54.7	22.4	0.0269	64.7	1.7	9.0*
	Total	1.83	56.0	18.7	0.0490	64.7	1.8	9.1*
Ramat Hanegev	Ripe fruit (FW)	11.3	67.4	22.0	0.320	106.0	N/A	

*See Shalhevet et al., 1986

Table 3 Comparisons between measured and calculated values of yield using global and local values of input parameters

A. GLOBAL PARAMETER ESTIMATES

Crop	Yield parameters	n	Correlation coefficient	Mean deviation (%)	$\frac{Y_p}{Y_m}$
Gilat	Sweet corn	20	.85	9.7	1.18
	Total	20	.85	9.0	1.04
Reim	Forage corn	16	.90	25.2	0.98
	Total	16	.93	20.5	1.06
Harnegev	Tomatoes	14	.95	60.6	0.45

B. LOCAL VALUES FOR EQ. (1) ONLY

Gilat	Sweet corn	20	.88	14.6	1.26
	Total	20	.93	10.4	1.12
Reim	Forage corn	16	.92	21.4	1.02
	Total	16	.95	18.5	1.10

C. LOCAL VALUES FOR EQS. (1) and (2)

Gilat	Sweet corn	20	.89 (.88)*	24.6 (9.0)*	0.78 (0.96)*
	Total	20	.90	22.6	0.79
Reim	Forage corn	16	.90	21.4	0.96
	Total	16	.94 (.97)*	19.5 (22.4)*	0.99 (1.22)*

C. LOCAL VALUE FOR EQ. (2) ONLY

Harnegev	Tomatoes	14	.96	9.2	0.94
----------	----------	----	-----	-----	------

* refer to transient state corrections

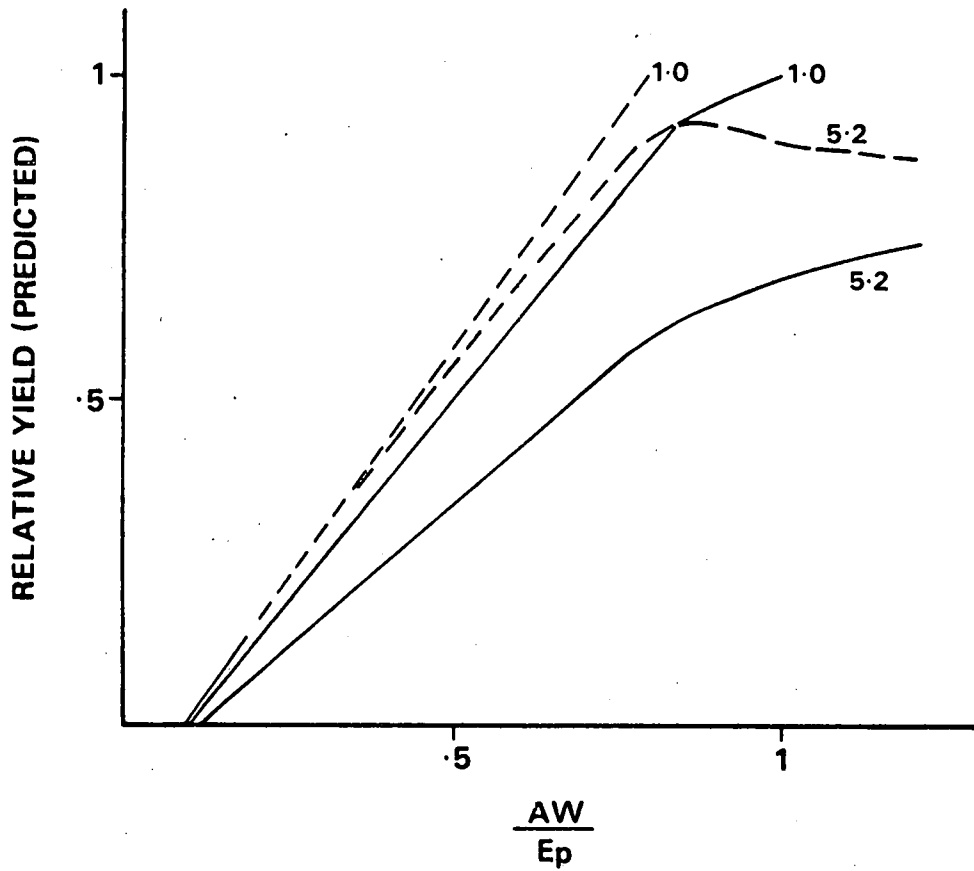


Fig. 1. Yield predictions when irrigating with two irrigation water salinities using the steady state model (—) and the transient state modification to the model (---). Figures on the curves refer to the EC_i of the water. Local parameters for forage corn (Table 2) are used. Low initial soil salinity.

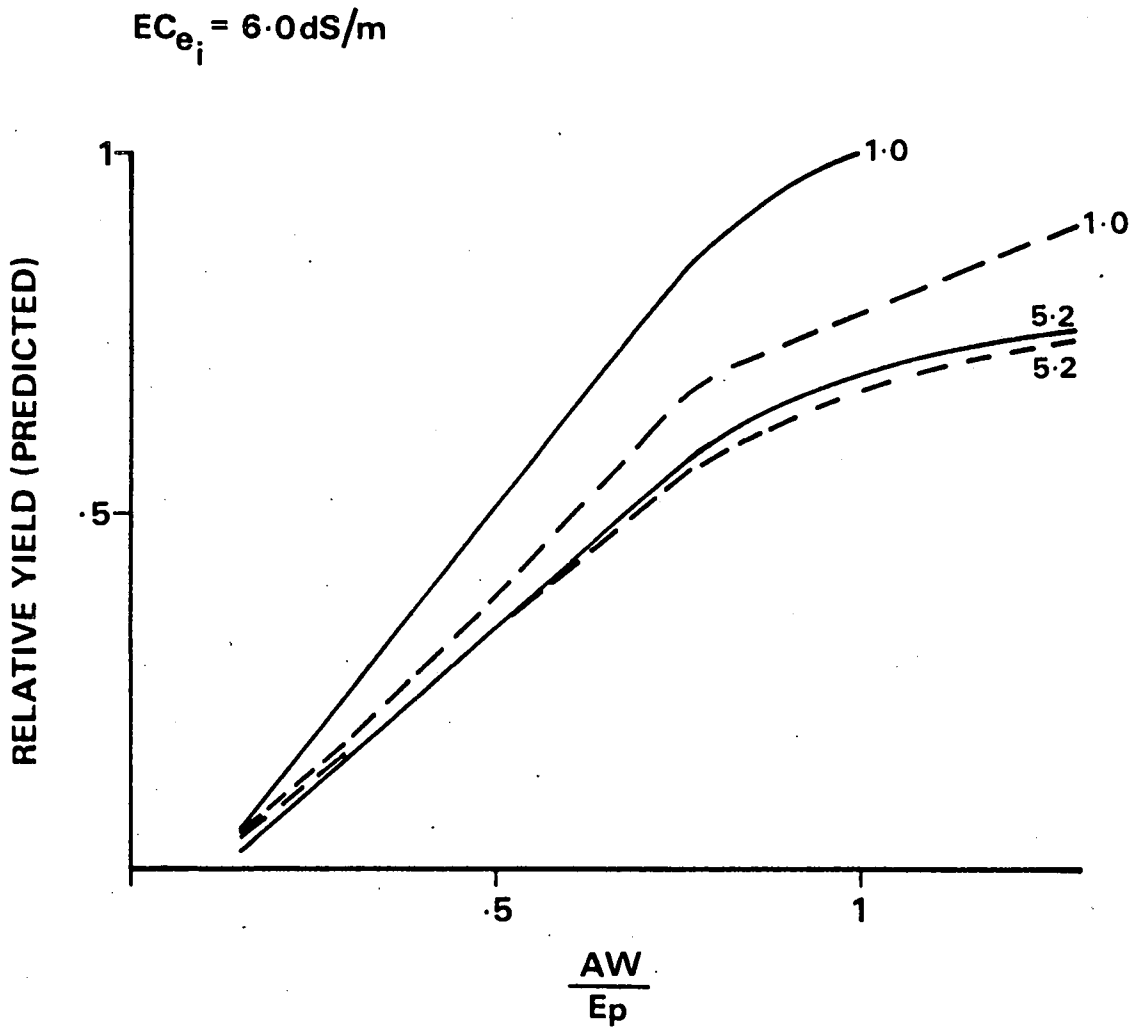


Fig. 2. Yield predictions when irrigating with two irrigation water salinities using the steady state model (—) and the transient state modification to the model (---). Figures on the curves refer to the EC_i of the water. Local parameters for forage corn (Table 2) are used. High initial soil salinity.

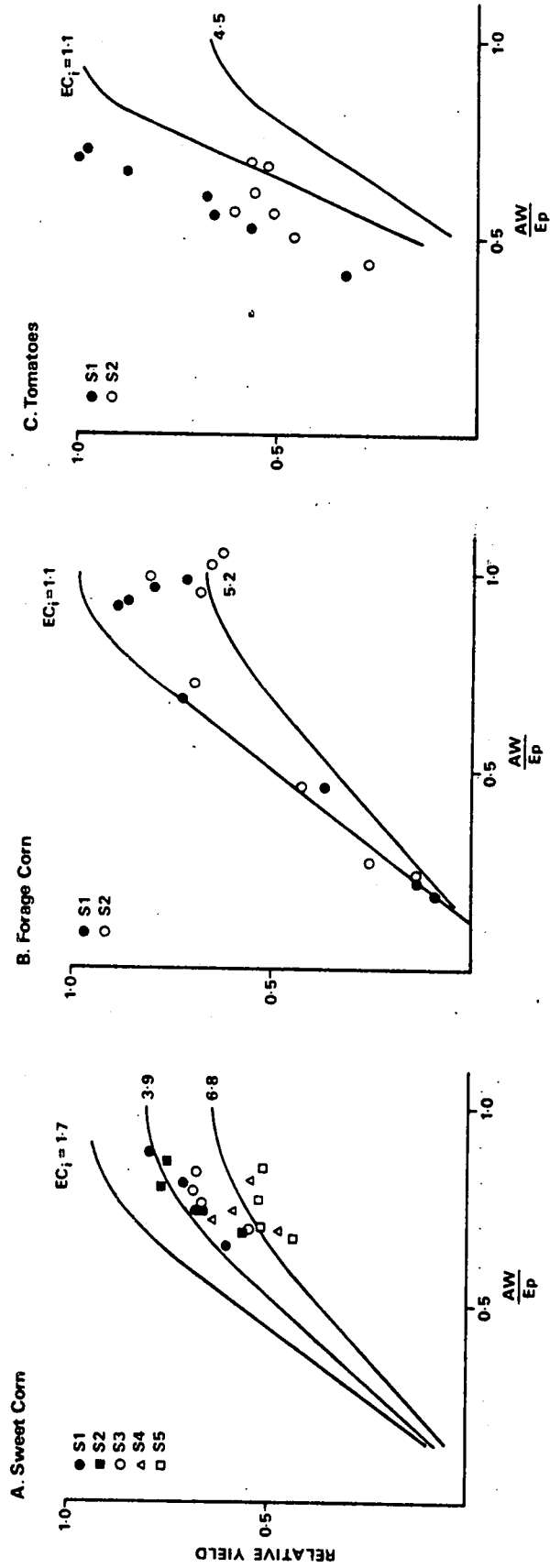


Fig. 3. Measured response of: (A) Sweet corn - ear dry matter; (B) Forage corn - total dry matter; (C) Tomatoes - fresh weight to irrigation with water of different salinities, compared with predictions of Letey and Dinar's original model, using global parameters.

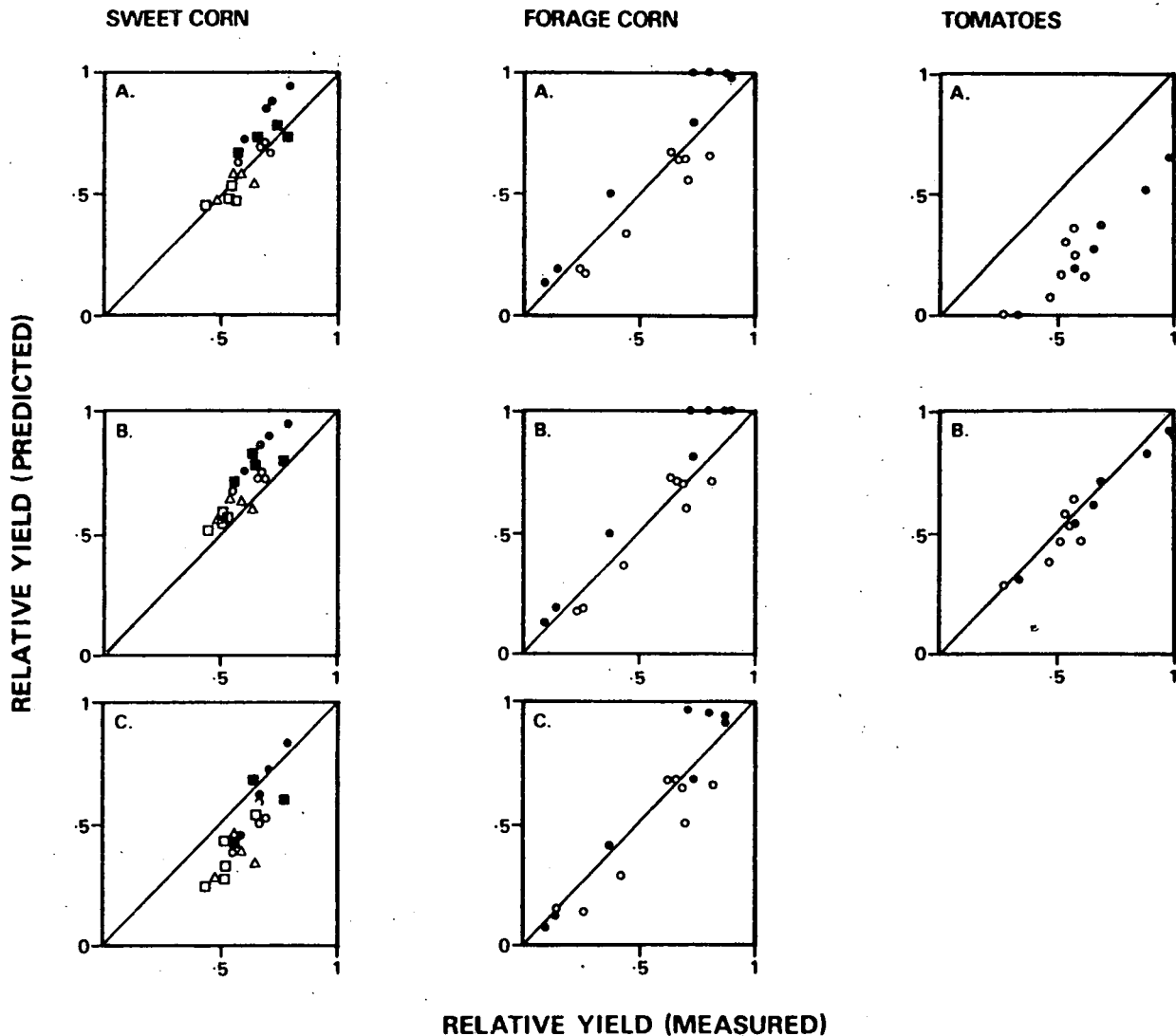


Fig. 4I. Comparison between measured (Y_{Mr}) relative yield and predicted (Y_{Pr}) relative yield of sweet corn ear dry matter using (A) global parameter estimates for eq. (1) and eq. (2); (B) global estimates for eq. (2) and local estimates for eq. (1); (C) local estimates for both eq. (1) and eq. (2).

Fig. 4II. Comparison between measured relative yield and predicted relative yield of forage corn total dry matter using (A) global parameter estimates for eq. (1) and eq. (2); (B) global estimates for eq. (2) and local estimates for eq. (1); (C) local estimates for both eq. (1) and eq. (2).

Fig. 4III. Comparison between measured relative yield and predicted relative yield of processing tomatoes using (A) global parameter estimates for eq. (1) and eq. (2); (B) global estimates for eq. (1) and local estimates for eq. (2).

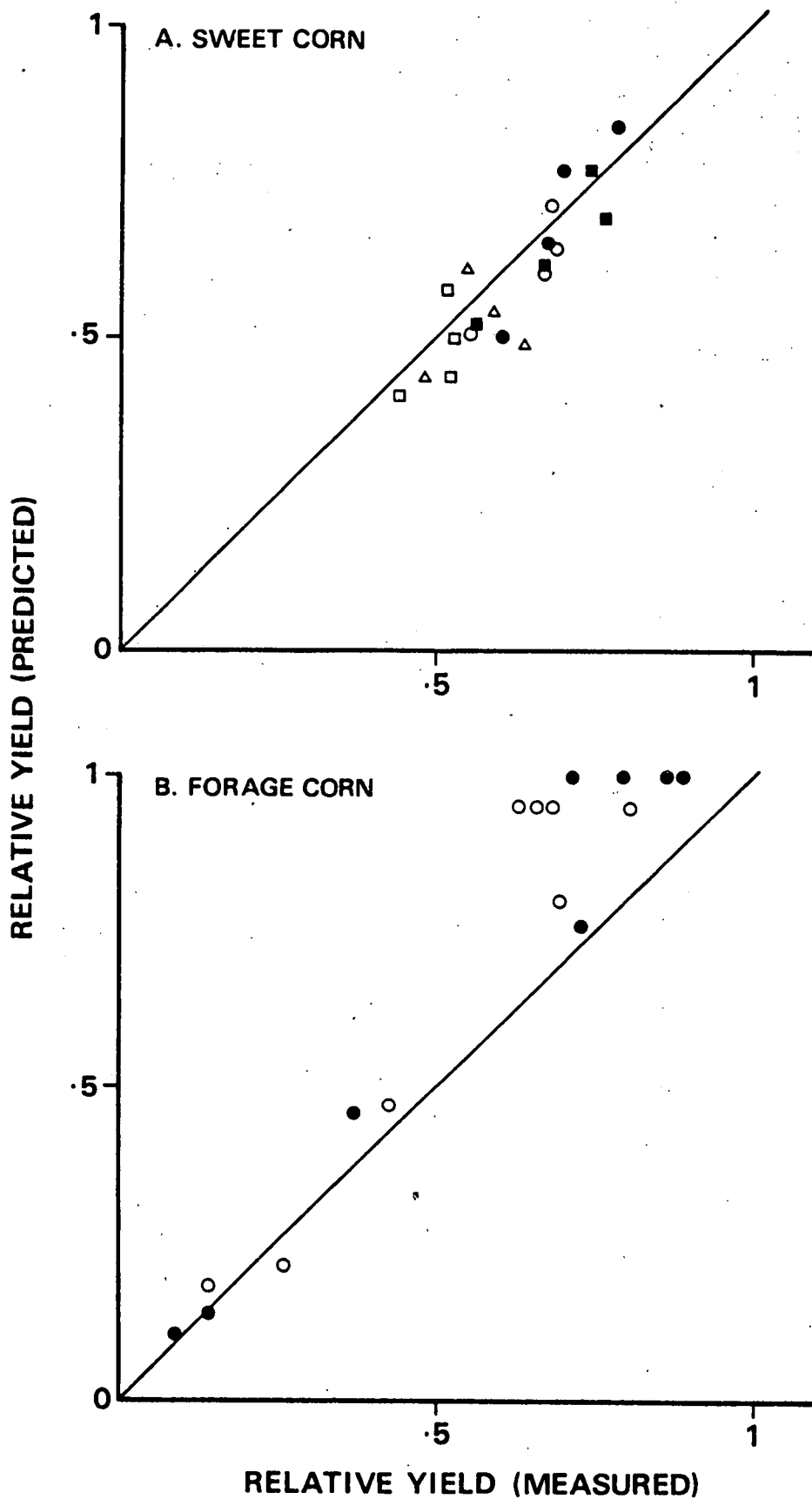


Fig. 5. Relationship between predicted and measured yields using the transient state correction to the Letey and Dinar model.

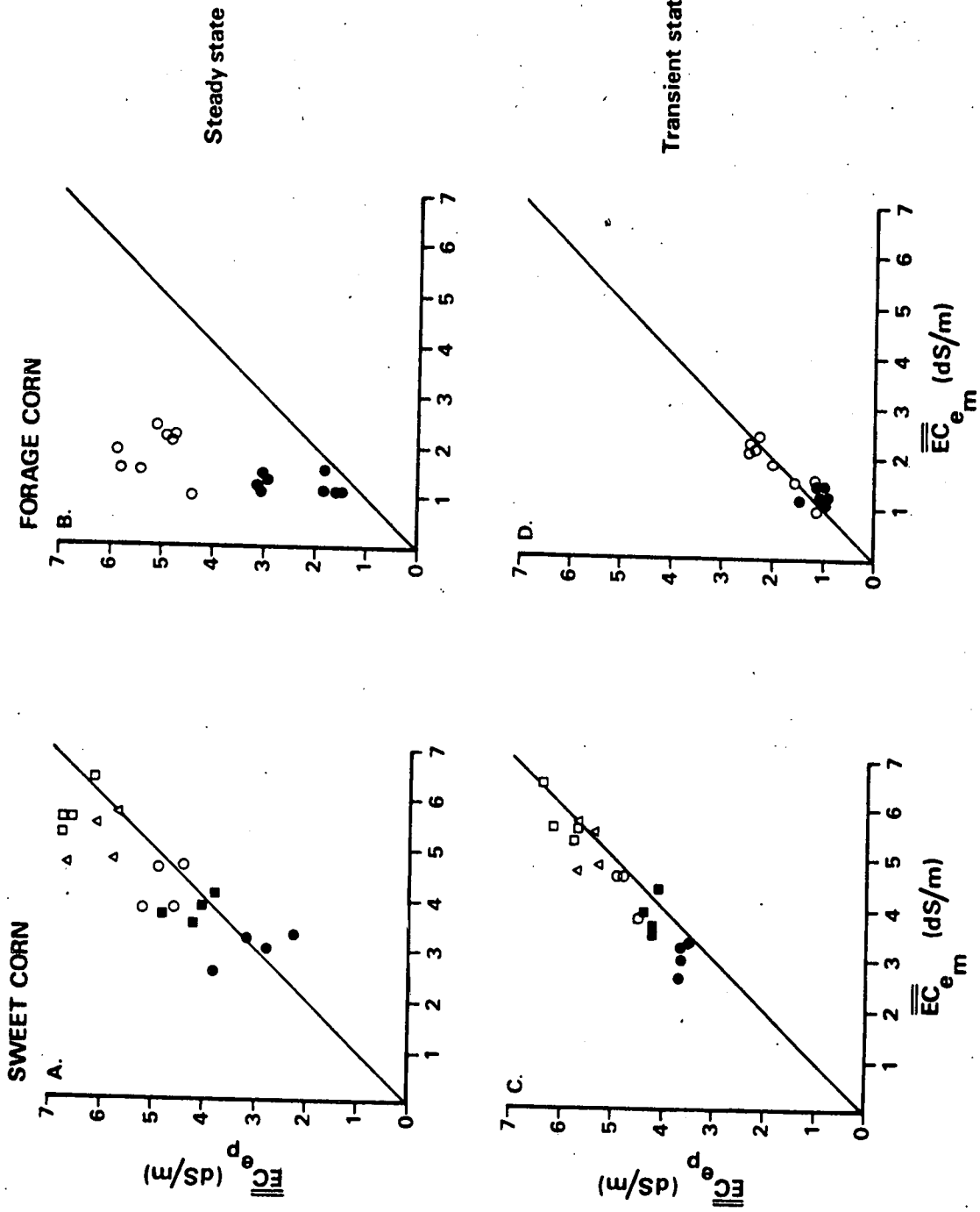


Fig. 6. Relationship between predicted and measured average seasonal root zone salinity, using the original model (A and B) and the transient state correction (C and D).

(A) Sweet Corn; (B) Forage Corn

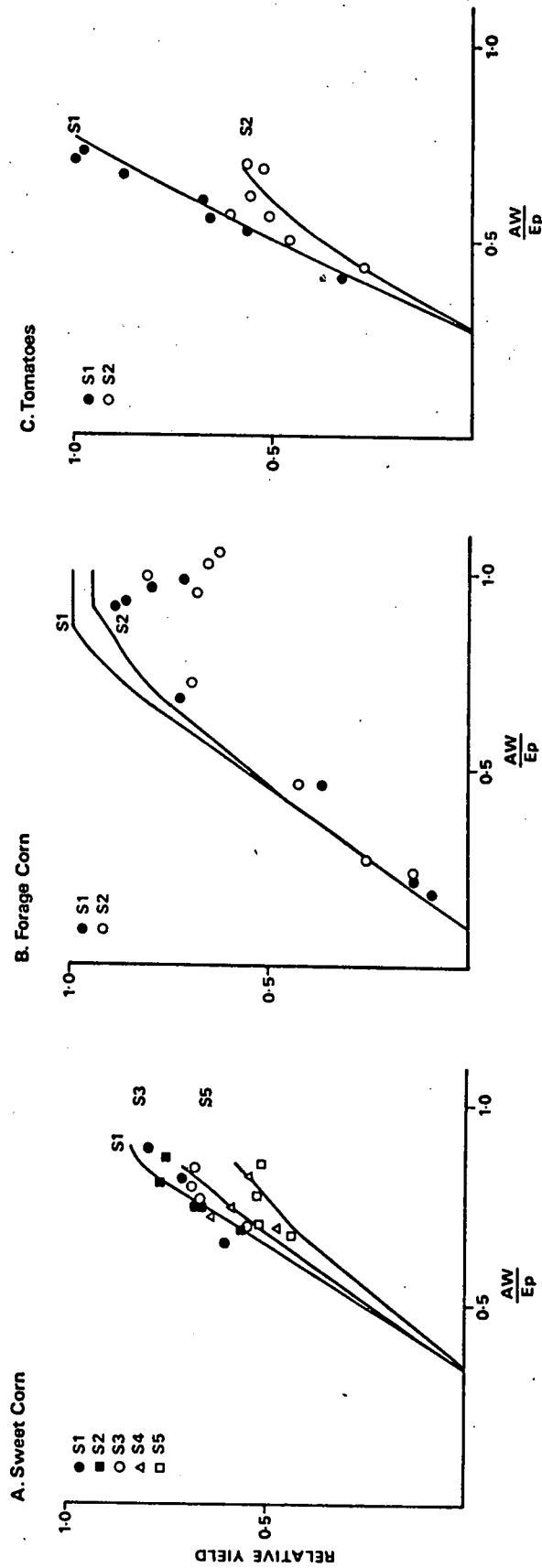


Fig. 7. Measured response of: (A) Sweet corn - ear dry matter; (B) Forage corn - total dry matter; (C) Tomatoes - fresh weight to irrigation with water of different salinities, compared with predictions of the modified version of Letey and Dinar's model, using local parameters.

Publications arising from the project

1. Frenkel, H., Mantell, A., Vinten, A. and Meiri, A. (1987)
Double line-source sprinkler system for determining separate and interactive effects of water and salinity on crop growth. 79th Ann. Meet., Amer. Soc. Agron., Atlanta, Georgia. Agron. Abstracts: 250.
2. Frenkel, H., Mantell, A., Vinten, A. and Meiri, A. (1988)
Double line-source sprinkler system for determining the separate and interactive effects of water and salinity on crop growth.
Isr. Agresearch (in press).
3. Frenkel, H. and Mantell, A. (1988) Comparison of methods for measuring soil salinity. Isr. Agresearch (in press).

